جمهورية العراق
وزارة التعليم العالي والبحث العلمي
جامعة بابل
كلية التربية للعلوم الصرفة
قسم الفيزياء

تحضير وخصائص خليط بوليمري مشوب بجسيمات نانويه للتطبيقات الحديثه

رسالة مقدمة

إلى مجلس كلية التربية للعلوم الصرفة في جامعة بابل
وهي جزء من متطلبات نيل درجه دكتوراه فلسفه
في التربية / الفيزياء

من قبل الطالبة

شيماء مظهر مهدي كاظم

ماجستيرتربيه فيزياء
2019 م

بأشراف

أ.د. مجيد علي حبيب

1445هـ **2023م**

Republic of Iraq
Ministry of Higher Education
and Scientific Research
University of Babylon
College of Education for Pure Sciences
Department of physics

Preparation and Properties of Nanoparticles Doped polymeric Blend for Modern Applications

A Thesis

Submitted to the Council of the College of Education for Pure Sciences University of Babylon in Partial Fulfillment of the Requirements for the Degree of Doctor of philosophy in Education/Physics

By

Shaimaa Mazhar Mahdi Kazem

Master of Education Physics
University of Babylon (2019)

Supervised by

Prof. Dr. Majeed Ali Habeeb

2023 A.D **1445A.H**

Abstract

In this work, two types of PEO-PVA-$SrTiO_3$-NiO and PEO-PVA-$SrTiO_3$-CoO nanocomposites were prepared by solution casting method, with different weight ratios (0,1,2,3 and 4) wt %,from nanoparticles. Optical microscopy and scanning electron microscopy images indicate that the distribution of the strontium titanate, nickel oxide and cobalt oxide nanoparticles was homogeneous in the polymeric blend. FTIR indicates that there is no change in the chemical compositions between the mixture and the additives. The experimental results of the optical properties of PEO-PVA-$SrTiO_3$-NiO and PEO-PVA-$SrTiO_3$-CoO nanocomposites showed that the absorption ,absorption coefficient, refractive index ,extinction coefficient and real and imaginary part of dielectric constant and optical conductivity of PEO-PVA mixture increased with increasing concentrations of $SrTiO_3$,NiO and CoO NPs, while the transmittance and energy gap (allowed and forbidden) decrease with increasing concentration of $SrTiO_3$,NiO and CoO NPs.

The AC electrical properties of these nanocomposites were studied in the frequency range (100Hz-5MHz) at room temperature. The results show dielectric constant and dielectric loss of PEO-PVA-$SrTiO_3$-NiO and PEO-PVA-$SrTiO_3$-CoO nanocomposites decreased with increasing frequency of the applied electric field, while increase with the increase of the concentrations of strontium titanate , nickel oxide and cobalt oxide NPs , while A.C electrical conductivity increases with increasing the concentrations of nanoparticles and frequency.

The antibacterial properties of PEO-PVA-$SrTiO_3$-NiO and PEO-PVA-$SrTiO_3$-CoO were tested against Gram-positive bacteria *(S. aureus)* and Gram-negative bacteria *(E. coli).* The results showed that the inhibition zone increases with increasing concentrations of strontium titanate, nickel oxide and cobalt oxide NPs .The results of pressure sensor of PEO-PVA-$SrTiO_3$-NiO and PEO-PVA-$SrTiO_3$-CoO nanocomposites showed that, the applied pressure rises, electrical capacitance (Cp) increase as applied pressure rises. As a result, pressure sensors have a higher sensitivity. Gamma ray shielding application results show that the attenuation coefficient of PEO-PVA-$SrTiO_3$-NiO and

PEO-PVA-$SrTiO_3$-CoO NCs is increase by increasing concentration of $SrTiO_3$,NiO and CoO nanoparticles.

الخلاصـــــــــــــــة

في هذه العمل ، تم تحضير نوعين من المتراكبات النانوية PEO-PVA-$SrTiO_3$-NiO PEO-PVA-$SrTiO_3$-CoO بطريقة صب المحلول. بنسب وزنيه مختلفة (0,1,2,3, 4) wt % من الجسيمات النانويه. تشير صور المجهر الضوئي والمجهر الالكتروني الماسح الى التوزيع متجانس للجسيمات النانويه تيتانات السترونتيوم وأكسيد النيكل وأكسيد الكوبالت في الخليط البوليمري. تشير تحولات فوريه للاشعه تحت الحمراء الى عدم وجود تغير في التراكيب الكيميائيه بين الخليط والمضافات .حيث اظهرت النتائج التجريبيه للخواص البصريه للمتراكبات النانويه PEO-PVA-$SrTiO_3$-NiO و PEO-PVA-$SrTiO_3$-CoO ان الامتصاصيه ومعامل الامتصاص ومعامل الانكسار ومعامل الخمود والجزء الحقيقي والخيالي من ثابت العزل الكهربائي والتوصيله الضوئيه لخيلط PEO - PVA تزداد بزياده تراكيز الجسيمات النانويه $SrTiO_3$, NiO and CoO .بينما النفاذيه وفجوه الطاقه (الممنوعه والمسموحه) تقل بزياده تركيز الجسيمات النانويه $SrTiO_3$ و, NiO CoO

تمت دراسة الخواص الكهربائيه المتناوبه لهذه المتراكبات النانويه في مدى من التردد (100 Hz 5MHz-) وبدرجه حراره الغرفه . اظهرت النتائج نقصان ثابت العزل وعامل الفقد للمتراكبات النانويه PEO-PVA-$SrTiO_3$- NiO و-PEO PVA-$SrTiO_3$-CoO وبزياده تردد المجال الكهربائي المسلط بينما يزدادان بزياده تراكيز الجسيمات النانويه تيتانات السترونتيوم وأكسيد النيكل وأكسيد الكوبالت بينما التوصيليه الكهربائيه المتناوبه تزداد بزياده تراكيز الجسيمات النانويه والتردد.

تم اختبار الخصائص المضاده للبكتريا للمتراكبات النانويه PEO - PVA - $NiO-SrTiO_3$ وPEO - PVA - $SrTiO_3$ - CoO ضد البكتريا الموجبه الغرام(*S. aureus*) والبكتريا سالبه الغرام (*E. coli*) اظهرت النتائج ان منطقه التثبيط تزداد بزياده الجسيمات النانويه تيتانات السترونتيوم وأكسيد النيكل وأكسيد الكوبالت اظهرت النتائج تطبيق متحسس الضغط للمتراكبات النانويه PEO- PVA - $SrTiO_3$ - NiO و PEO - PVA - $SrTiO_3$ - CoOان السعة الكهربائية (Cp) تزداد بزياده الضغط المسلط . نتيجة لذلك ، يمتلك متحسس الضغط بحساسية أعلى. تظهر نتائج تطبيق التدريع بأشعة جاما أن معامل التوهين لـمتراكبات النانويه PEO - PVA - $SrTiO_3$ - NiO و PVA - PEO - $SrTiO_3$ - CoO NCs يزداد بزيادة تركيز الجسيمات النانوية $SrTiO_3$, NiO and CoO

﴿قَالُوْا سُبْحَانَكَ لاَ عِلْمَ لَنَا إِلاَّ مَا
عَلَّمْتَنَا إِنَّكَ أَنْتَ العَلِيْمُ الْحَكِيْمُ﴾

صدق الله العظيم

سورة البقرة (الآية ٣٢)

Dedication

sincerity

I dedicate this effort to

My dad

My mom

My husband

My children

My brothers

My sisters

My colleagues

My country is Iraq

Iraqi martyrs with love and appreciation

for my teacher

Who provides me with the keys to success

Shaimaa ✍

Acknowledgments

First of all, I thank the gracious God for helping me complete this letter.

After that, I would like to express my sincere appreciation and deep gratitude to my supervisor Prof. Dr. Majeed Ali Habeeb for suggesting the topic of this thesis and for the guidance, suggestions and continuous encouragement throughout the research work.

A word of thanks to the faculty members of the Department of Physics, College of Education for Pure Sciences.

Shaimaa ✍

Contents

List of Figures

List of Address Tables

List of Symbols

Symbols	
A	Area
A_{abs}	Absorbance
c	Light Speed in Vacuum
$C_{\circ}$	Capacitance
D	Electrical Displacement
d	Sample Thickness
E	Electric Field
E_{ele}	Electronic Energy
E_f	Final Energy
E_g^{opt}	Optical Energy Gap
E_i	Initial Energy
E_{rot}	Rotational Energy
E_{trans}	Translation Energy
E_{vib}	Vibration Energy
f	Frequency
h	Blank Constant
$I_{\circ}$	Incident Light
I_p	Conduction Current
I_q	Capacitate Current
I_t	Transmission Light
K	Extinction Coefficient
k_B	Boltzmann Constant
L	Length
n	Refractive Index
n^*	Complex Refractive Index
N_o	Means the Number of Molecules for a unit per Volume
P	Total Dipole Moment
P_e	Electronic Polarization
P_i	Ionic Polarization
P_o	Orientation Polarization

P_s	Space Charge Polarization
R	Electrical Resistance
R_{ref}	Reflectance
T	Transmittance
v	Light Speed in Medium
α	Absorption Coefficient
λ	Wavelength
μ_e	Average Dipole Moment
$\sigma_{a.c}$	A.C electrical Conductivity
σ_{opt}	Optical Conductivity
ω	Angular Velocity
ε	Permittivity of the dielectric material
$\varepsilon_{\circ}$	Permittivity of Vacuum
ε''	Dielectric Loss
ε'	Relative Permittivity
ε_1	Real Part of Dielectric Constant
ε_2	Imaginary Part of Dielectric Constant

List of Abbreviations

Abbreviations	
PEO	Poly Ethylene Oxide
PVA	Poly Vinyl Alcohol
$SrTiO_3$	Strontium Titanate
NiO	Nickel oxide
CoO	Cobalt Oxide
NPs	Nanoparticles
A.C	Alternative Current
C.B	Conduction Band
V.B	Valence Band
FT-IR	Fourier Transformation Infrared ray

UV	Ultra violet Ray
S.aureas	Staphylococcus. Aureas
E.Coli	Escherichia coli
DNA	Deoxyribo Nucleic Acid
PBs	Polymer Blends
C-C	Carbon –Carbon
1D	One Dimension
2D	Two Dimension
3D	Three Dimension
NCs	Nanocomposites
SEM	Scanning Electron Microscope

1-1 Introduction

Concept of nanoscience as their use as antibacterial impact leads to investigations have introduced impetus by giving cutting-edge solutions in various sectors as materials science, biomedical, electronics, and optics. The field of study known as nanoscience focuses on measurements made at the nanoscale. The capacity to regulate the movement of atoms and molecules to create materials, composites, components, and electronics at the nanoscale is part of nanotechnology and nanoscience. The researchers have come to the conclusion that materials with different characteristics than the same materials with greater sizes can exist in small materials, microscopic particles, and thin films. For instance, silver, which is typically thought of as benign, becomes hazardous to viruses when it is converted into nanoparticles and comes into touch with them. Additionally, as a substance shrinks to the size of a nanoparticle, its characteristics change, including color, electrical conductivity, and strength. Metal, for instance, can transform into an insulator or a semiconductor when it reaches the nanoscale level [1].

Nowadays use of polymer materials is attributed to their properties, low weight and ease of processing. However for improvement of some properties such as thermal and mechanical stability, large numbers of additives were added to polymeric matrix and formed polymer matrix composite. A composite is defined as a combination of two or more materials with different physical and chemical properties. In recent years, it has been observed that when we add nanoparticles into polymers leads to dramatic changes in structural , optical and electrical properties of the polymer [2].

Over the past few years, a little word with big potential has been rapidly insinuating itself into the world's consciousness. That word is "Nano" . Nanotechnology is one of the leading scientific fields today since it combines knowledge from the fields of physics, chemistry, biology, medicine, informatics, and engineering. It is an emerging technological field with great potential to lead in great that can be applied in real life. Novel nano and biomaterials, and nanodevices are fabricated and controlled by nanotechnology tools and techniques, which investigate and tune the properties, responses, and functions of living and non-living matter, at sizes less than100 nm by understanding these different the infinite

promises for improved structures, devices and materials. Nanomaterial can be used for several reasons as tiny size, light weight and strong. The major important points in nanotechnology are [3]

1. Small size, usually equal or less than 100 of nanometers.
2. Due to small size it gets unique characterizations.
3. The structure and composition in the (nm) scale can be controlled of them hence control the properties.

The advancement of nanoscience and nanotechnology in materials has led to the creation of nanomaterials, which differ from traditional materials in structure and chemistry and can have one or more dimensions on the nanoscale. get a lot of interest in the realm of study [4]The dimensions of nanomaterials can be categorized as follows:

1.Three dimensions as nanoparticles, nanoshells and quantum dots.

2.Two dimensions as fibers, nanotube and nanowire.

3.One dimensions as thin films, coating and layers.

4. Zero-dimension confinement (quantum dot).

There are two types of nanomaterials, naturally and industrial nanomaterials. The naturally nanomaterials are found in environment without human intervention as viruses, proteins, DNA molecules, and nanoparticles were generated from volcanoes explosion. The industrial nanomaterials are fabricated by human and without intention as nanoparticles were generated during diesel burning [5].

1-2 Polymers

polymer any huge molecule, or macromolecule, made up of several repeating subunits. Both synthetic and natural polymers play a crucial and pervasive role in daily life as a result of their wide variety of characteristics. Natural biopolymers like DNA and proteins, which are essential to biological structure and function, can be found alongside more well-known synthetic plastics like polystyrene. Numerous tiny molecules, referred to as monomers, are polymerized to produce polymers, both natural and artificial. They have unusual physical characteristics, including as toughness, and a propensity to form glasses

and semi-crystalline structures rather than crystals [6], as a result of their relatively large molecular mass in comparison to small molecule compounds .Polymers are present in a wide variety of everyday goods, including clothes, shoes, personal care items, furniture, electrical and electronic gadgets, packaging, cutlery, vehicle parts, coatings, paints, tires, and more. These a few illustrations out of an unlimited list should give you a sense of how crucial synthetic polymers are to contemporary civilization, both in terms of their practicality and their economic worth [7].

1-3 Classification of Polymer

Polymers passes different chemical structure, physical properties, mechanical behavior, thermal characteristics etc., and on the basis of properties of polymer it is being classified in different way [8], as shown in Table (1-1).

Table (1-1) Classification of polymer [8].

No	Basis of Classification	Polymer Type
1	(Origin)	Natural, Semi synthetic, Synthetic
2	Thermal Response	Thermoplastic, Thermosetting
3	Mode of formation	Addition, Condensation
4	Line structure	Linear, Branched, Crosslinked
5	Application and physical Properties	Rubber, Plastic, Fibers
6	Tacticity	Isotactic, Syndiotactic, Atactic
7	Crystallinity	Non crystalline (amorphous), Semi crystalline, Crystalline

1-4 Polymer Blends (PBs)

Is previously earlier several synthesis processes relied heavily on alloys. The polymer mixes, however, are now essential in many areas of life, including the industrial, medicinal, and commercial fields larea .In order to create a unique polymer with new physical characteristics, polymer blends (PBs) should comprise at least two different types of polymers. Each polymer's shape and content is characteristics that influence the efficacy of a polymer mix. The price of mixes

depends on the content, composing method, and morphology [9]. Miscible and immiscible polymer mixes are the two main categories into which they fall. Due to their compatibility and popularity as biodegradable plastics, PEO-PVA blends were used in this study. They have the characteristics of miscible polymer blends, which include a strong bond or adhesion between them, homogeneous blend, single phase structure, and one glass transition temperature. Low bond or adhesion, a scattered phase structure with a variety of morphologies, and two glass transition temperatures are the characteristics of immiscible polymer blends [10]. There are several justifications for using filler in polymers and polymer blends, including:

1. The price of a polymer product may be calculated, and inexpensive fillers are frequently utilized.
2. To improve the mechanical (toughness, bending, and strength) and electrical (as well as optical) characteristics of polymers.
3. Using pigments allows for the creation of colored polymer products.
4. The filler content of a polymer may be used to create composite materials.
5. Functional fillers are added in this case to give the polymer new characteristics, such as conductive filler (Ni, Co, or scattered metals), which changes the filled polymer from insulating to conducting.

1-5 Nanocomposites Materials (NCs)

In recent years, the majority of industries and our everyday lives have required new materials. Therefore, polymer nanocomposites may be defined as materials that include minute amounts of fillers dispersed uniformly across polymers at various concentrations. Compared to microcomposites, the space between adjacent additives in nanocomposites is substantially less. In nanocomposites, fillers and polymers should interact substantially more [11]. A promising subject in the realm of nanoscience is represented by nanocomposites, a new construction material. They exhibit extraordinary benefits in terms of structure, electrical, optical, biocompatibility, and biodegradability in a variety of industrial, medicinal, and drug release packaging applications .In addition to these characteristics[12],the interaction between the nanoparticle filler and polymer blend creates molecular bridges for nanocomposites. This is the reason why the nanocomposite's structural, electrical, and optical characteristics are better than those of traditional microcomposites[13]. Understanding the interactions between

polymer nanocomposites is necessary to manage their characteristics and structural linkages. This should be function within the limitations imposed by the industrial and biomedical applications' physical, chemical, and biological requirements[14]. As shown in figure(1-1), the matrix, reinforcement, and interfacial area are the three main components of nanocomposite polymers, the last is in charge of incorporating the nanofiller into the matrix [15].

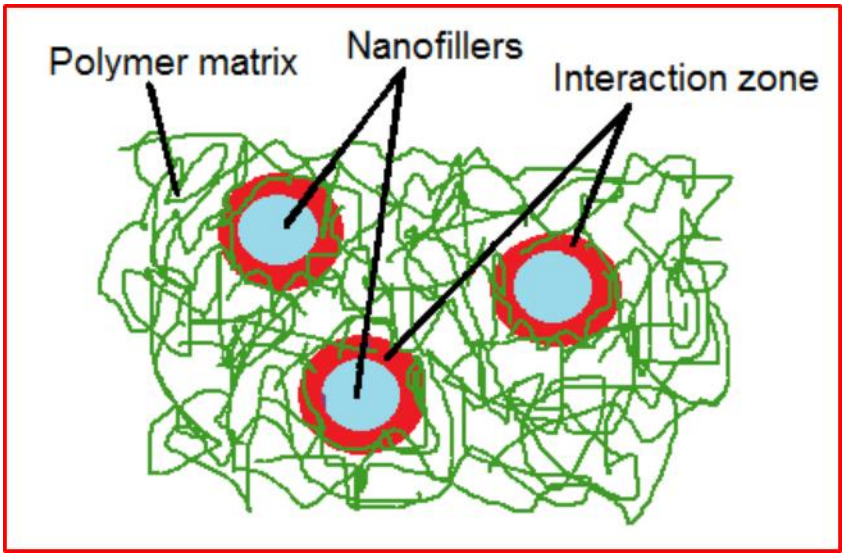

Figure (1-1) The component of nanocomposites polymer[15]

Filler of nanoparticles helps to enhance the foaming properties of polymer. The large surface with comparing volume ratio of the foaming polymer leads to increase the rate of gas and heat release in incident of fire. But with present nanoparticles as nickel oxide, the rate of burning can be mainly reduced[16,17].

1-6 Poly Ethylene Oxide (PEO)

The highest chemical and thermal stability of any base material makes polyethylene oxide particularly intriguing. PEO is a semi-crystalline polymer that, at ambient temperature, may exist in both amorphous and crystalline states. Even at extremely high salt concentrations, a wide range of salts may be solvated. The interaction of metallic actions with oxygen atoms in the backbone of salts causes them to dissolve. However, as it has been demonstrated that ionic conduction occurs mostly in the amorphous phase of PEO, its multiphase characteristic is frequently viewed as a significant issue in actual functioning systems. The reduction of polymer chain crystallinity enhances polymer chain mobility, which in

turn promotes improved ionic conduction. One of the most efficient ways to increase the amorphous content and decrease the crystalline content is polymer mixing. Polymer blends frequently have qualities that are better than those of the separate component polymers [18]. Recent years have seen a rise in interest in poly(ethylene oxide) because to its water solubility, biodegradability, non-toxicity, and biocompatibility. It may be used for a variety of things, including electrical gadgets, paper coating, textile fibers. Structure of PEO is shown in figure (1-2) [19]. Table (1-2) Physical and chemical properties of Poly ethylene Oxide [20]

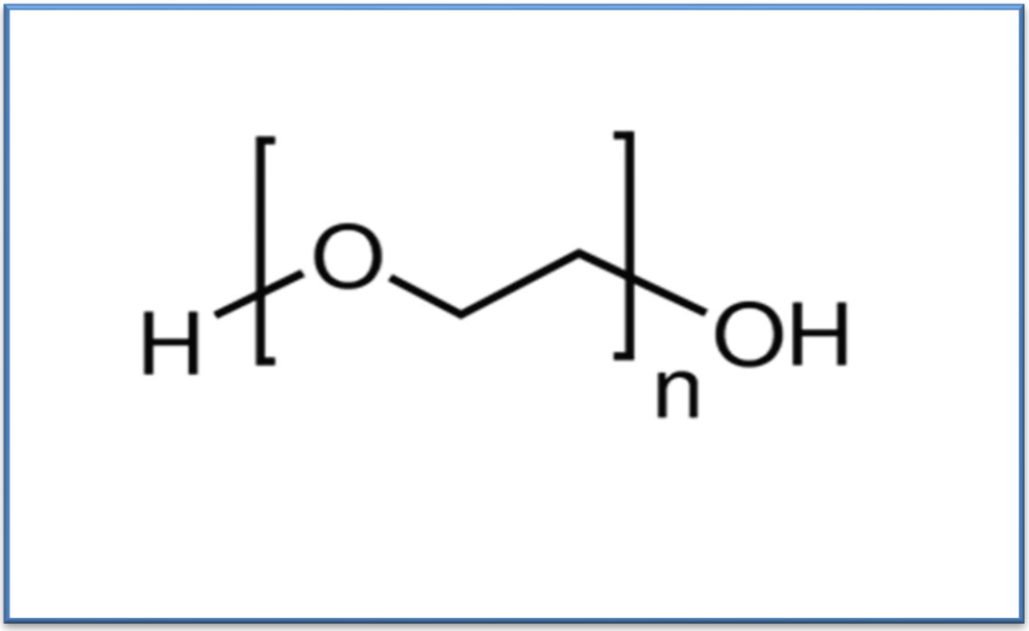

Figure (1-2) structure of Polyethylene Oxide[19]

Table (1-2) Physical and chemical properties of Poly ethylene oxide (PEO)[20].

Appearance	PEO
Molecular Formula	H(OCH2CH2)nOH
Appearance	White to very pale yellow
Melting Point	64-66°C
Density	1.27g/mLat 25°C
Flash Point	423 - 425 °C
Boling Poin	>250°C
Water Solubility	Soluble in water
Solubility	Slightly hygroscopic. It melts easily when heated. Soluble in water and ethanol
Vapor Presure	<0.01 mm Hg (20 °C)
Vapor Density	>1 (vs air)
Appearance	waxy solid
Maximum wavelength(λmax)	'λ: 260 nm Amax: 0.6،' , 'λ: 280 nm Amax: 0.3']
PH	5.5-7.0 (25℃, 50mg/mL in H2O)
Specific Gravity	1.128
Gravimetric analysis	0.3 -0.8 wt%
Viscosty:	497 - 536
Packing	250g per bag sealed in vaccum (moisture content<2%RH)

1-7 Poly Vinyl Alcohol (PVA)

Poly Vinyl Alcohol's primary physical characteristics include being water soluble, semi-crystalline, nontoxic, biocompatible, eco-friendly, better at creating films and fibers, superior mechanical capabilities, great chemical resistance, and biodegradable. The physical characteristics of it are the result of the polymerization of vinyl acetate to form polyvinyl acetate (PVAc) and the subsequent hydrolysis to produce PVA. Due to its outstanding biocompatibility and biodegradability, the hydrophilic polymer polyvinyl alcohol (PVA) finds particular use in the medical field. A semi crystalline nature, or the occurrence of both amorphous and crystalline patches, which causes interfacial effects and

amplifies the physical properties, is a significant characteristic of (PVA). Because of its distinctive properties, poly vinyl alcohol is employed in the majority of synthetic polymers[21,22].

PVA is frequently used in the packaging, cosmetic, adhesive, food, paper, filtration, optics, and catalysis are three of the main functional applications of poly vinyl alcohol. Because of the polarity of the hydroxyl group, which produces intermolecular hydrogen bonding, PVA has a significant cohesive energy that contributes to a number of its key features .However, PVA is sensitive to plasticization in humid settings because to the same characteristics that give it distinctive performance and hydrophobicity. Additionally, water and biological fluids have a significant degree of swelling or rubberiness. The melting point of polyvinyl alcohol is T_m = 230 ^oC, and it has a density of 1.3 g/cm^3 and a glass transition temperature of T_g = 85 ^oC. Structure of PVA is shown in figure (1-3)[23]. Table (1-3) Physical and chemical properties of poly vinyl alcohol(PVA) [24].

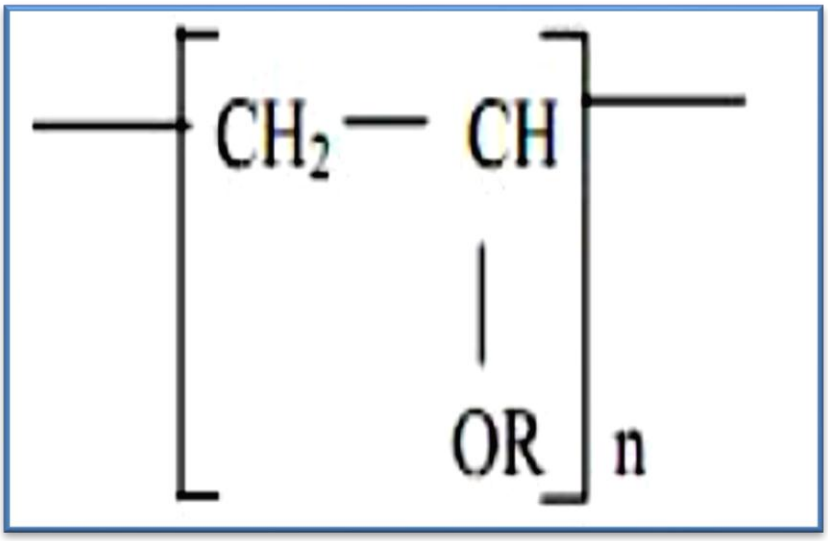

Figure (1-3) structure of polyvinyl alcohol where R= H or $COCH_3$[23].

Table(1-3)Physical and chemical properties of poly vinyl alcohol (PVA) [24]

Appearance	White –to-cream granule powder
Solution PH	5.0-6.5
Bulk density, kg/m^3	400-432
Resin density, kg/m3	1294
Specific gravity	1.27-1.31
Specific volume, m^3/kg	7.7 x 10^{-4}
Specific heat, J/kg·K	1674
Thermal conductivity, W/(m.K)	0.2
Thermal Stability	Gradual discoloration about 100 ^{0}C ,darkens rapidly above 150^{0}C ,rapid decomposition above 200^{0}C
Melting point (un plasticized) ^{0}C	230 for fully hydrolyzed grades ,180-190 for partially hydrolyzed grades
Tg ^{0}C (dry film)	75-85
Storage Stability (solid)	Indefinite when protected from moisture
Flammability	Burns similarly to paper
Stability to sunlight	Excellent
Molecular weight	26,300-30,000
Degree of hydrolysis	(86.5-89)%

1-8 Strontium Titanate ($SrTiO_3$) Nanoparticles

Having the chemical formula $SrTiO_3$, is a titanate and strontium oxide. It has a Centro symmetric perovskite structure and functions as a cento electric material at ambient temperature. It becomes a quantum pare electric when, at low temperatures, it approaches a ferroelectric phase transition with an extremely large

dielectric constant of 104 and stays Para electric down to the lowest temperatures observed as a result of quantum fluctuations. [25] believed to be a completely substance. In nature ,been used in advanced ceramics, optics, and varistors in its synthetic form, $SrTiO_3$ has a direct band gap of 3.75 eV and an indirect band gap of 3.25 eV [26] With a low electric field and a relatively large dielectric constant (300) at ambient temperature, synthetic strontium titanate is an excellent material. For very pure crystals, specific resistivity of over 10^9 cm. In high-voltage capacitors [27].Table (1.4) Physical and chemical properties of strontium titanate ($SrTiO_3$) [28].

(1-4) Physical and chemical properties of Strontium Titanate ($SrTiO_3$) [28].

Chemical_ formula	$SrTiO_3$
Molar_mass	183.49 g/mol
Appearance	White, opaque crystals
Density	5.11 g/cm3
Melting_point	2,080 °C (3,780 °F; 2,350 K)
Aqueous_solution	insoluble
Refractive_index	2.394
Crystal_structure	Cubic Perovskite
Cubic Perovskite	Pm3m, No. 221

1-9 Nickel Oxide (NiO) Nanoparticles

Nickel oxide is a light green a cubic FCC structure. At low temperatures .In the periodic table's group (II-VI) of semiconductor compounds, nickel oxide (NiO) is a compound with a crystalline structure like that of sodium chloride salt (NaCl) [29]. Table (1-5) lists some significant physical characteristics of NiO. The sample's hue serves as a general indicator of the stoichiometry of NiO. Even in traces, higher valence states of nickel may drastically alter the hue of NiO. Depending on the production procedure and resulting defect configuration, it shows vastly disparate magnetic, optical, electrical, and electrochemical characteristics [30]. The covalent bond between the nickel oxide ions and the unit cell of a centralized faceted type (FCC) is produced by the participation of two electrons between the nickel atoms and oxygen atoms [31,32].

Due to its substantial exciton binding energy and big energy gap (3.6-4.0 eV), nickel oxide (NiO) is a potential p-type semiconducting material . Compared to bulk nickel oxide, the nanostructured NiO material shows unique physical characteristics in the areas of mechanical, electrical, optical, and magnetic properties. Particle size and shape have an impact on the physical properties of NiO NPs. The larger surface to volume ratio, which is shown by the smaller size NPs, has an impact on the NPs' physical characteristics. Higher surface-to-volume ratios give nanoscale particles more surface energy, which lowers i the number of co-ordinations at the surface relative to the volume within, (ii) changes in crystal symmetry, and (iii) increases disorder/defects in the crystals. The surface and particle size effects brought on by quantum confinement at the nanoscale are what have improved the physical characteristics of NiO. NiO nanoparticles (NPs) are a versatile material that may be employed in a wide range of applications, including catalysts. Electrocromic films have been used in gas sensors nanoscale optoelectronic devices p-n junction heterojunction [33]. NiO NPs can also be employed as a medication delivery vehicle and in magnetic resonance imaging since they have super-paramagnetic properties. To enhance the structure-optical nature of the unique physical characteristics, such as mechanical, electrical, optical, and magnetic capabilities against the bulk nickel oxide, intrinsic and surface detects produced during the synthesis of NiO NPs are used. NiO NPs' physical properties are dependent on the size and form of the particles [34]

Table (1-5) The physical characteristics of NiO [30].

Property	**NiO**
Density (g/cm^3)	6.8
Melting point (^oC)	1955
Molar mass (g/mol)	74.69
Energy Gap (eV) at (300K)	3.5
Type of optical transition	Direct
Electronic Affinity (eV)	1.47
Effective mass of carriers (Holes) m^*/m_o	0.6-1
Dielectric constant ε_o	11.9
Crystal Structure	Cubic
Lattice Constant(a=b=c) (nm) at (300K)	0.4178
α (deg) = β (deg) = γ (deg)	90
Appearance	green crystalline solid

1-10 Cobalt Oxide (CoO) Nanoparticles

Cobalt oxide (Π) is in the form of a crystalline powder of olive green color in the pure state, but it is often found in the state of impurities and the color of the compound at that time is dark gray, and in the presence of moisture it easily oxidizes to cobalt trihedral oxide. Or cobalt monoxide is prepared from double and triple cobalt oxide at a temperature of 1220 K [35]. Cobalt is used in the manufacture of magnets, ceramics and special types of glass, as well as pure cobalt. In the manufacture of cathode tubes for X-rays and some special industries. Cobalt is often used in alloying, refractory and hardening, and in the manufacture of magnets and cofactors. It is also considered one of the three natural minerals for

making magnets, by adding it to iron and nickel. Aerobic oxygen slowly, does not ignite and reacts with most acids to produce hydrogen. It does not react with water at room temperature.Cobalt oxide is used in the manufacture of ceramics as well as in the manufacture of chemicals, including cobalt salt . Cobalt oxide (CoO) has been used for centuries as a pigment for pottery , and it has an energy gap of 3.7eV electrons. Table (1-6) The physical and chemical properties of (CoO)nanoparticles [36].

Table (1-6) The physical and chemical properties of (CoO)nanoparticles[36]

Properties	**Cobalt oxide nanoparticles (CoO)**
Color	Green, red, gray, or black powder
Sensitivity	Air moisture sensitive
Molecular Weight, (g/mol.)	74.9326
Structure	Fcc
Decomposition temperature	Not determined
Crystallography	Cubic
Bulk Density,(g/cm^3)	0.966
Melting temperature (°C)	~1935
Boiling temperature (ºC)	Not determined
Specific gravity	6.11
Form	Powder
Odor	Odorless
Solubility	Negligible
Manufacture	Shimadzu corporation, japan
Purity	99.7% (Co: >78%)
PH	5.5-6.0
Morphology	Nearly spherical

1-11 Literature Review

Patel *et al* in (2014) [37] have studied spectroscopic investigation of (PAAm/PEO) blend films: preparation and its characterizations, they found that the absorption spectra of the pure and blended polymer films. Increased with increasing the weight percentage of PEO and absorption coefficient (α) was determined from the absorption spectra and the values of direct and indirect band gap for the pure and blended films are decreases with increasing PEO percentage.

Dawood .K. A, *et al* in (2014). [38] studied the nanocomposites of polyvinyl alcohol- poly-acrylic acid- cobalt oxide nanoparticles. The cobalt oxide nanoparticles was added to polymers with diffrent concentrations. The results show that the absorbance of naoocomposites is increased with the increase of cobalt oxide nanoparticles and optical constants (absorption coefficient, extinction coefficient, refractive index. Real and imaginary dielectric constants) are increased with the increasing of cobalt oxide nanoparticles concentrations. The energy band gap of nanocomposites is decreased with the increase of cobalt oxide nanoparticles concentrations.

Sujumaran .S, *et al* in (2015). [39]] studied the characterization of the (PVA-$Al2O_3$) composite thin films prepared by the dipping method. They found that dependence of temperature and frequency for dielectric properties. The results also showed the study of insulating properties. The results indicated a higher refractive index, dielectric constant and lower dielectric loss for (PVA-Al2O3).

Chatterjee .B, *et al* in (2015) **.** [40] examined the electrical properties of starch-PVA polymer blend with different concentrations of KCl. The results showed that the conductivity and dielectric constant of starch-PVA polymer blend increased with an increase in the salt concentrations.

Mathen .J. J ,*et al* in (2016) .[41] studied the improve of the optical and dielectric properties of PVA matrix with nano-ZnSe: synthesis and characterization. The results showed that the constant and loss dielectric increase with increasing of ZnSe nanoparticles concentration. The optical conductivity increases with increasing the nanoparticles concentration

Karpuraranjith .M, *et al* .in (2017) . [42] have studied produced the (cesium/zinc oxide-polyvinyl pyrrolidone) nanocomposites by using precipitation process. Antibacterial activity of chitosan,(cesium/zincoxide polyvinyl pyrrolidone) ,and (polyvinyl pyrrolidone–zinc oxide) nanocomposites was examined versus gram negative bacteria Escherichia coli (E.coil) and gram positive bacteria Staphylococcus aureus) S.aureus) .The results indicated that gram positive bacteria are more susceptible to inhibition than gram negative bacteria.

Goswami .A, *et al* ,in (2017) .[43] they study carboxy methyl cellulose (CMC)and (PVA) thin films by solution casting. Vanadium pentagonal oxide was prepared for the production of bio-nanocomposites ($CMC/PVAV_2O_5$(by in situ precipitation. The electrical conductivity of alternating current was measured at different frequencies. It was found that the conductivity rises at a higher frequency, and the band gap decreases at UV-VIS spectra. The nanocomposites appear to have a strong electrical behavior.

Gurswamy.B, *et a*l,in (2018) [44] .They study The doping of SnO2 nanoparticles on the structural, optical, electrical and thermal properties of the polymer blend (PVA-PVP). Membranes of the nanocomposites (PVA-PVP-SnO2) were prepared using the solution casting technique. Aninfrared Fourier transform study showed that SnO2 nanoparticles react with the (OH) group of (PVA) and the carboxyl group (PVP) to form the compound within the mixing matrix. The optical study showed increased absorption in the UV region and transparency in the visible region.

Ningaraju S,*et a*l ,in.(2018). [45] studies the free volume controlled electrical properties of PVA/NiO and PVA/TiO2 polymer nanocomposites. The Scanning Electron Microscopy (SEM) studies demonstrate the formation of nanoclusters by the agglomeration of nanoparticles at higher wt% of nanofiller loading. The increased AC/DC conductivity of PVA/NiO and at lower concentration of TiO2 in PVA/TiO2 polymer nanocomposites suggests the increased mobility of ions and electric charge carriers. The decreased conductivity at higher concentration of TiO2 indicates the reduced conducting pathways for the mobility of ions and electric charge carriers due to the increased ion aggregation. The increased dielectric constant and dielectric loss up to 0.1 wt% of NiO and 0.4 wt% of TiO2 suggests the increased dipole polarization. The decreased dielectric constant after

0.4 wt% of TiO2 is attributed to the reduced dipole polarization by the formation of thin immobile nano-layers and hence the polymeric chain mobility.

Ueda K, in (2019). [46] studied the optical, electrical and thermal properties of organic–inorganic hybrids with conjugated polymers based on POSS having heterogeneous substituents. They found demon strated that poss "element-blocks" en able trans formation of conjngated polymers into thermally – stable hybrid materials with out critical and electronic properties provided by the organic components

Jebur Q, *et al*, in(2020). [47] have studied the dielectric and structural characteristics of (PVA-PEO-Fe_2O_3) nanocomposites. The results indicate that when the frequency of the applied electric field increases, the dielectric loss and dielectric constant decreased while the electrical conductivity increases. The optical experiments revealed that the absorbance for (PVAPEO-Fe_2O_3) increases with increasing iron oxide nanoparticle concentrations. With increasing concentrations for iron oxide nanoparticles, the indirect (Eg) energy gap for the (PVA-PEO) blend reduces. The optical constants of (PVA-PEO) blend, such as , extinction coefficient, absorption coefficient, refractive index, real and imaginary dielectric constants, and optical conductivity, altered as the weight percentage of iron oxide nanoparticles increased.

Abid .A, *et al*, in (2021). [48] have studied examined polymer blend(PVA-PVP)-carbon black (C.B N375) nanocomposites. The nanocomposites (PVA-PVP-C.B) are prepared by the use of a casting method. The dielectric constant and dielectric loss of the samples decreased as the frequency of the applied electric field increased, however the A.C electrical conductivity results increased as the frequency increased. With increasing carbon black concentrations, the dielectric constant, dielectric loss, and electrical conductivity (A.C) of all films increased

Cao Y, *et al*, in (2022). [49] have studied, the solution blow spinning (SBS) technique was used to rapidly create polyvinyl pyrrolidone(PVP),polycaprolactone (PCL), and PCL/PVP nanofibrous films to encapsulate chromogenic acid (CGA). The PVP Nano fibrous film did not show any inhibition activity against E. coli or S. aureus, while the PCL/PVP and PCL films showed will antimicrobial activity. In

summary, the above findings indicated that PCL and PCL/PVP nanofibrous films containing CGA had interesting applications in food packaging

Zainab *et al*, in (2023) [50] have studied new type of nanocomposites made of polyvinyl alcohol (PVA) with different concentrations (0, 1, 2 and 3) wt% of cobalt oxide and zirconium dioxide (CoO-ZrO2) nanoparticles by using casting method. Microscopic photographs demonstrate the fact that the additive distribution amount of NPs in the polymer was uniform, and (CoO-ZrO2) NPs formed a continuous network within the polymer when the concentration reached 3wt.%. The outcomes of optical properties indicate that the absorbance of nanocomposites improves as the concentrations of cobalt oxide and zirconium dioxide nanoparticles increase while transmittance and the optical energy gap decrease. On the other hand, optical constants of nanocomposites (refractive index, absorption coefficient, extinction coefficient, real and imaginary the dielectric constants) and optical conductivity are increase with increases in the weight percentages of (CoO-ZrO2) nanoparticles.

1-12 The Aims of The Study

The principle aims of this research are:

1- In this study, the formation of new types of PEO-PVA-SrTiO3-NiO and PEO-PVA-SrTiO3-CoO nanocomposites for use in improving physical properties.

2-Investigating the structural, electrical, and optical characteristics of PEO-PVA-$SrTiO_3$-NiO and PEO-PVA-$SrTiO_3$-CoO nanocomposites

3-Applications for PEO-PVA-$SrTiO_3$-NiO and PEO-PVA-$SrTiO_3$-CoO nanocomposites as antibacterial activity , pressure sensors and gamma ray shielding.

2-1 Introduction

This chapter includes a general description of the theoretical part of this study, relationships, physical concepts, scientific clarifications, and laws used to interpret the study results.

2-2 Structural Properties

The structural properties represent important tool to study the crystallographic structure of the films.

2-2-1 X – ray diffraction (XRD)

X-ray is an electromagnetic wave with specific wavelength between the ultraviolet (UV) and gamma ray (0.1-10 Ao). Therefore, it is preferable to use in most crystalline diffraction experiments. In general, diffraction depends on crystalline structure, wavelength used should be equal to or approximate to lattice constant [51]. X-ray diffraction provides important information about the shape and specification of the unit cell and the crystalline structure of the films prepared whether they are single crystalline polycrystalline or amorphous [52]. Bragg supposed that the Chapter Two Theoretical Background crystal is a large groups of parallel surfaces of atoms repeat itself periodically in three-dimensional space and the space between any two successive surfaces is "d" so he imagined the crystal . Therefore, Bragg assumed the X-ray of wavelength with monochromatic from source falls on the sample to be examined at an angle (θ) in (degree) and reflected at an angle value of twice the fall angle recorded on the detector, the fall angle changed once after (160^{o}) depending on the need for this range. This technology provides information on characteristic peaks locations which represent the direction of crystalline growth prevailing within the crystal lattice, the mid-width represents the greatest level of intensity through which granular boundary information can be obtained the knowledge of growth in granular size of the test sample [53]. As a result of construction interferences, X-Ray diffraction peaks characteristic of the prepared films are between the reflected rays from the characteristic surfaces groups of the prepared films at specific angles called "Bragg's angles", the characteristic surfaces of a similar phase which the optical path difference between them equals to an integer number of wavelengths with monochromatic X-Ray [54].Bragg deduce the following law [55]:

$$n\lambda = 2\, dhkl\, sin\theta \ldots\ldots\ldots \quad (2\text{-}1)$$

where

n : integer number representing diffraction order

λ : X-ray wavelength (1.5406 Å)

d : distance between two successive leve

hkl: Miller index

θ **:** Bragg diffraction angle

2-2-2 Scanning Electron Microscope (SEM)

A scanning electron microscope (SEM) is a type of electron microscope that produces images of a sample by scanning the surface with a focused beam of electrons. The electrons interact with atoms in the sample that contain information about the sample's surface topography. The most common SEM mode is detection of secondary electrons emitted by atoms excited by the electron beam. The number of secondary electrons can be detected depending on specimen topography [56]

2-2-3 Fourier Transform Infrared Ray (FTIR)

Spectroscopy is the study of molecular or atomic structure of a substance by observation of its interaction with electromagnetic radiation (here infrared (IR) radiation). The transition energy of most molecular vibrations falls within the infrared region of the electromagnetic spectrum, which can therefore be detected in an infrared spectrum .Fourier transform infrared (FTIR) is one of the important analytical techniques. This type of analysis can be used for characterizing samples in the forms of liquids, solutions, pastes, powders, films, fibers, and gases. This analysis is also possible for analyzing material on the surfaces of substrate . Compared to other types of characterization analysis, FTIR is quite popular. This characterization analysis is quite rapid, good in accuracy, and relatively sensitive [57].

In the FTIR analysis procedure, samples are subjected to contact with IR radiation. The IR radiations then have impacts on the atomic vibrations of a molecule in the sample, resulting the specific absorption and/or transmission of energy. This makes the FTIR useful for determining specific molecular vibrations contained in the sample Infrared spectroscopy detects the vibration characteristics of chemical functional groups in a sample. When an infrared light interacts with the matter, chemical bonds will stretch, contract and bend. As a result, a chemical functional group tends to adsorb infrared radiation in a specific wavenumber range regardless of the structure of the rest of the molecule [58]. Modern infrared spectrophotometers analyze light of all chosen wavelengths at the same time. This is done by use of Fourier transformation, and this spectroscopy method is thus called FTIR. The key component of an FTIR instrument is the interferometer [59]. The basic construction of an interferometer is illustrated in figure (2.1).

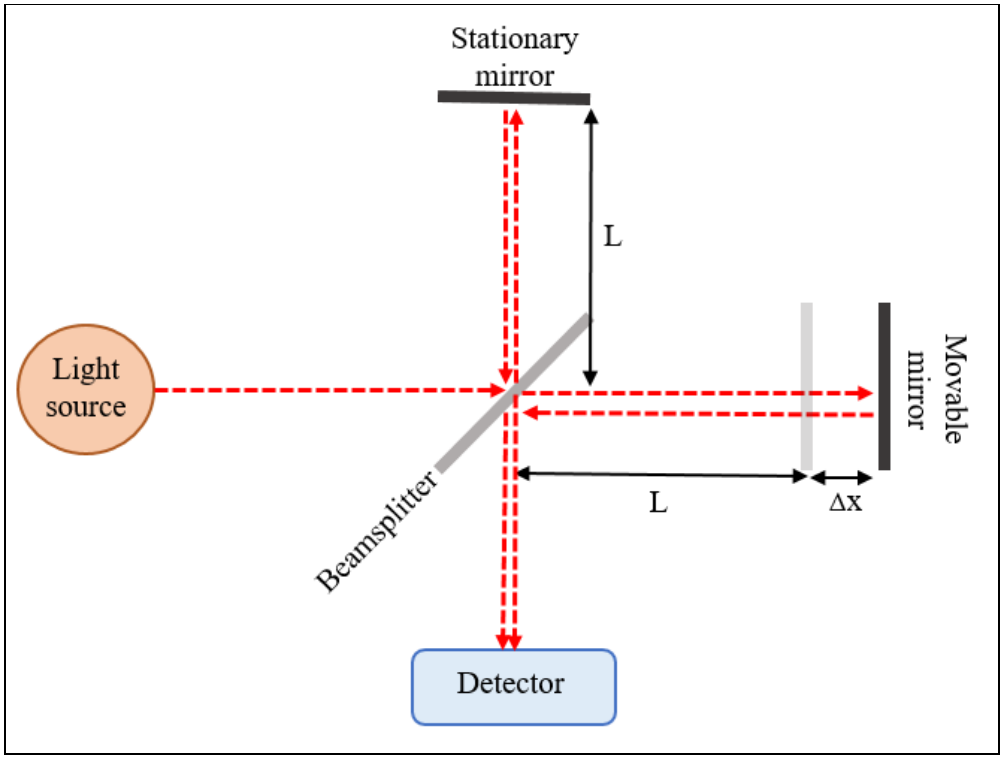

Figure (2.1) Basic construction of an interferometer [60].

In the interferometer, radiation from an infrared light source hits a beam splitter. Approximately 50% of the light is reflected towards a stationary mirror. When it hits the mirror, it will have travelled a length of *L* from the beam splitter. The other 50% of the light is transmitted towards a movable mirror. This beam will travel a

distance. The difference in travelled path length between the two beams will be $2\Delta x$ when they meet in the beam splitter. This difference is called the retardation. As the mirror moves back and forth, the retardation is changing. This will lead to a pattern of constructive and destructive interference. A plot of light intensity, measured by the detector, against the retardation is called an inter fogram. A computer transforms the inter fogram into a plot of absorbance against wavenumber by Fourier transformation. Since light of all wavenumbers are investigated at once, the analysis only takes a few seconds. The main idea gained from the FTIR analysis is to understand what the meaning of the FTIR spectrum. The spectrum can result "absorption versus wavenumber" or "transmission versus wavenumber" data . The IR spectrum is divided into three wavenumber regions: far-IR spectrum (<400 cm^{-1}), mid-IR spectrum (400-4000 cm^{-1}), and near-IR spectrum (4000-13000 cm^{-1}). The mid-IR spectrum is the most widely used in the sample analysis, but far- and near-IR spectrum also contribute in providing information about the samples analyzed [60].

The mid-IR spectrum (400-4000 cm^{-1}) can roughly be divided into four ranges. The first is the high-frequency area (4000-2400 cm^{-1}) where the stretching vibrations of single bonds O-H, C-H and N-H occur. The second area (2400-1900 cm^{-1}) is where triple bonds have stretching frequencies. The double bonds (stretching) and the single bond of N-H (bending) have vibration frequencies in the third area (1900-1500 cm^{-1}). The last area (1500-400 cm^{-1}), which is called the fingerprint area, contains frequencies of most of the bending and stretching vibrations of some single bonds. The fingerprint area contains complex absorption patterns and each molecule has its own characteristic fingerprint area. The absorption peaks in the region above 1500 cm^{-1} are distinct and may be used for identification of the functional groups in the molecule [61].

2-3 The Optical Properties

The discipline of nano optics, which focuses on how light interacts with nanoscale particles, has grown significantly recently. Materials with fascinating features, particularly optical properties, include metals, semiconductors, dielectrics, and polymers on the nanoscale scale. Innovative techniques to create thin film coatings have attracted a lot of interest among the many uses. To create materials with adjustable refractive indices and improved

optical qualities, nanocomposite has been developed [62].The interaction of light with a substance has to be given more attention, both in depth and detail. Three basic outcomes are conceivable when light interacts with a substance: absorption, transmission, and reflection of light. In comparison to bulk materials, the nanoparticles have higher specific surface area, surface energy, and density. Thus, adding nanoparticles at even lower filler loadings will have a significant impact on the matrix's physical, thermal, and mechanical characteristics [63]. When coupled with polymers, nanomaterials have improved mechanical and optical characteristics (such as refractive index and coefficient of absorption) and are used in optical sensors, light-emitting diodes, solar cells, polarizers, and light-stable color filters. New properties like light emission are also brought forth by [64]. For use in UV filters, bio imaging, photo thermal treatments, oxygen sensors, and other applications, nanoparticles' optical characteristics have been studied [65].

2-3-1 Light Absorbance and Electronics Transitions

The total energy for molecular can be divided into electronic (Eele) , vibration (Evib) , translation (Etrans) and rotational energy (Erot). The light absorbance leads to changing in molecular energy as a result to change of other energies. As following[66].

$$\Delta E_T = \Delta E_{ele} + \Delta E_{rot} + \Delta E_{trans} + \Delta E_{vib} \quad (2.1)$$

Ultra violet and visible light are the electronics absorbance. The reaction between molecular and photon leads to electric field to excitement the electronic structure of molecular where the photon disappear and the molecular trans to excited state.

2-3-1-1 Direct Transitions

In semiconductors, this transformation occurs when the (C.B) base is exactly above the top (V.B). This implies that the wave vector has the same value ($\Delta k=0$). The absorption occurs in this condition ($h\upsilon = Eg^{opt}$). This form of transition calls for energy and momentum conservation laws. There are two forms for direct transitions. [67]

a) Direct allowed transition

It occurs from the top (V.B) points and the bottom (C.B), as seen in the figure (2.2-a).

b) Direct forbidden transitions

As given in this figure (2.2-b), this transition occurs between the close high points of (V.B) and the lower points of (C.B) [68]. For this transition form, the absorption coefficient is indicated:

$$\alpha h\upsilon = B\,(h\upsilon - Eg^{opt})^{r} \qquad (2.2)$$

Where: Eg^{opt} . energy gap between direct transition.

α: is the absorption coefficient.

B: constant depended on type of material.

h: is the Planck's constant.

υ: is the photon frequency. r: exponential constant, its value depended on type of transition.

r =1/2 for the allowed direct transition.

r =3/2 for the forbidden direct transition

2-3-1-2 Indirect Transitions

In the curve (E-K), in these transitions the bottom (C.B.) is not above the top of (V.B.) The electron transits between (V.B.) and (C.B.) are not perpendicular if the magnitude of the electron's wave vector is not identical before and after transfer. This kind of transformation occurs with the beneficial "Phonon" particle for energy conservation and energy law. Two kinds of indirect transitions exist [69].

c)Allowed indirect transitions:

These transitions occur between the top of the (V.B.) and the bottom of (k space), as shown in figure (2.2-c) (C.B).

d) Forbidden indirect transitions

As shown in the figure, such transitions occur between points near the top of (V.B.) and points near the bottom of (C.B) [70]. (2.2-d). The coefficient of transition absorption is denoted by Phonon on absorption:

$$ah\upsilon = B(h\upsilon - Eg^{opt} \pm E_{ph})^{r} \quad (2.3)$$

Where: E_{ph} : Phonon energy :

(-) is absorbed by phonon, and

(+) is emitted by phonon. (r = 2) for the allowed indirect transitions (r = 3) for the forbidden indirect transitions

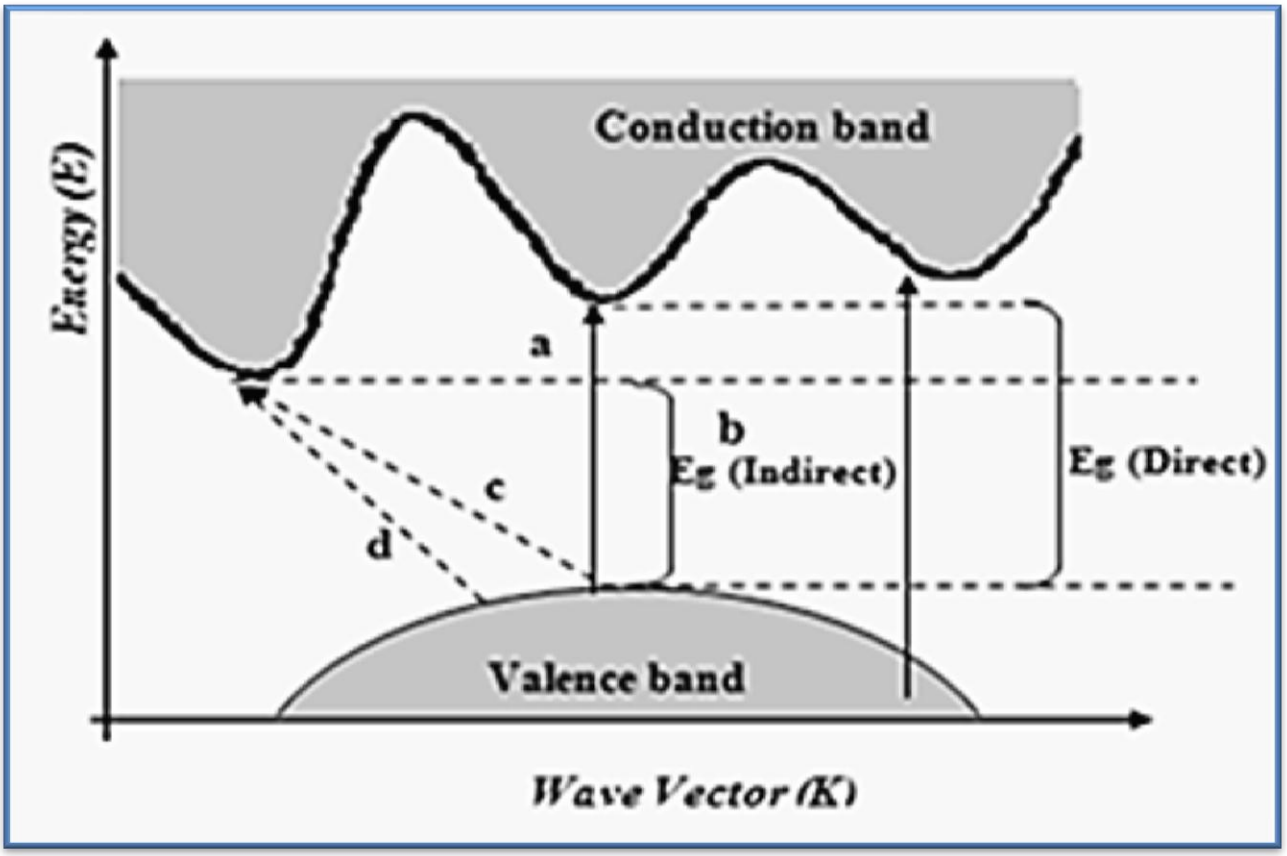

Figure (2-2) The electronic transitions types of (a) allowed direct, (b) forbidden Direct Transition, (c) allowed indirect and d) forbidden indirect transitions [71].

2-3-2 Absorbance (A)

The intensity of the absorbed light (I_a) by the material to the incident intensity of light (I_o) as a ratio is defined as absorbance that is giving in the following equation [72].

$$A = \frac{I_a}{I_o} \quad (2.4)$$

2-3-3 Transmittance (T)

Transmittance (T) is given by ratio of the intensity of the transmitting rays (I_T) through the film to the intensity of the incident rays (I_o) on it as follows [73]

$$T=I_T/I_\circ \quad (2.5)$$

2-3-4 Reflectance (R)

Reflectance is defined as fraction of light reflected at an interface[74]

$$R=I_R / I_\circ \quad (2.6)$$

Where (I_R) are the reflected beam intensity

We can obtained reflectance from absorbance and transmittance spectrum in according to the law of conservation of energy by the equation[75].

$$R+T+A=1 \quad (2.7)$$

2-3-5 Absorption Coefficient (α)

Absorption coefficient is defined as a ratio decrement in flux of incident rays energy relative to the distance unit in the direction of incident wave diffusion. Absorption coefficient (α) depends on incident photon energy (hυ) and on semiconductor characteristics (n or p) type, where electronic transitions type (n) or (p) and forbidden energy gap. Photon energy is given by the following equation [76].

$E = h\upsilon$ When incident photon energy is less than forbidden energy gap, then photon will be transmitted, and transmittance gives the following equation [77]

$$T= (1-R)^2 \exp (- \alpha d) \quad (2.8)$$

Where : T is transmittance, R : is the reflectance.

If the light of intensity (Io) incident on the film of thickness (d), the transmitted intensity (I_T) can be given as [78].

$$I_T = I_o \exp (- \alpha d) \quad (2.9)$$

$I_T / I_o = \exp(-\alpha d)$ (2.10)

where : $T = I_T / I_o$

$T = \exp(-\alpha d)$ (2.11)

$1/T = \exp(\alpha d)$ (2.12)

Then:

$\alpha d = 2.303 \log (I_o / I_T)$ (2.13)

But $A = \log (I_o / I_T)$

$\alpha d = 2.303 \times A$ (2.14)

Then:

$\alpha = (2.303 \times A) / d$ (2.15)

Where: d is the sample thickness in cm , A is the absorption of the material.

2-3-6 Extinction Coefficient (k)

The extinction coefficient represents the amount of attenuation of an electromagnetic wave that is traveling in a material, where it values depends on the density of free electrons in the material and also on the structure nature, this coefficient can be calculated by using the following equation [79].

$k=\alpha\lambda/4\pi$ (2.16)

It can be noted that (k) has same behavior of absorption coefficient, absorption coefficient has a direct related with (k) as in the above equation [80].

2-3-7 Refractive Index (n)

Refractive index (n) represents the ratio of the light speed in space (c) to the light speed inside the material (v). Equation (2-17) gives the law which used to calculate the refractive index [81].

$$n=\left(\frac{4R-K^2}{(R-1)^2}\right)^{1/2}-\frac{(R+1)}{(R-1)} \quad (2.17)$$

Complex refractive index (n^*) can be written as following:

$$n^* = n - iK \quad (2.18)$$

Where, n is the real part of refractive index. (k) it is the extinction coefficient represents the imaginary part. (n^*)it is a complex number represent the complex refractive index that depends on several characteristic factors such as crystal defect and crystal structure [82].

2-3-8 Dielectric Constant (ε)

The dielectric constant (ε) is defined as the ratio of the electric permeability of the material to the electric permeability of free space. The dielectric constant is generally a complex number which describes the interaction of a material with an electric field:

$$\varepsilon = \varepsilon_1 - i\varepsilon_2 \quad (2.19)$$

Where (ε_1) is a real part of the dielectric constant , (ε_2) is an imaginary part of the dielectric constant.

The real part of the complex dielectric constant (ε_1) is a measure of how much energy from an external field is stored in a material.

The imaginary part of the complex dielectric constant (ε_2) is a measure of how dissipative or lossy a material is to an external field [83].

The dielectric constant (ε) is not constant by changing either the frequency or the temperature [84].

The relation between the complex dielectric constant (ε) and the complex refractive index (n^*) is expressed by [85].

$$\varepsilon = (n^*)^2 \quad (2.20)$$

It can be concluded that

$$\varepsilon_1 - i\varepsilon_2 = (n - iK)^2 \quad (2.21)$$

The real and imaginary parts of the dielectric constant thus related to (n) and (K) values and can be calculated using the following formulas [85].

$$\varepsilon_1 = n^2 - K^2 \qquad (2.22)$$

and

$$\varepsilon_2 = 2nK \qquad (2.23)$$

2-3-9 Fundamental Absorption Edge

1.High Absorption Region: Direct electron transitions occur in this region.an absorption coefficient with a value higher than or equal to 10^4 cm^{-1}.

2.Exponential Region: it is represent the transition between extended levels in valence band to localize levels in conduction band. Also from localize levels in top valence band to extended levels in bottom conduction band. The magnitude of absorption coefficient between ($1<\alpha<10^4$) cm^{-1}.

3.Low Absorption Region: the electron transitions in this region attribute to density as a result of structure defects. The magnitude of absorption coefficient is very small ($\alpha<1cm^{-1}$). Figure (2-3) which shows the absorption regions[86]

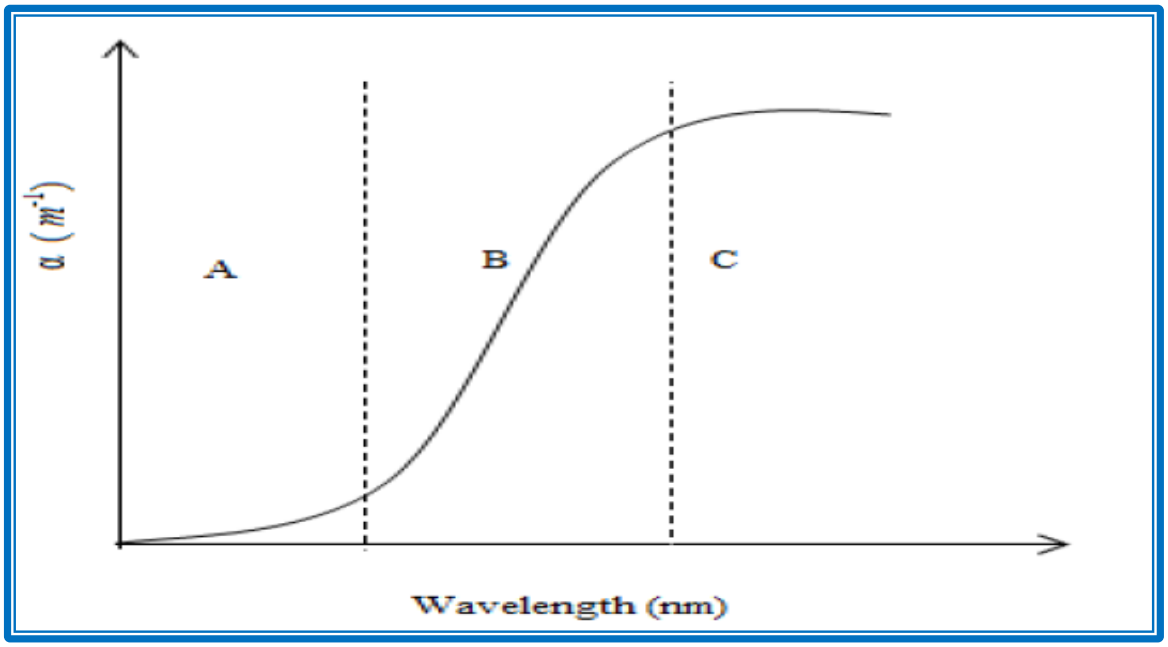

Figure (2-3) Typical absorption spectra for materials [86]

2-3-10 Optical Conductivity

The Optical Conductivity was calculated using the relation[87].

$$\sigma_{opt} = \alpha nc/4\pi \quad (2.24)$$

c:the velocity of light.

2-4 The A.C Electrical Properties

Due to their unusual characteristics, such as low density, the ability to create complicated structures, flexible electrical properties, and inexpensive manufacturing costs, polymers are receiving a lot of interest from scientists, engineers, and industrials [88].The most practical and effective techniques for examining the structure of polymers are dielectric constant and loss factors [89]. A specific conductive filler can be included into insulating polymer materials to increase their electrical conductivity . The dielectric constant value becomes equal to its value in a static field when an insulator is placed in a low-frequency electrical field where induced or permanent electrical dipoles can move along with the variation of the applied electrical field without leaving any residue, making the insulator ideal (ohmic conductivity equals to zero). On the other hand, a complex dielectric constant will exist when the electric field's frequency is higher and the electric polarization is frequency-dependent .The definition of the dielectric constant is "the ratio of the capacitance of a capacitor containing an insulator material between its conducting plates to the capacitance of a capacitor of the same size with a vacuum between the Insulator plates" . When an alternating potential is put across a capacitor, the current can flow through the device because the insulator-filled capacitor is ahead of the potential by a phase of $\pi/2$ [90].

$$I = j\omega c v_m \quad (2.25)$$

ω, means the applied filed angular frequency ($\omega=2\pi f$), j, means the number of imaginary and equal to $\sqrt{-1}$, C, means capacitance of a capacitor and $V_{m,}$ means the maximum voltage.

The angle between electric current and voltage is less than $\pi/2$, as illustrated in figure (2-4 B). The sum of the conduction current (I_p) is considered the electric current. This is in the same phase with voltage and the capacitates

current (I_q) with a phase difference of ($\pi/2$). The current is symbolized using the equation (2.26):

$$I = I_P + jI_q \quad (2.26)$$

The capacitance of a capacitor constructed of two parallel plates is given by the equation[91].

$$C = \varepsilon \varepsilon_o \, {}^{bL}/_{t} \quad (2.27)$$

When, equation (2.27) substituted in relation (2.25), we get

$$I = j\varepsilon \varepsilon_o VL. \, {}^{b}/_{t} \quad (2.28)$$

The permittivity (ε) is a complex quantity. The permittivity is formed from the real and imaginary parts, as mentioned in equation (2.29).

$$\varepsilon = \varepsilon' - j\varepsilon'' \quad (2.29)$$

ε" = Dielectric loss and ε'= dielectric constant, it's become.

$$I = j\omega \varepsilon_o (\varepsilon' - \varepsilon'') \, {}^{bL}/_{t} \quad (2.30)$$

By comparing equation 2.26 with 2.30, then:

$$I_P = V \omega \varepsilon'' \varepsilon \varepsilon_{\circ} \, {}^{bL}/_{t} \quad (2.31)$$

$$I_q = V \omega \varepsilon' \varepsilon_O \, {}^{bL}/_{t} \quad (2.32)$$

ω : Angular frequency

Figure (2-4 B) shows that the loss factor is:

$$\tan \delta = \frac{I_P}{I_q} = \frac{\varepsilon''}{\varepsilon'} \quad (2.33)$$

I_p = conduction current, I_q = capacitate current

Where, in the insulator, this represents the transformed the lost electrical energy to the thermal energy. At high frequencies, excessive power factor could result in heat in the insulator at high frequencies [92].

At low frequencies, the ideal capacitor when connecting with a resistance R_p in parallel is can be represented capacitor C [93].

$$I = I_P + jI_q = \frac{v}{R_P} + j\omega C_P v \qquad (2.34)$$

Hence, get the impedance:

$$\frac{1}{Z} = \frac{1}{R_P} + j\omega C_q \qquad (2.35)$$

From the relations (2.31, 2.32 and 2.34), the following equation can be written:

$$R_P = \frac{t}{\omega \varepsilon'' \varepsilon_o L.b} \qquad (2.36)$$

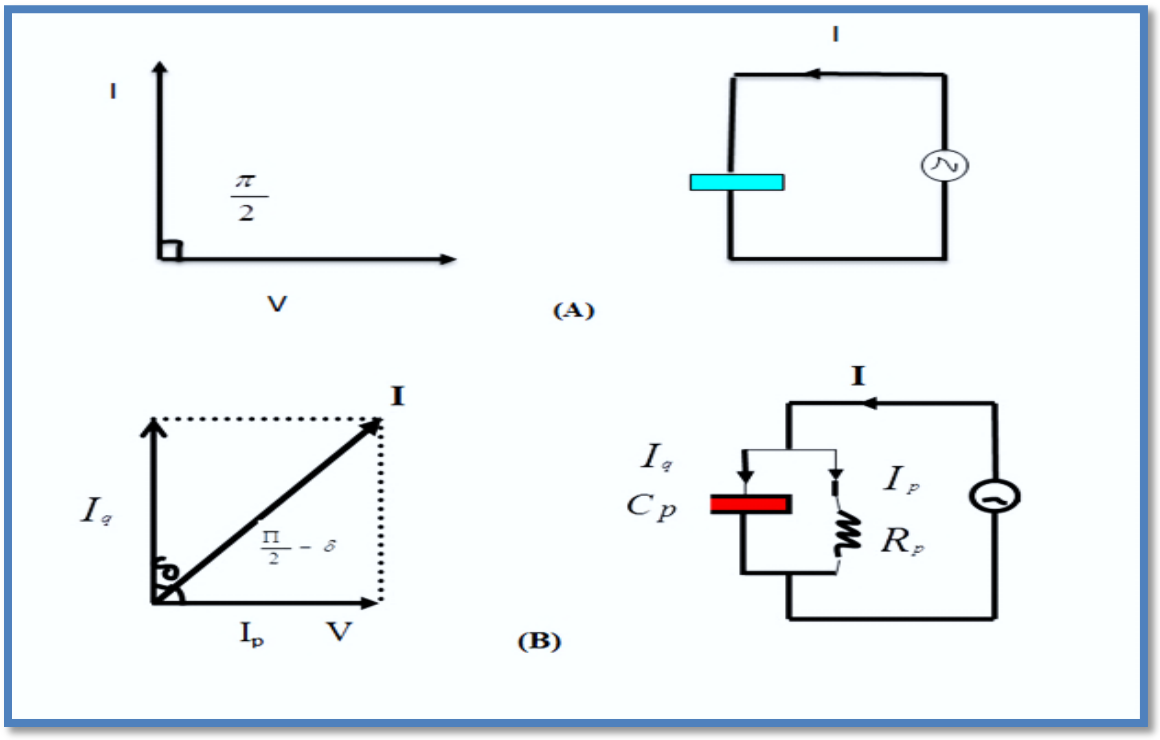

Figure (2-4) The circuit equivalent of (A) ideal capacitor and (B) non- ideal capacitor [94]

$$\varepsilon'' = \frac{1}{\omega R_P C_O} \quad (2.37)$$

$$C_P = \varepsilon' \varepsilon_0 \frac{L.b}{\omega R_P C_O} \quad (2.38)$$

$$\varepsilon' = \frac{C_P}{C_0} \quad (2.39)$$

C_p and C_o mean the capacitor having an insulator material and vacuum, respectively .The alternating conductivity is a function that used to the existence of alternating potential that could represent the dissipated power in the insulator, as could using the equation (2.36) to represent it[95].

$$\sigma_{AC} = w\varepsilon_o\varepsilon'' \quad (2.40)$$

In the insulating material, σ_{AC} has represented the calculation of the generated temperature that is resulted from the rotation of the dipole in their positions, as a result of the field alternating [96].

2.4.1 The Electrical Polarization

Electrical polarization is the phenomenon in which the centers of positively and negatively charged particles do not line up. When a dielectric material is subjected to an electrical field, this often happens [97]. A local shift in positively and negatively charged centers happens when electrical fields are given to a condenser terminal with an electrical insulator between its surfaces. This movement in charge is what causes the electrical polarity to change. According to this quantity, which equates to the sum of all the moments in the sample's unit volume (dipoles)[98].

$$\mu_e = P_m E_i^- \quad (2.41)$$

μe means the moment of the electrical dipole, P_m means the polarity of molecule or atom E_i^- means the molecule internal field that is proportional to the external field. Where, for a unit volume, the total dipole moment P is:

$$P = N_o \mu_e \quad (2.40)$$

N_o means the number of molecules for a unit per volume.

The polarization of electrical occurs in all insulators for the reason that of impurities, atoms, molecules and ions that have either charges to be negative or positive [99]. The effect of an electrical field lead to present the electrical polarization that can calculate form the following relation [100]:

$$P = D - \varepsilon_o E \quad (2.38)$$

D means the displacement of the electrical, E means field intensity of the electrical and ε_0 means the free space or vacuum permittivity (8.85×10^{-12} F/m) [101].

$$D = P + \varepsilon_o E = \varepsilon_o \varepsilon' E \quad (2.39)$$

Despite

$$\therefore \varepsilon' = \frac{D}{\varepsilon_o E} \quad (2.40)$$

And

$$\because \varepsilon' = 1 + \frac{P}{\varepsilon_o E} \quad (2.41)$$

where ε' represented the constant of the dielectric.

The equation of the Clausius Mossotti explains the relative between the constant of dielectric with the polarizability for a volume per unit [102].

$$\frac{N_o P}{3\varepsilon_o} = \frac{\varepsilon' - 1}{\varepsilon' + 2} \quad (2.42)$$

this equation can be applied to ionic crystals and non-polar electric insulators[103].

2-5 Types of Electrical Polarization

A. Electronic Polarization (P_e)

This opposite type of polarization is caused by distortion in the charge distribution that occurs when an external electric field is projected. What is happening here is the effect of the nucleus and the electrons with two opposing forces in the direction that work to displace the nucleus towards the electric field and the electrons in the direction, This produces induced polar diodes as seen, in

figure (2.5.a). That this polarization occurs in all materials regardless of the appearance of other types of polarization, and that it occurs during a very small period (10^{-15} s). It is also called optical polarization because its effect is visible at high frequencies (optical frequencies) and does not depend on temperature [104,105].

B. Ionic Polarization (P_i)

It is generated in the ionic compound that possesses the ionic character and occurs when the material falls under the influence of an electric field, resulting in the displacement of the negative and positive ion from each other within the molecule and as a result of this, it creates a bipolar moment in the molecule that was not previously found in the form of (2.5.b). It takes a short period of time to reach (10^{-13} s), that is, what corresponds to the frequency in the infrared(IR) region of the spectrum, after which the polarization effect begins to diminish when the frequency exceeds (10^{14} Hz) as the ions cannot follow the rapid change of the field dominated at these frequencies and thus a decrease in the polarization value occurs. As shown in Figure (2-5), this polarization depends on little temperature [106].

C. Orientation Polarization (P_0)

Rotational polarization occurs only in materials whose molecules have a permanent diode (Permanent Dipole moment), even in the absence of the electric field and called polar molecules, though, the polarization result is equal to zero because the molecular moments are random in directions, which leads to the cancellation of each other [107], but when an electric field is shed on these materials, the polar diodes revolve around their axis and are arranged toward the field as in the form that presented in Figure (2.5.c), it is known that when the temperature increases, it becomes more difficult to control the orientation of the particles by the electric field. Accordingly, the directional polarization is highly dependent on the temperature and this polarization occurs in a rather large period of time [108].

D. Interfacial Polarization (P_d)

This type of polarization occurs in the materials as a result of containing impurities, space, or a structural defect, as a group of opposite charges is produced on both ends of the impurity, and this is the emergence of polar diodes in the atom or molecule or areas of the atom that presented in Figure (2.5.d). The amount of homogeneity of the material and the percentage of its defects or impurities, and its effect appears in radio frequencies are determined by the polarization. It extends to subsonic frequencies (f) depending on the type of defect that causes this polarization [109].

Thus, the total polarization of the material is.

$$P=P_e+ P_i + P_o+ P_d \qquad (2.43)$$

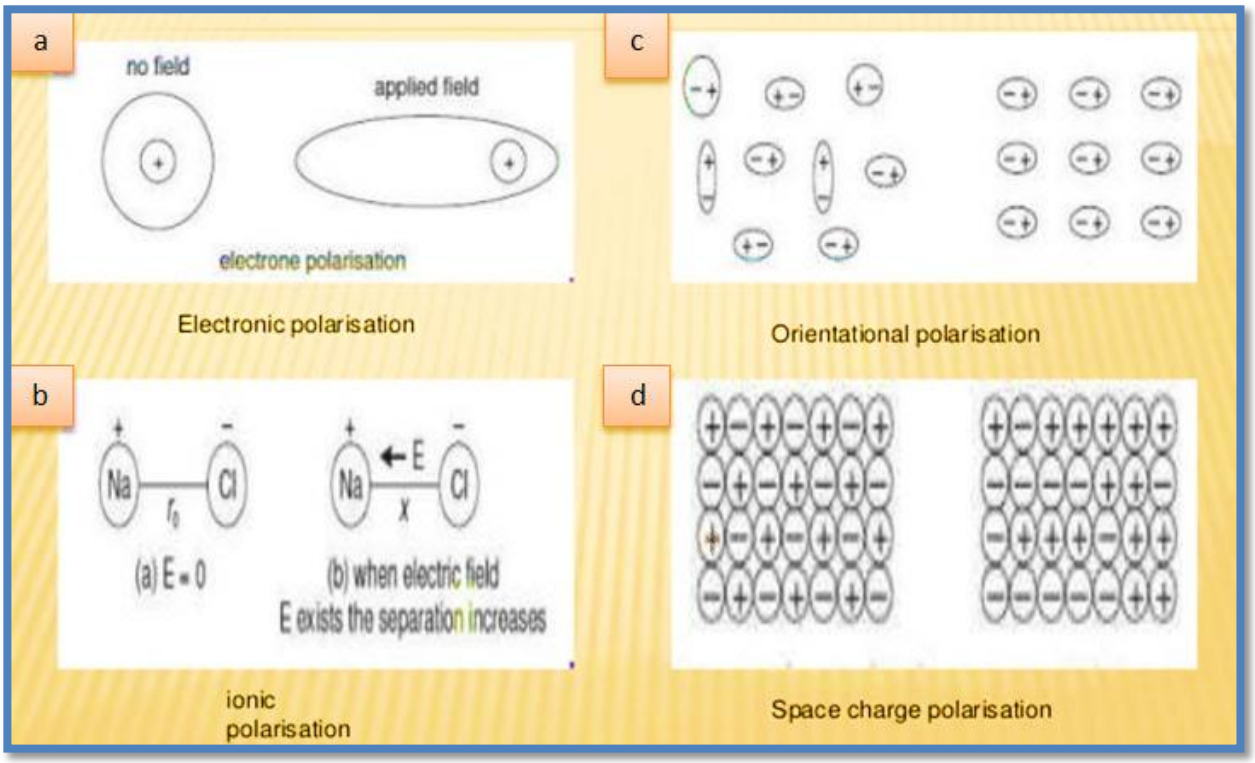

Figure (2-5) schematic representation of different types of polarization of (a) electrical polarization, (b) ionic polarization, (c) orientational polarization and (d) space charge or interfacial polarization [110].

2-6 Antibacterial Effect Systems

Antibiotics often lose their effectiveness over time due to the emergence and spread of drug resistance by bacterial pathogens, which leads to the generation of the so-called “antibiotic resistance crisis” and infections in addition to the huge amounts of medical costs that may reach billions of dollars annually[111].Particles and nanomaterials have become the global platform for many therapeutic applications because of the unique physical and chemical properties of these materials and provide treatment for drug-resistant bacteria. The antibacterial activity of multiple nanomaterials is expected to play an important and alternative role for other antibacterial agents[112]. The important and unique properties of some nanomaterials such as changing their size or shape, surface properties, optical properties, low cell toxicity, and high stability make them attractive in many fields of medicine. Because of those qualities and properties that characterize some of these nanomaterials, they have anti-fungal and anti-bacterial activity, so nanomaterials can be combined with other certain biological materials to transfer anti-bacterial properties to the material, thus improving the value of that material and its applications[113].The nanoparticles are attached to the antibacterial drugs via covalent or non-covalent bonds whereby the antibacterial drugs reach the site of action effectively[114]. When bacteria are active in the affected sites in the body, whether on the skin or in the intestines, the rates of secretion of their output and waste naturally increase, which increases the acidity of the medium in it; It drops below 5 degrees, and the more you activate the degree more, and therefore this medium is ideal for changing the charge of the nanocomposite from negative to positive, only when the body has a bacterial infection, and this is what is required, and then attraction occurs between the nanocomposite and the cell membrane of bacteria cells to eliminate therefore. This process also ensures that the compound is not attracted to healthy cells, as long as there are no bacteria in the medium, which makes it biologically safe [115].

2-7 Pressure Sensors

Sensor technology is one of the widely used technologies for applications in the industry and medicine. It can be used to measure pressure, temperature, quality, and amount of energy, and to monitor health. Various types of sensors have been fabricated from polymer matrices such as pressure , thermal/infrared , vapor,

humidity , gas , electrical , and temperature/thermal sensor[116] . resistive ,capacitive, optical and thermal conductivity have been proposed and examined , low response time, high sensitivity, repeatability, reversibility and noise immunity are required. pressure is one of the most important physical quantities in our environment. Pressure is a significant parameter in such varied disciplines as thermodynamics, aerodynamics, acoustics, fluid mechanics, soil mechanics and biophysics. As an example of important industrial applications of pressure measurement we may consider power engineering. Hydroelectric**,** thermal, nuclear, wind and other plants generating mechanical, thermal or electrical energy require the constant monitoring and control of pressures . pressure enters into the control and operation of manufacturing units that are automated or operated by human operators . All these activities require instrument chains in which the first element is the pressure sensor [117].

2-8 Gamma Ray Shielding

Depending on distance and time, there are some fundamental principles for radiation protection. The type and quantity of shielding needed depending on the type of radiation, radiation source activity, and dose rate. However, there are other factors such as their cost and weight for the choice of shielding material. A good shield leads to a large energy loss at a small penetration distance without radiation emission [118]. There have been several experimental and theoretical work on radiation protection that has wide different application areas with different materials (e.g. concrete, polymer, etc.) [119].

A study of radiation absorption from gamma and neutron is an important subject in the field of radiation physics. For example, most of the previous studies focused on photon attenuation coefficients . There are two main radiation protection methods. First, protective materials are furnished on or directly inside the wall surface . Secondly, these materials are covered by the source of radiation. Any radiation shielding material can be used if it is thick enough to absorb incident radiation to a safe level. In the field of protective materials and the design of some research, various types of glass have been reported as new protective materials .With the use of active gamma-ray isotopes in industry, agriculture and medicine, researching the attenuation index of different materials

has become significant both biologically and technologically .The following equation shows the properties of the radiation attenuation[120].

$$N= N_0 \exp(-\mu x) \quad (2.22)$$

Where (N_0) represents the number of radiation particles counted at a given time. The period shall be without any absorber. (μ) is the attenuation coefficient of gamma radiation. (N) is the amount of counted radiation particles at the same time, with the thickness of the sampled [121].

3-1 Introduction

This part involves the steps of samples preparation for PEO-PVA-$SrTiO_3$-NiO and PEO-PVA-$SrTiO_3$-CoO NCs, samples tests and measurements steps such as: optical microscopic , scanning electron microscope (SEM), Fourier transformation infrared radiation (FTIR) , optical measurements (A.C electrical measurements), antibacterial activity pressure sensors and gamma ray shielding applications.

3-2 The materials used in this work

3-2-1 Polymers

Two polymers are used in this work:

A) Poly ethylene oxide (PEO)

The white material PEO and a semi-crystalline polymer are used Panveac Spain company with high purity (99.8%)

B)Polyvinyl alcohol (PVA)

Used as powder form and could be obtained from Panveac Spain company with high purity (99.8%).

3-2-2 Metals Oxides Nanoparticles

A) Strontium Titanate ($SrTiO_3$)

It was got as powder with particle diameter (30-45) nm cubic phase from Research Nanomaterials USA Company and high purity (99.95%).

B) Nickel Oxide (NiO)

It was got as powder with particle diameter (15-35)nm from Research Nanomaterials USA Company and high purity (99. 5%)

C) Cobalt Oxide(CoO)

It was got as powder with particle diameter (20-50)nm from Research Nanomaterials USA Company and high purity (99. 5%).

3-3 Preparation of PEO-PVA-$SrTiO_3$-NiO and PEO-PVA-$SrTiO_3$-CoO Nanocomposites

Polyvinyl alcohol, polyethylene oxide, and nanocomposite films composed of strontium, titanium, and cobalt were made using a casting technique, which involved dissolving 1 gram of PEO and PVA (50/50) in 40 mL of distilled water using a magnetic stirrer for 45 minutes at a temperature of 70 °C. to make a more consistent solution. Nanoparticles of strontium-titanium and nickel oxide were introduced into the polymer mixture to prepare PEO-PVA-SrTiO3-NiO nanocomposites. On the other hand, add strontium-titanium and cobalt oxide to prepare PEO-PVA-SrTiO3-CoO nanocomposites in different concentrations (0.1, 2, 3 and 4) wt%. When the solution was dried for 4 days at room temperature, PEO-PVA-SrTiO3-NiO and PEO-PVA-SrTiO3-CoO NC polymer nanocomposites were formed and the solution was poured into a petri dish and used for measurement. Samples thickness around (16 ± 2) μm Structural, optical and AC properties, of PEO-PVA-SrTiO3-NiO and PEO-PVA-SrTiO3-CoO NCs. Figure (3-1) shows the schematic diagram of the experimental work

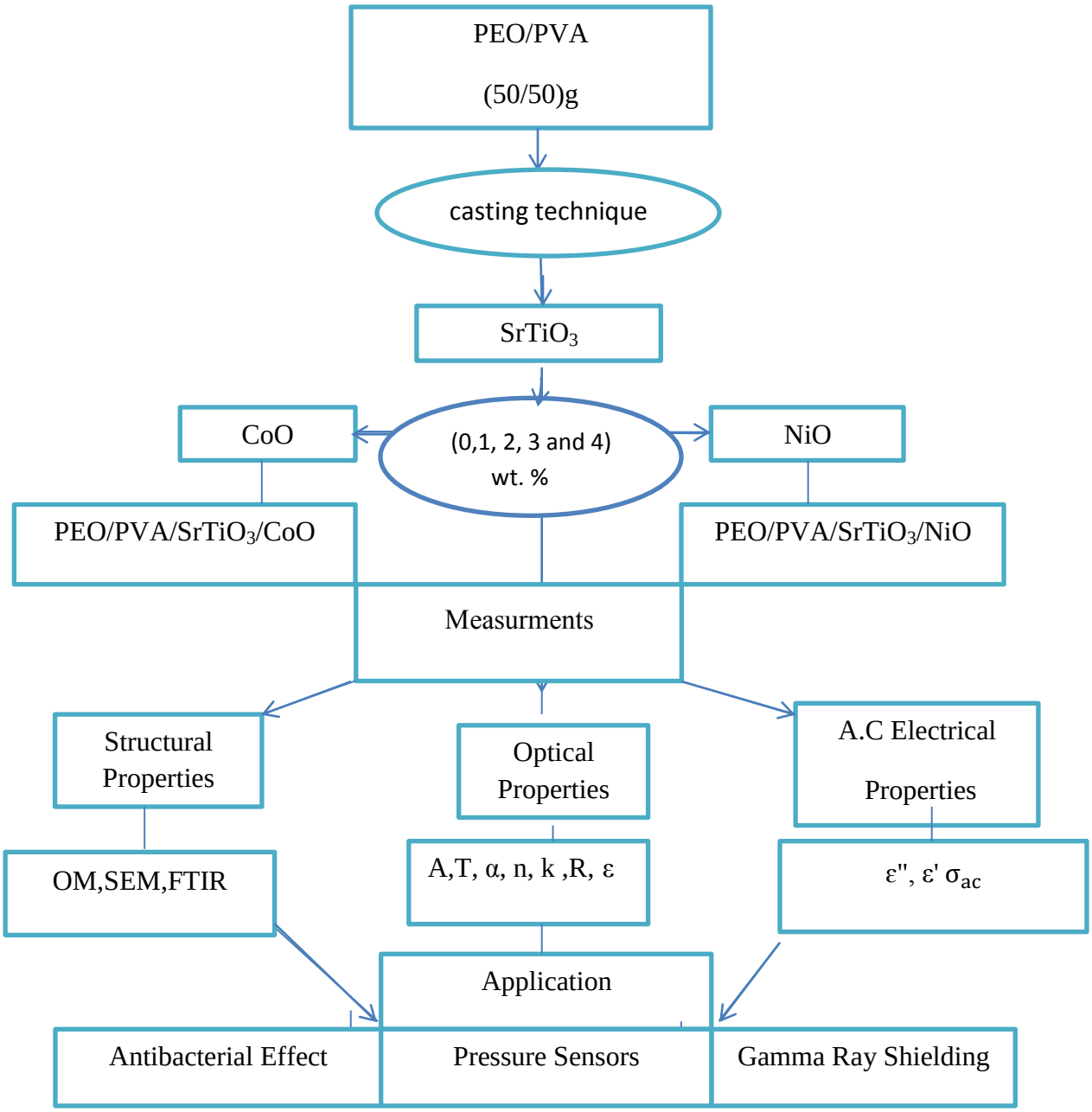

Figure (3-1) Scheme of experimental part

3-4 Structural Properties for PEO-PVA-$SrTiO_3$-NiO and PEO-PVA-$SrTiO_3$-CoO NCs

3-4-1 Optical Microscopic Investigation

PEO-PVA-$SrTiO_3$-NiO and PEO-PVA-$SrTiO_3$-CoO nanocomposite samples were examined using a light microscope (provided by Olympus (ToupView) type (Nikon- 73346) at University of Babylon/College of Education for Pure Sciences with magnification (x10) .

3-4-2 Scanning Electron Microscope (SEM)

The scanning electron microscope (SEM) is an electron microscope that images the sample surface by scanning it with a high -energy beam of electrons in a raster scan pattern .The specimens for an SEM testing must be electrically conductive, at least at the surface, and electrically grounded to prevent the accumulation of electrostatic charge at the surface. Small part of ($1cm^2$) was taken from the sample to examine it by SEM. In this work low vacuum scanning electron microscope was used. The surface morphology of PEO-PVA-$SrTiO_3$-NiO and PEO-PVA-$SrTiO_3$-CoO NCs was observed using Tescan mira3 SEM microscope. is equipped with dual Bruker Flash EDS detectors and Bruker Flash HD EBSD(Czech Tescan Instrument Co.) for analytical studies at the University of Tehran .The advantage was observed using this technique (Low vacuum SE detecto) is beam deceleration technology (BDT) for high resolution imaging and high surface sensitivity at very low kv and variable pressure operation, fully integrated active anti-vibration system. as shown by diagram SEM in figure (3-2).

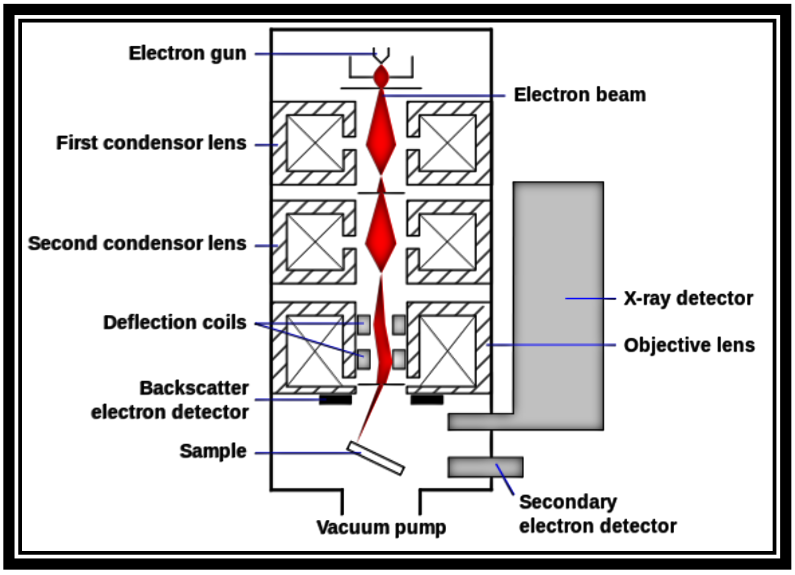

Figure (3-2) Diagram SEM device.

3-4-3 Fourier Transforms Infrared Spectrometer

FTIR spectra for PEO-PVA-$SrTiO_3$-NiO and PEO-PVA-$SrTiO_3$-CoO NCs ere detailed by FTIR (Bruker company, German origin, type vertex-70) at University of Babylon, College of Education for Pure Sciences. The FTIR spectrometer is in the wavenumber range (400 – 4000)cm^{-1}

Figure (3-3) Fourier transform infrared (FTIR) spectroscopy device .

3-5 Measurement of A.C Electrical Conductivity for PEO-PVA-$SrTiO_3$-NiO and PEO-PVA-$SrTiO_3$-CoO NCs

The A.C electrical properties have been measured by LCR meter type (HIOKI 3532-50 LCR Hi TESTER (Japan)).It is found in University of Babylon, College of Education for Pure Sciences/Department of physics, as shown in figure (3-4). Only (1cm) from each one of the samples have been taken and put between two electrodes and at different frequencies from (100Hz-5MHz) at room temperature which shows a diagram of A.C circuit. The capacity and dissipated factor have been recorded for all samples.

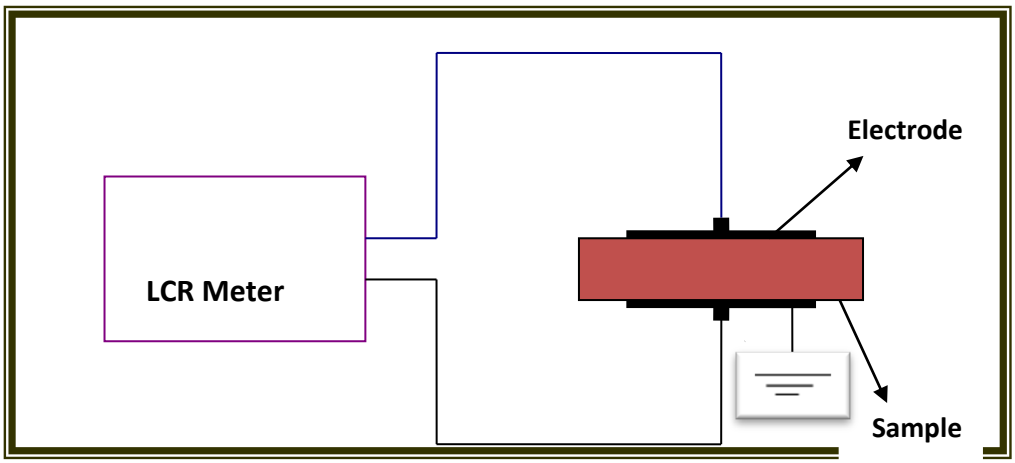

Figure (3-4) Schematic diagram for A.C electrical properties measurement

3-6 Optical Properties Measurements for PEO-PVA-$SrTiO_3$-NiO and PEO-PVA-$SrTiO_3$-CoO NCs

The optical properties of PEO-PVA-$SrTiO_3$-NiO and PEO-PVA-$SrTiO_3$-CoO NCs the absorption spectrum films have been recorded in the wavelength range (200-800) nm by using the double beam spectrophotometer (Shimadzu model UV-1800 Ao (JAPAN) as shown in figure (3-5). It found in University of Babylon /College of Education for Pure Sciences/Department of Physics. The absorption spectrum have been recorded at room temperature. A computer program was employed to obtain the optical constants, absorption coefficient, extinction coefficient, refractive index and energy gaps.

Figure (3-5) UV Photographic Spectrophotometer

3-7 Antibacterial Activity Effect Measurements of PEO-PVA-$SrTiO_3$-NiO and PEO-PVA-$SrTiO_3$-CoO NCs

Antibacterial activity of the PEO-PVA-$SrTiO_3$-NiO and PEO-PVA-$SrTiO_3$-CoO NCs tested samples was determined using a disc diffusion method. The antibacterial activities were done by using gram positive organism(Staphylococcus aureus) and gram negative organisms (Escherichia coli). Bacteria (Staphylococcus aureus and Escherichia coli) were cultured in Muller-Hinton Medium. The solution of the PEO-PVA-$SrTiO_3$-NiO and PEO-PVA-$SrTiO_3$-CoO NCs were injected inside the media and incubated at 37°C for 24 hours. The inhibition zone diameter was measured. The device is located in Al-Najaf Al-Ashraf Governorate

3-8 Pressure Sensors Application Measurements PEO-PVA-$SrTiO_3$-NiO and PEO-PVA-$SrTiO_3$-CoO Nanocomposites

The pressure sensors application of the PEO-PVA-$SrTiO_3$-NiO and PEO-PVA-$SrTiO_3$-CoO NCs were investigated by measuring capacitance between two electrodes on top and bottom of sample for different pressures range (80–160) bar in University of Babylon/College of Education for Pure Sciences/Department of physics

3-9 Gamma Ray Shielding Application Measurements of PEO-PVA-$SrTiO_3$-NiO and PEO-PVA-$SrTiO_3$-CoO NCs

The gamma-ray attenuation properties of samples with different concentrations of SrTiO3, NiO and CoO nanoparticles were investigated using radial shielding measurements of PEO-PVA-SrTiO3-NiO and PEO-PVA-SrTiO3-CoO. Different concentrations of test samples were placed in front of a collimating beam emitted from a gamma-ray source (Cs-137). The gamma ray source is 3 cm away from the detector, the nanocomposite sample is 2 cm away from it and the time used was 10 seconds. Geiger counter is used to estimate the linear attenuation coefficients by measuring the gamma ray fluxes transmitted through the samples at University of Babylon/College of Education for Pure Sciences/Department of Physics.

4-1 Introduction

This chapter involves the results of structural, optical and (A.C) electrical measurements for PEO-PVA-$SrTiO_3$-NiO and PEO-PVA-$SrTiO_3$-CoO nanocomposites and discussions. As affected with adding filler of $SrTiO_3$-NiOandCoO nanoparticles on structural ,optical characterize and (A.C) electrical for PEO-PVA blend. Beside this discuss each of the antibacterial activity ,pressure sensors and gamma ray shielding applications for PEO-PVA-$SrTiO_3$-NiO and PEO-PVA-$SrTiO_3$-CoO nanocomposites.

4-2 The Structural Properties of PEO-PVA-$SrTiO_3$-NiO and PEO-PVA-$SrTiO_3$-CoO Nanocomposites

4-2-1 XRD powder materials analysis

Figure (4-1) shows XRD for powder materials used in this study to confirm these materials compared of standard charts (ASTM), on the other hand, FTIR spectraconfirm polymer materials (PEO and PVA). Table 1 shows crystallite size of $SrTiO_3$ and CoO nanoparticles

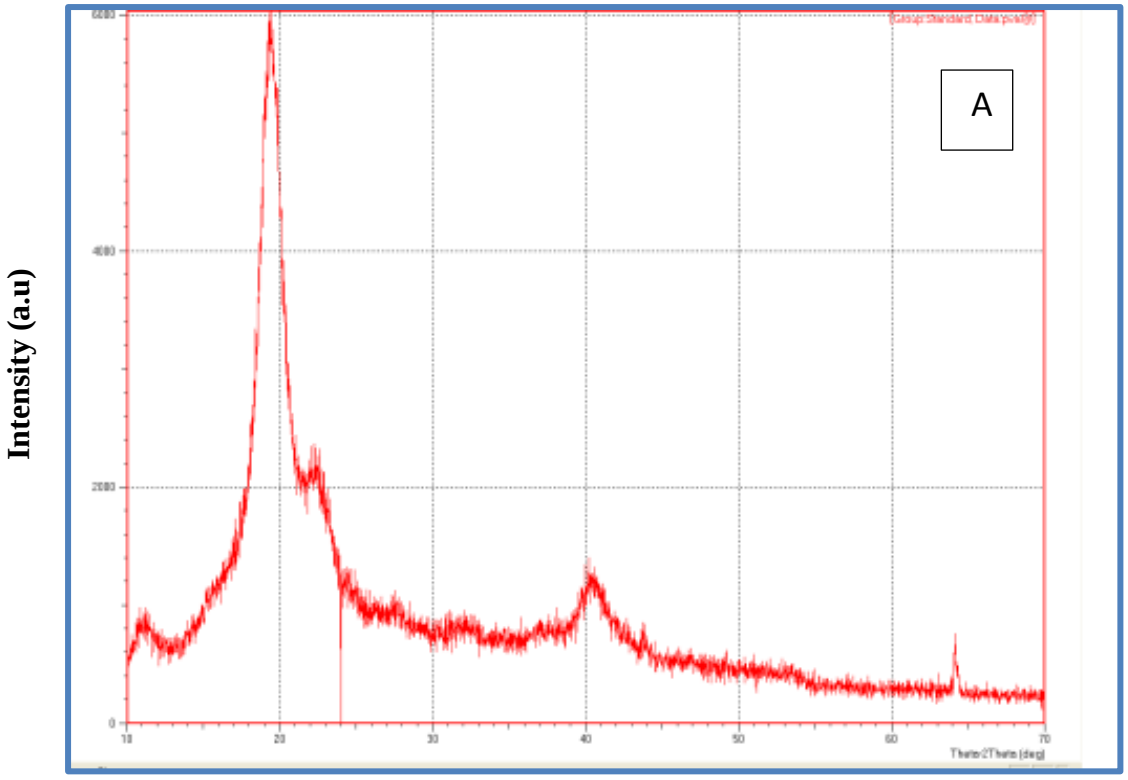
A
Intensity (a.u)
2θ(degree)

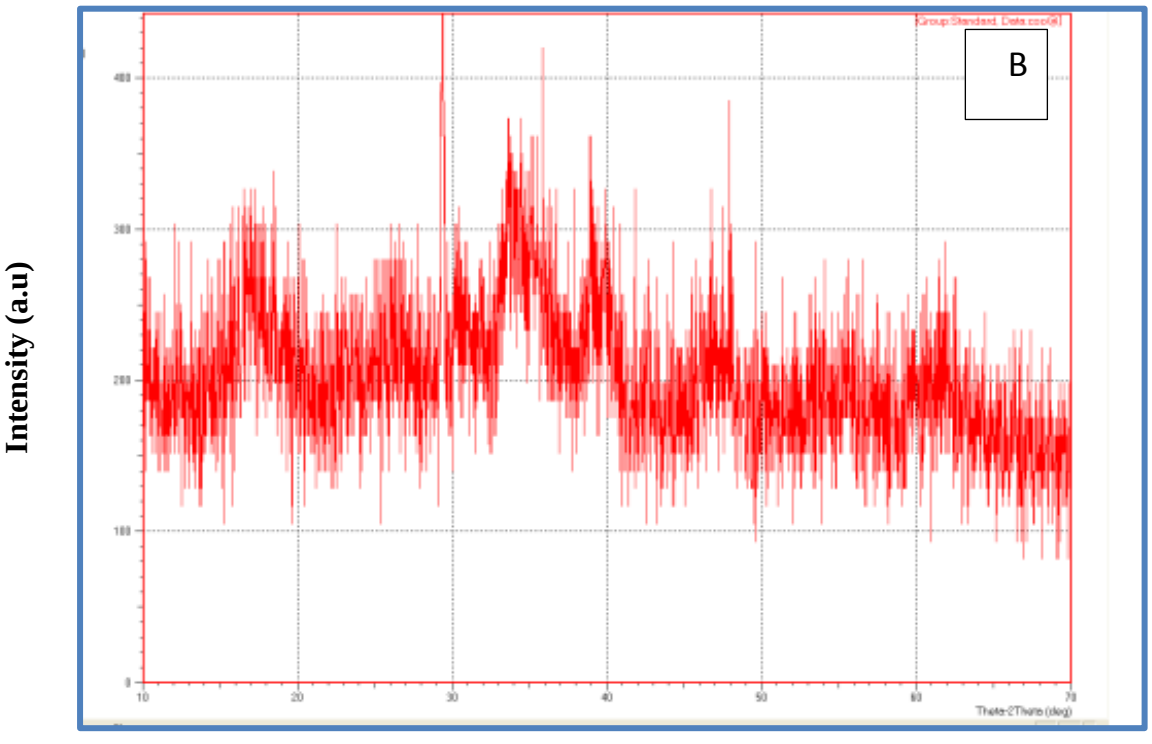
B
Intensity (a.u)
2θ(degree)

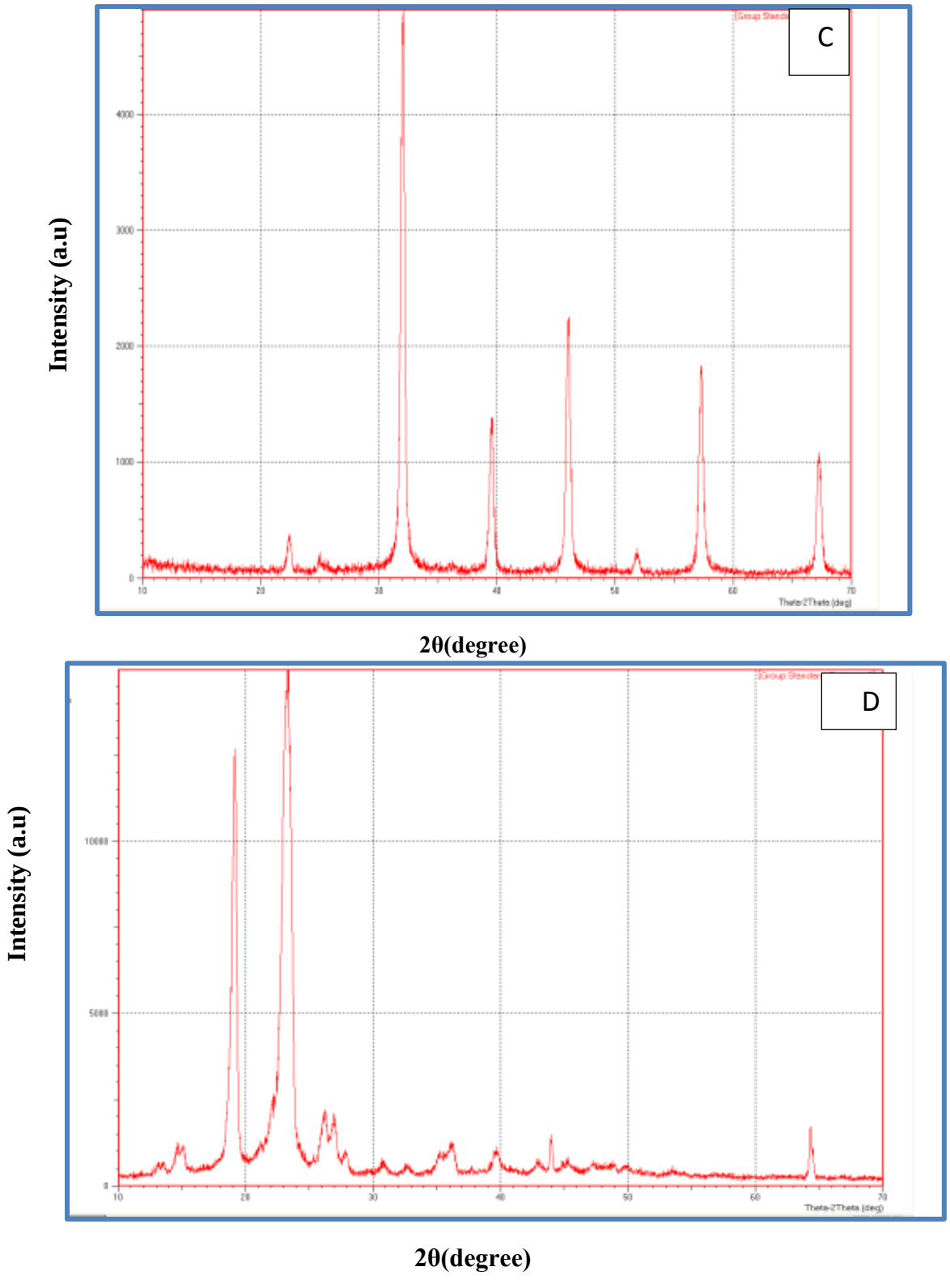

Figure. (4-1): XRD pattern of A) PEO , B) PVA , C) $SrTiO_3$, D) CoO

Table (4-1) Summary of mean crystal size estimated from XRD patterns using Scherer formula for PEO, PVA polymer and $SrTiO_3$,CoO nanoparticles

PEO	2θ (degree)	hkl	FWHM (degree)	Crystallite size (nm)
1	14.65		0.0087	16.7113
2	19.09		0.0078	18.7247
3	23.33		0.0143	10.3666
4	26.06		0.0109	13.6874
5	36.10		0.0139	10.9864
6	39.36		0.0110	13.9864
7	43.96		0.0061	27.2716
$SrTiO_3$				
1	22.35	100	0.007546804	19.54835285
2	31.93	110	0.007257428	20.74206581
3	39.52	111	0.007422885	20.7176043
4	46.08	200	0.007962192	19.75264219
5	51.86	210	0.008304277	19.37924875
6	57.25	211	0.007656759	21.53476284
CoO				
1	19.14	111	0.0148	9.8814
2	22.25	200	0.0305	4.8072
3	40.59	220	0.0184	8.0504
4	64.12	311	0.0080	21.4056

4-2-2 Optical Microscope

Figures (4-2) and (4-3) displays optical microscope images for PEO-PVA-$SrTiO_3$-NiO and PEO-PVA-$SrTiO_3$-CoO nanocomposites films with different concentrations at magnification strength (100x).As shown in the images, there is a clear difference between the samples (a, b, c, d, e) in figures (4-2) and (4-3). When increasing ratiosof $SrTiO_3$,NiO and CoO NPs in PEO / PVA blend, the NPs create a continuing network inside the polymers, reaching to 4 wt% for PEO-PVA-$SrTiO_3$-NiO and PEO-PVA-$SrTiO_3$-CoO nanocomposites. This network is made up of indoor routes, and nanocomposites allow charging carriers to move through such pathways[122,123].

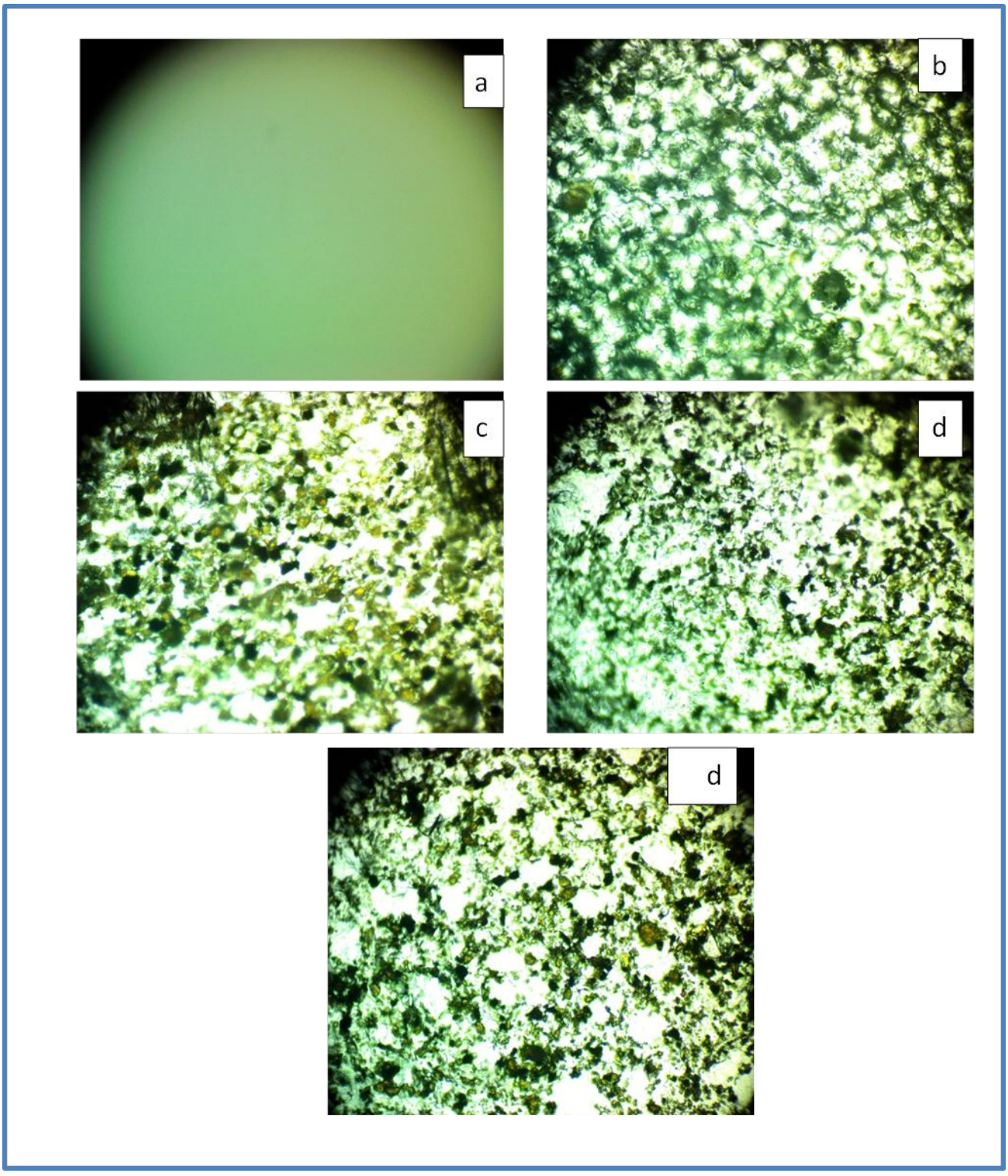

Figure(4-2) Photomicrographs for PEO-PVA-$SrTiO_3$-NiO nanocomposites at 100× magnification (a) PEO-PVA pure, (b) 1 wt% $SrTiO_3$-NiO, (c) 2 wt% $SrTiO_3$-NiO,(d)3 wt% $SrTiO_3$-NiO, (f) 4 wt% $SrTiO_3$-NiO

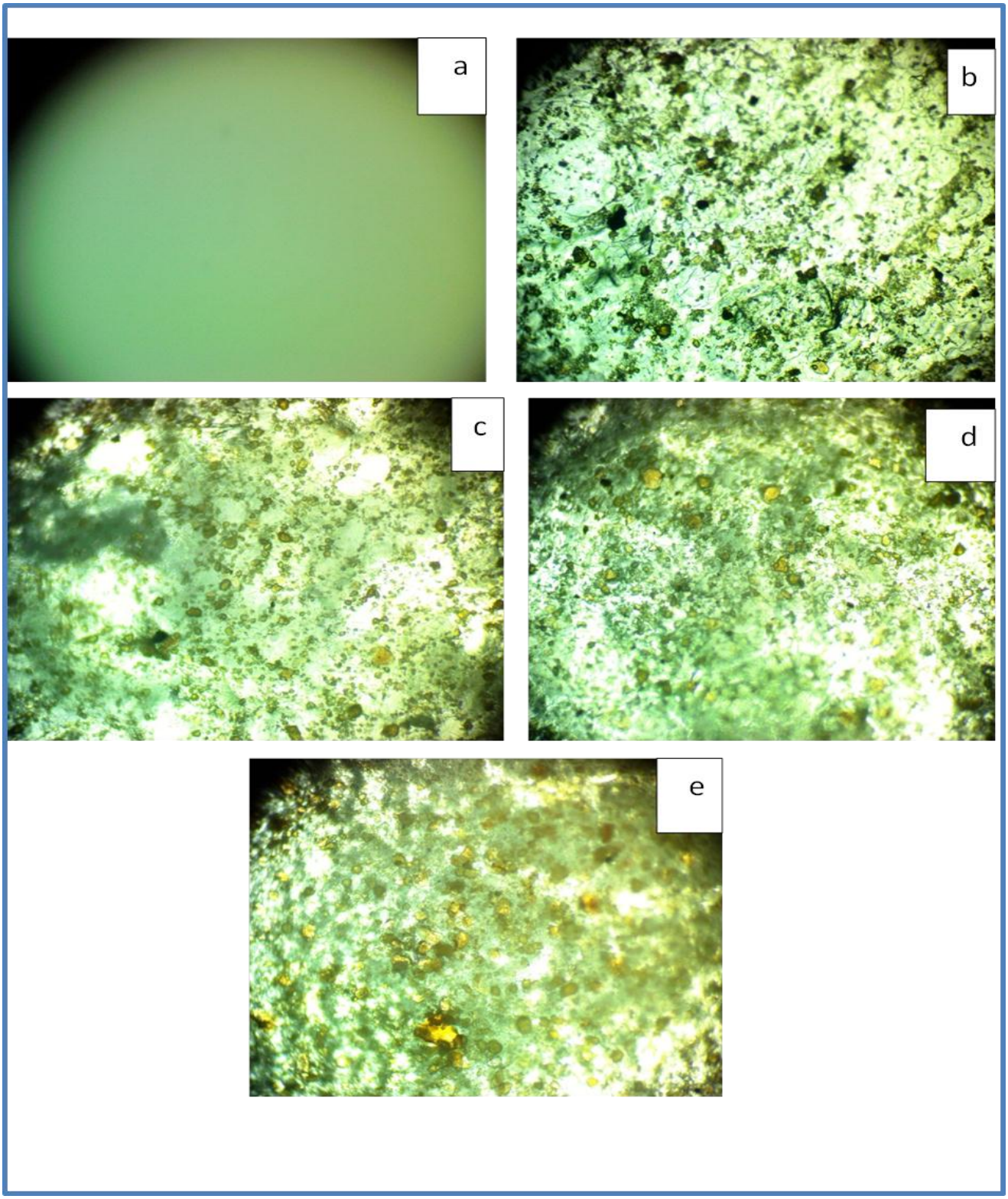

Figure(4-3) Photomicrographs for PEO-PVA-$SrTiO_3$-CoO nanocomposites at 100× magnification (a) PEO-PVA pure, (b) 1 wt% $SrTiO_3$- CoO, (c) 2 wt% $SrTiO_3$- CoO,(d)3 wt% $SrTiO_3$- CoO, (f) 4 wt% $SrTiO_3$- CoO

4-2-3 Scanning Electron Microscope (SEM)

Figures (4-4) and (4-6) show SEM images of the PEO-PVA mixture with different concentrations of strontium titanate , nickel oxide and cobalt oxide nanoparticles, respectively to study the morphology of the nanocomposites and the arrangement of the nanoparticles different at low and high concentrations of nanoparticles. SEM images reveal uniformly distributed nanoparticles within the PEO-PVA blend where charge carriers are allowed to pass through the tracks [124]. The nanocomposite membranes display many evenly dispersed and widely spaced spherical particle agglomerates or pieces on the surface. This may be a sign of a homeostatic growth mechanism .The surface profile varies with the proportion of nanoparticles in the polymer mixtures.

When $SrTiO_3$, NiO and CoO NPs rise, the grains agglomerate. The results will show the surface morphology of the membranes. when 4 wt% $SrTiO_3$, NiO and CoO NPs are added to PEO-PVA blend. $SrTiO_3$,NiO and CoO NPs ratio gradually growing in PEO-PVA blend, appearance of several spherical particle aggregates or chunks on the surface of nanocomposites indicates the presence of a homogenous growth mechanism. It gets softer as the concentration of both particles increases, where nanoparticles aggregate and are well distribution in PEO-PVA blend form a continuous network with in the polymers and this is similar to the results of the researchers [125]. Figures (4-5) and (4-7) show particle size for PEO-PVA-$SrTiO_3$-NiO and PEO-PVA-$SrTiO_3$-CoO nanocomposites calculate from SEM analysis.

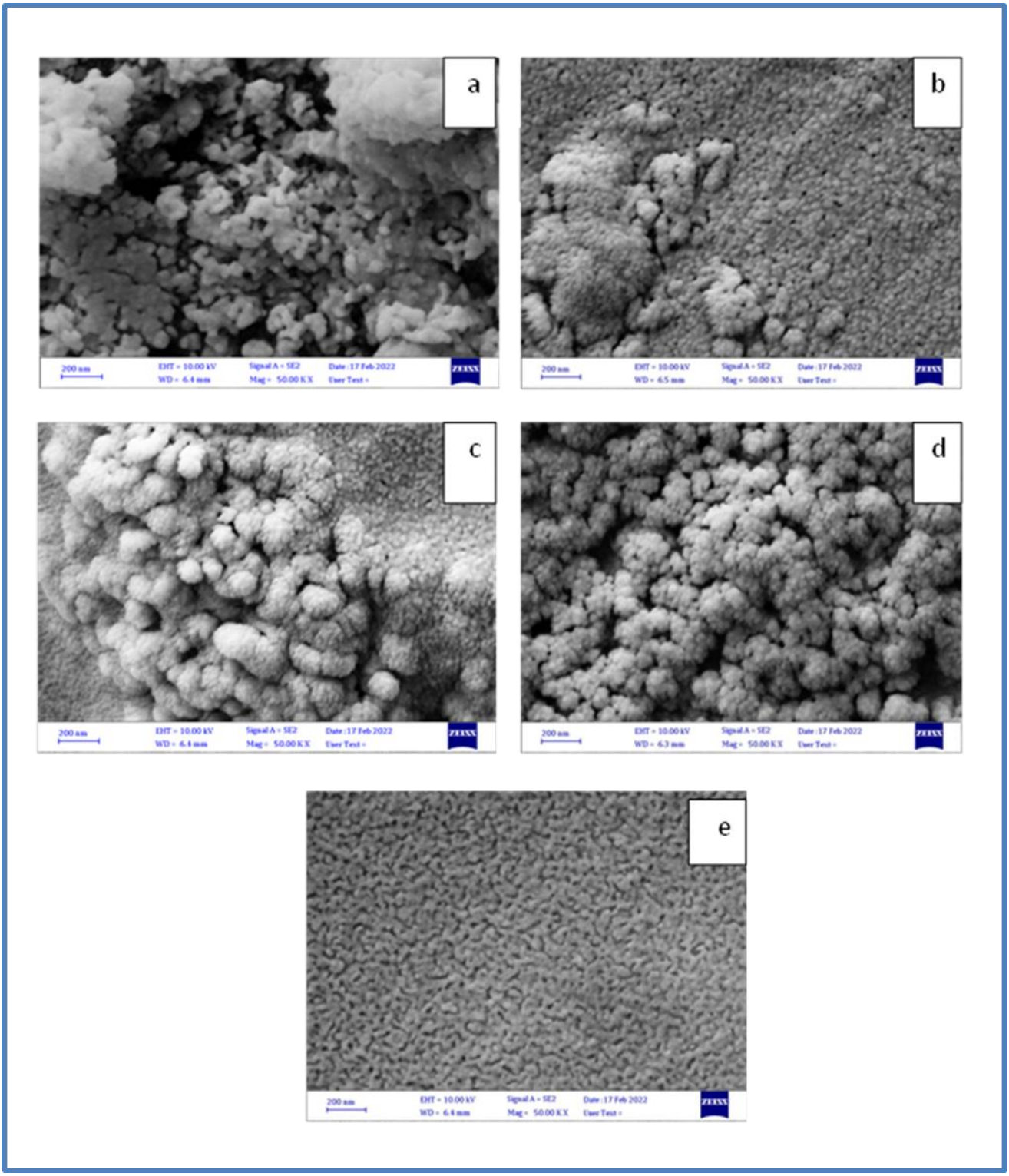

Figure (4-4) SEM for PEO-PVA-$SrTiO_3$-NiO NCs are shown in (a) for PEO-PVA, (b) for 1 wt% $SrTiO_3$-NiO, (c) for 2 wt% $SrTiO_3$-NiO, (d) for 3 wt% $SrTiO_3$-NiO and (e) for 4 wt% $SrTiO_3$-NiO

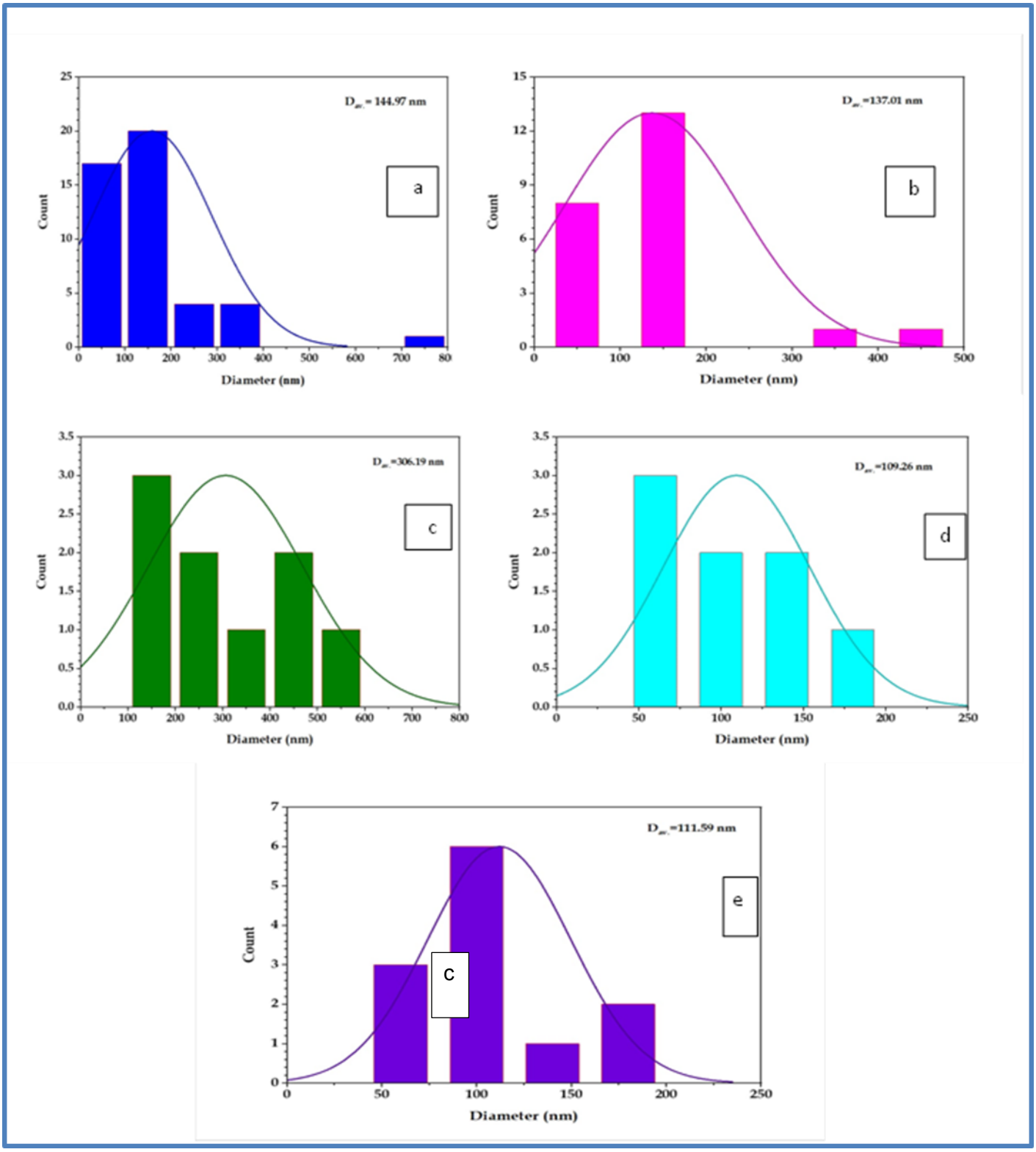

Figure (4-5) Partical size for PEO-PVA-$SrTiO_3$-NiO nanocomposites: a for PEO-PVA, b for 1 wt.% $SrTiO_3$-NiO, c for 2 wt.% $SrTiO_3$-NiO, d for 3 wt.% $SrTiO_3$/NiO, e for 4 wt.% $SrTiO_3$-NiO

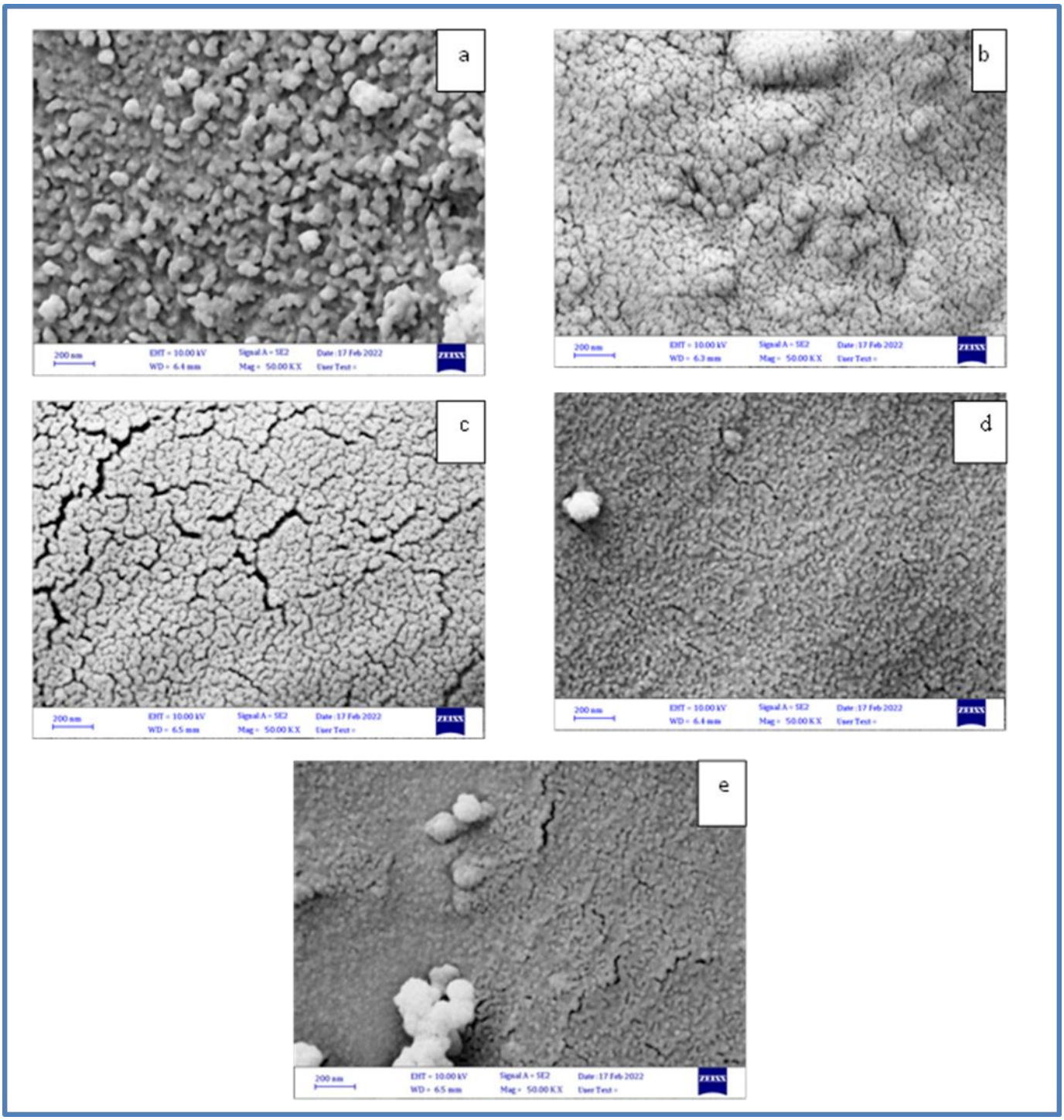

Figure (4-6) SEM for PEO-PVA-$SrTiO_3$-CoO NCs are shown in (a) for PEO-PVA, (b) for 1 wt% $SrTiO_3$- CoO, (c) for 2 wt% $SrTiO_3$- CoO, (d) for 3 wt% $SrTiO_3$- CoO and (e) for 4 wt% $SrTiO_3$- CoO

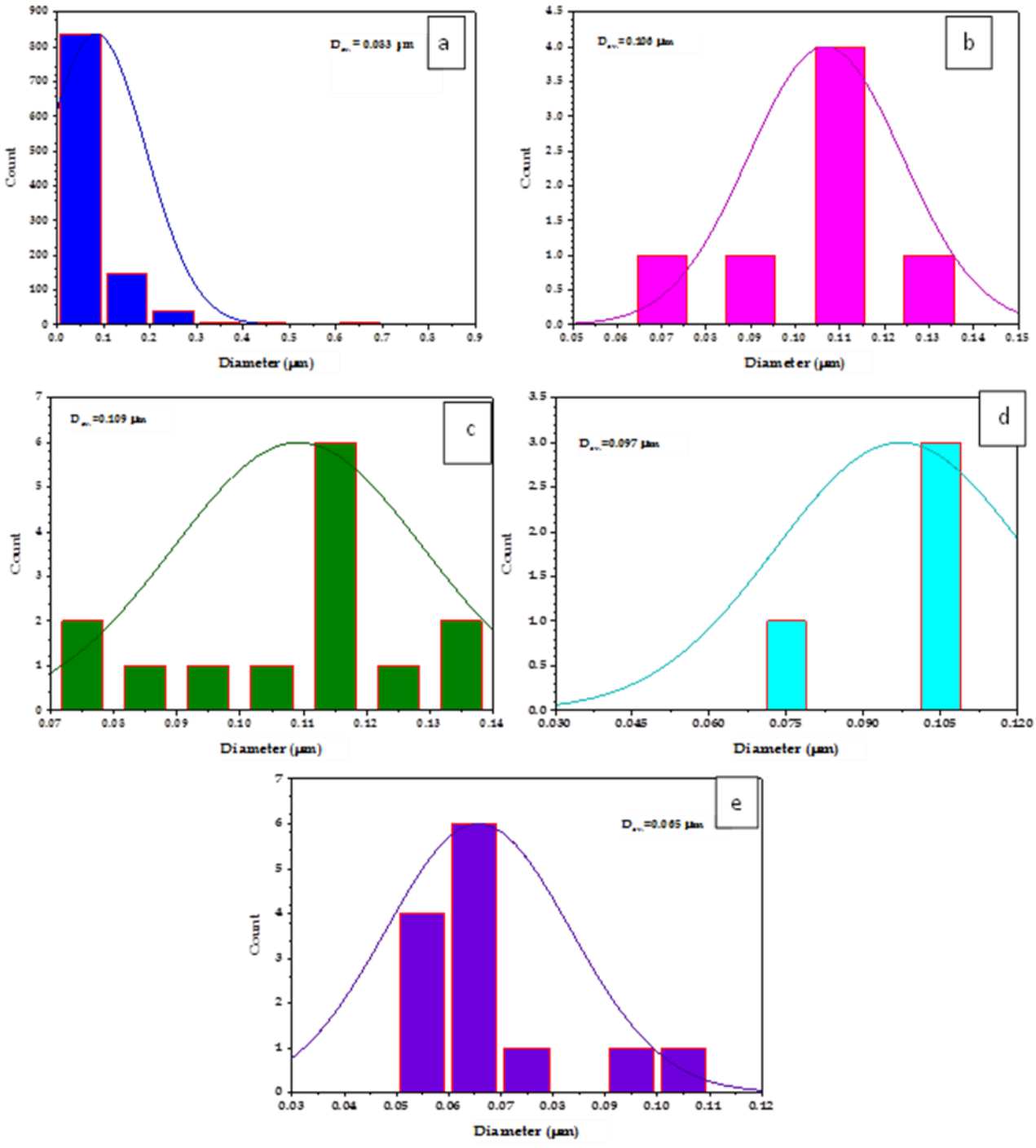

Figure (4-7) Partical size for PEO-PVA-$SrTiO_3$-CoO nanocomposites: a for PEO-PVA, b for 1 wt.% $SrTiO_3$-CoO, c for 2 wt.% $SrTiO_3$-CoO, d for 3 wt.% $SrTiO_3$-CoO, e for 4 wt.% $SrTiO_3$-CoO

4-2-4 Fourier Transformation Infrared Radiation (FTIR) for PEO-PVA-$SrTiO_3$-NiO and PEO-PVA-$SrTiO_3$-CoO nanocomposites

Figures (4-8) and (4-9) show that the FTIR spectra of PEO-PVA-$SrTiO_3$-NiO and PEO-PVA-$SrTiO_3$-CoO . At ambient temperature, FT-IR spectra of pure PEO/ PVA blend and doped by $SrTiO_3$,NiO and CoO nanoparticles in the range (1000–4000) cm^{-1} were collected. The presence of the stretching vibration appeared as bright spots in all of them with varying degrees of roughness in PEO-PVA 3wt% of nanoparticles generated samples , these bright spots appear to be agglomerates of $SrTiO_3$,NiOandCoO NPs that grow in size as the concentration of nanoparticles increases.

As seen in (4-8 e) and (4-9 e) 4wt % percent, the degree of roughness of the film surface increases. This could indicate filler segregation in the host matrix, implying additive-polymer interaction and complications. It may also refer to the formation of the hydroxyl group OH of PEO-PVA is responsible for the prominent peaks in the spectra at (2881) cm^{-1}. The C=O stretching mode is thought to be responsible for the absorbent peak at (2359) cm^{-1}. Asymmetric stretching and scissoring bending vibrations of the CH2 group appear at (1098) cm^{-1}. The photos demonstrate the bonding nature of PEO-PVA-$SrTiO_3$-NiO and PEO-PVA-$SrTiO_3$-CoO nanocomposites with polymers. According to the FT-IR analysis, there are no interactions between the PEO-PVA blend and the $SrTiO_3$,NiO and CoO NPs. Furthermore, we can see in these data that when the concentration of nanoparticles increases, the transmittance decreases dramatically due to the increased density of nanocomposites [126]

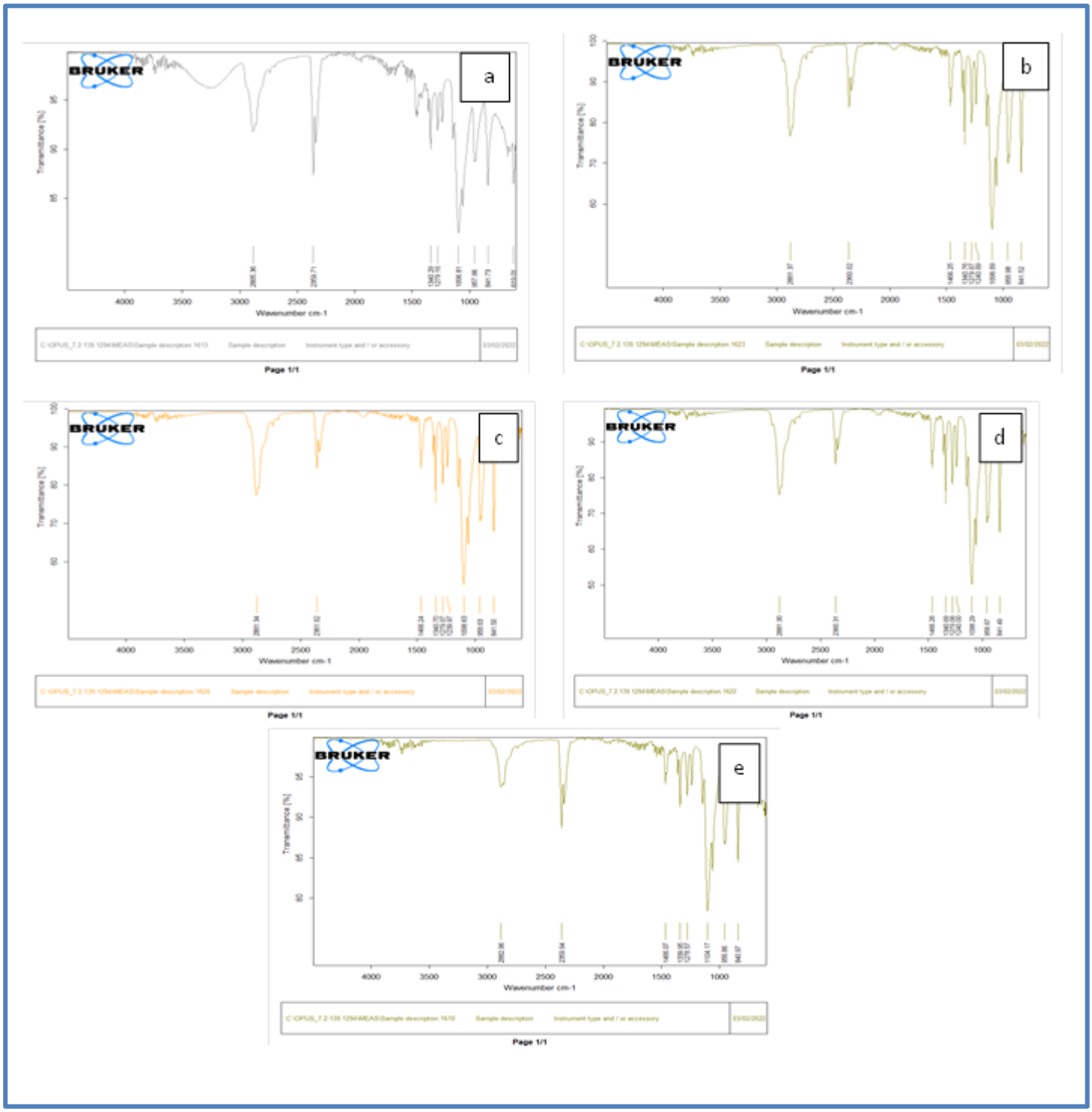

Figure (4-8) FTIR spectra for PEO-PVA-$SrTiO_3$-NiO NCs are shown in (a) for PEO-PVA, (b) for 1 wt% $SrTiO_3$-NiO, (c) for 2 wt% $SrTiO_3$-NiO, (d) for 3 wt% $SrTiO_3$-NiO and (e) for 4 wt% $SrTiO_3$-NiO

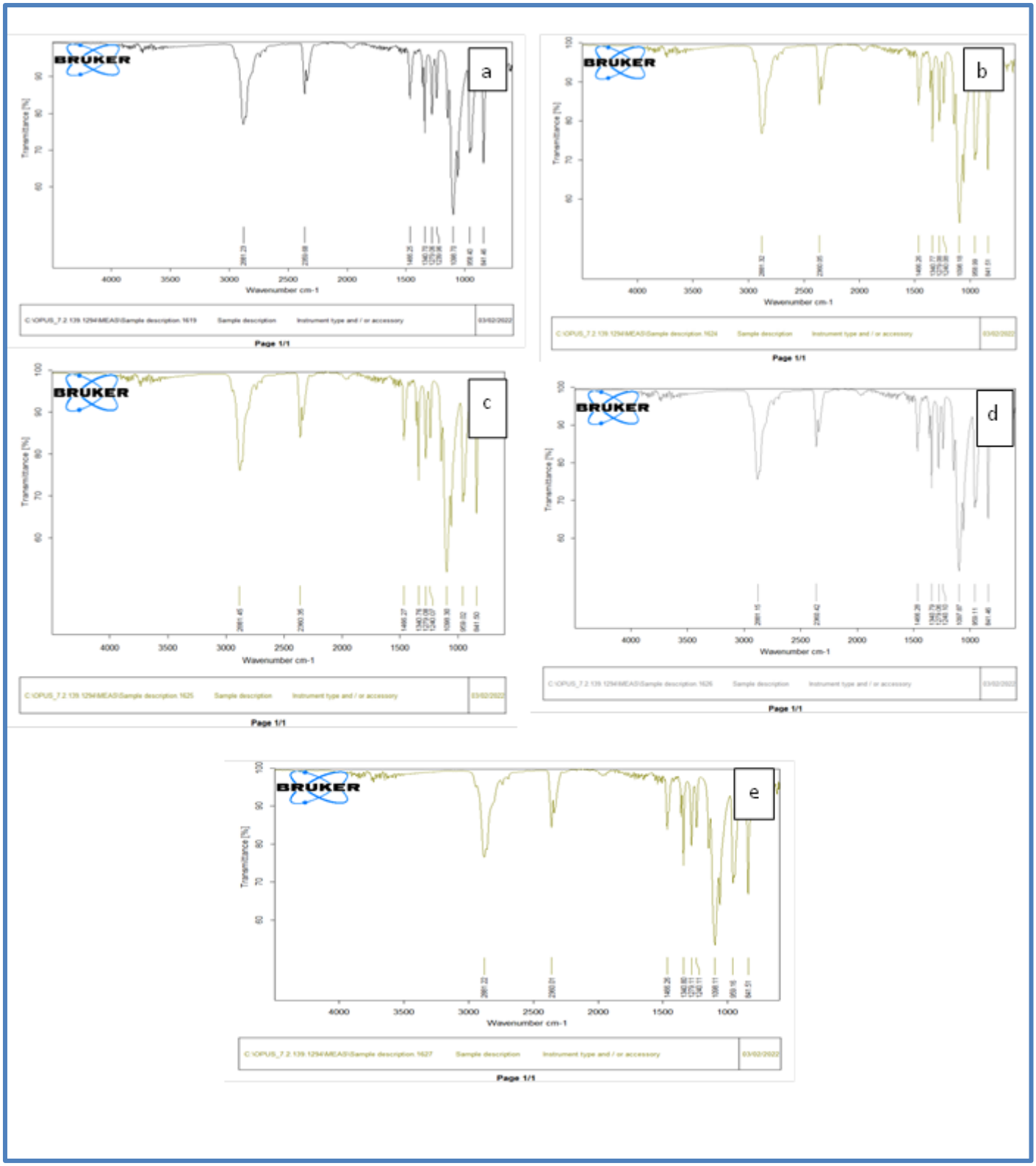

Figure (4-9) FTIR spectra for PEO-PVA-$SrTiO_3$-CoO NCs are shown in (a) for PEO-PVA, (b) for 1 wt% $SrTiO_3$- CoO, (c) for 2 wt% $SrTiO_3$- CoO, (d) for 3 wt% $SrTiO_3$- CoO and (e) for 4 wt% $SrTiO_3$- CoO

4-3 Optical Properties of PEO-PVA-$SrTiO_3$-NiO and PEO-PVA-$SrTiO_3$-CoO nanocomposites

The main purpose of optical properties study of PEO-PVA-$SrTiO_3$-NiO and PEO-PVA-$SrTiO_3$-CoO nanocomposites to know the effect of Strontium Titanate and nickel oxide and cobalt oxide nanoparticles additive on the optical properties of PEO-PVA blend and uses as antibacterial effect. The absorbance and transmittance have been recorded of the PEO-PVA blend with different concentrations of $SrTiO_3$,NiO and CoO nanoparticles.

4-3-1 The Absorbance (A)

Figures (4-10) and (4-11) show absorption spectra for PEO-PVA-$SrTiO_3$-NiO and PEO-PVA-$SrTiO_3$-CoO NCs .There is evidence to suggest that strontium-titanium oxide, nickel oxide and cobalt oxide filler levels boost the peak's intensity. Due to the establishment of intermolecular hydrogen bonds between strontium-titanium oxide ,nickel oxide and cobalt oxide and the adjacent OH groups of the main chain of PEO and PVA, as well as the specific weight $SrTiO_3$,NiO and CoO NPs and the absorption band moves. Because the valence and conduction bands are further apart, the PEO-PVA combination has a low absorption.The increased absorbance for PEO-PVA-$SrTiO_3$-NiO and PEO-PVA-$SrTiO_3$-CoO NCs absorbed the incident radiation by free electrons[127].

In addition to; specific weight of strontium titanate , nickel oxide and cobalt oxide nanoparticles compare with PEO-PVA blend, as a result increase in the specific weight of PEO-PVA-$SrTiO_3$-NiO and PEO-PVA-$SrTiO_3$-CoO nanocomposites . But appear new physical properties, due to the shift in the band edges and the absorption bands towards the higher wavelengths with different absorption intensities for different concentrations nanoparticles samples. The shift in the absorption band gives an idea of the formation intermolecular hydrogen bonding existing nanoparticles with the neighboring OH groups of the PEO-PVA main chain is caused by an increase in strontium-titanium oxide, nickel oxide and cobalt oxide nanoparticles [128].

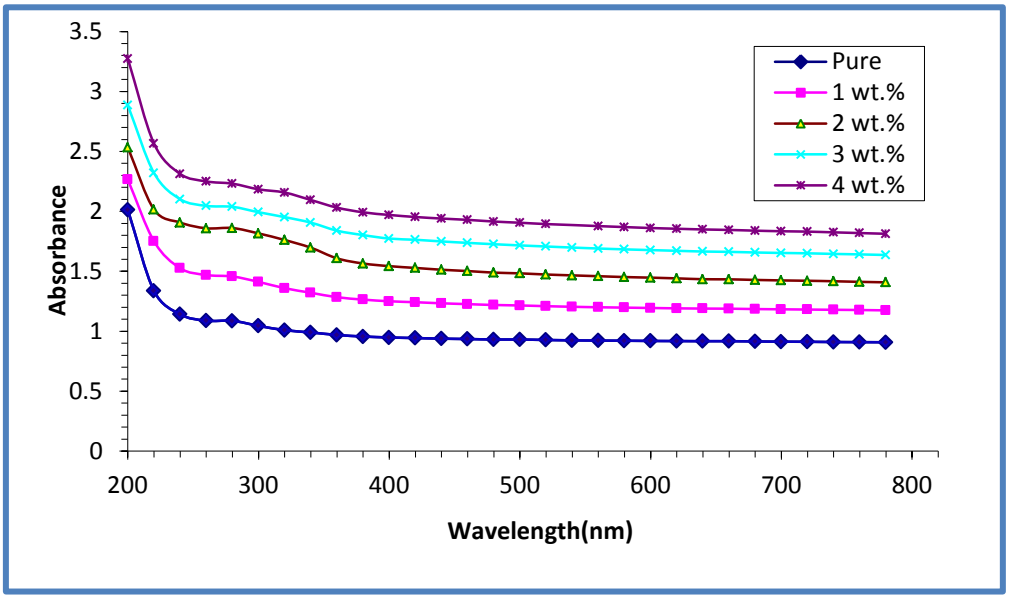

Figure (4-10) Variation of absorbance for PEO-PVA-$SrTiO_3$-NiO nanocomposites with wavelength

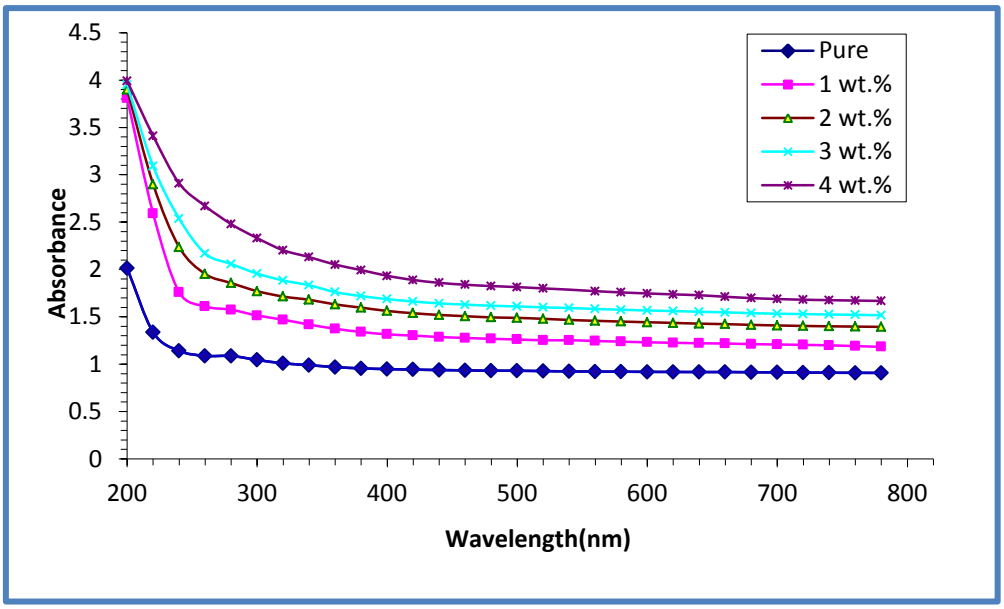

Figure (4-11) Variation of absorbance for PEO-PVA-$SrTiO_3$-CoO nanocomposites with wavelength

4-3-2 Transmittance Spectrum

Figures (4-12) and (4-13) show the transmittance spectra versus wavelength of the incident light on the PEO-PVA-$SrTiO_3$-NiO and PEO-PVA-$SrTiO_3$-CoO NCs.When the concentration of $SrTiO_3$, NiO and CoO nanoparticles is increased, the transmittance of PEO-PVA-$SrTiO_3$-NiO and PEO-PVA-$SrTiO_3$-CoO NCs decreases, which is the opposite of the absorbance behavior. This means that the $SrTiO_3$, NiO and CoO nanoparticles improve the absorbance of the PEO-PVA-$SrTiO_3$-NiO and PEO-PVA-$SrTiO_3$-CoO nanocomposites

This is due to the use of nanoparticles to fii the voids between the polymer chains of the PEO-PVA blend. Furthermore, the free electrons of nanoparticles absorbed the light incident on the samples, causing the free electrons to cross to a high level of energy and emit no rays, indicating that the electrons migrated to a high level of energy and took up a free position in the energy band [129].The nature of the reflected and refracted light in the samples may also account for the lower transmittance [130].

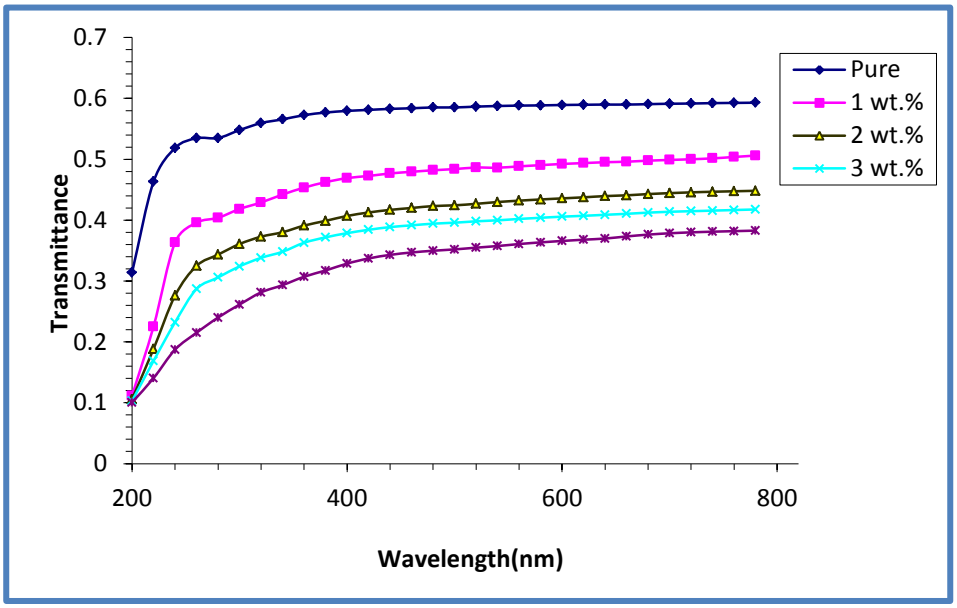

Figure (4-12) Variation of transmittance for PEO-PVA-$SrTiO_3$-NiO NCs with wavelength

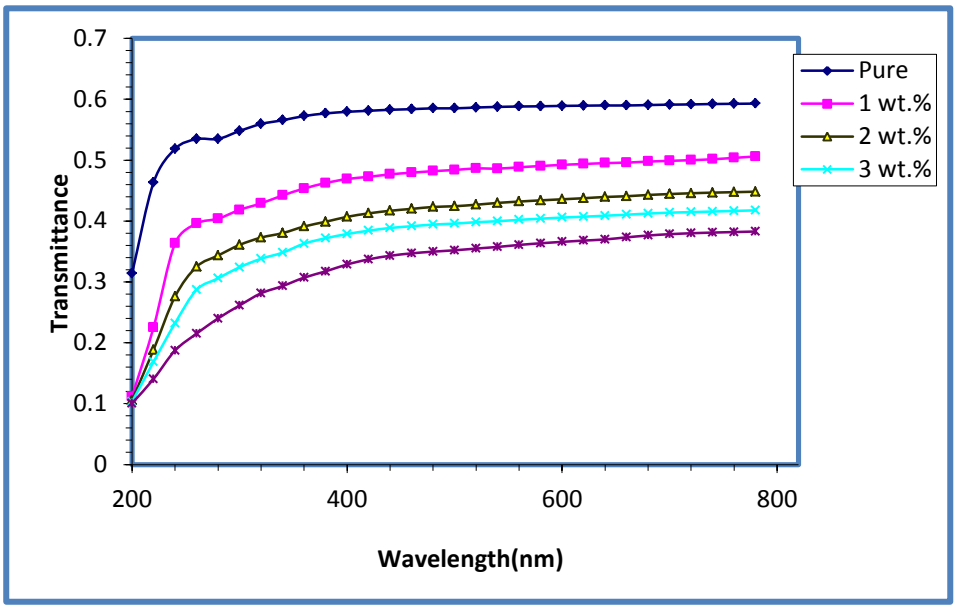

Figure (4-13) Variation of transmittance for PEO-PVA-$SrTiO_3$-CoO NCs with wavelength

4-3-3 Absorption Coefficient (α) for PEO-PVA-$SrTiO_3$-NiO and PEO-PVA-$SrTiO_3$-CoO NCs

Figures (4-14) and (4-15) show the absorption coefficient versus of incident photon energy for PEO-PVA blend with different concentrations of $SrTiO_3$, NiO and CoO nanoparticles. Figures show low absorption at low energy, this means the probability of electrons transition is low due to the incident of photon energy was not enough to transition of electron from valence to conduction band PEO-PVA-$SrTiO_3$-NiO and PEO-PVA-$SrTiO_3$-CoO nanocomposites.

But in the high energy, the absorption is large this is indicated high probability for electrons transitions. On other hand; the incident photon energy becomes greater than of forbidden energy gab. From the same figures; can be noted an increasing in absorption coefficient PEO-PVA-$SrTiO_3$-NiO and PEO-PVA-$SrTiO_3$-CoO nanocomposites when increase of a filler of $SrTiO_3$, NiO and CoO nanoparticles. This increases attributed to increase the number of carries charges of nanoparticles which cause to increase the absorbance[131]. In addition to; creates new location levels which means degradable or expand in covalent bond between valence and conduction bond, which additive of $SrTiO_3$, NiO and CoO nanoparticles made to degradable and break the covalent between PEO-PVA blend. Because of the oxygen leads to make degradable covalent band where the

prevent free roots to corporate in the end of polymer chain. In spite of the energy gap of nanoparticles large but the conduction band filled of free electrons because of oxygen vacancies which due to from non-stoichiometry [132].

Absorption coefficient can be helped for concluding the nature of transition electrons, when the value of is high (greater than $10^4 cm^{-1}$) in the higher energy expected direct transitions of electrons. Whaite the value of absorption coefficient is low (less than $10^4 cm^{-1}$) in the low energy expected indirect transitions of electrons. From the results, it's indicated the absorption coefficient for PEO-PVA-$SrTiO_3$-NiO and PEO-PVA-$SrTiO_3$-CoO nanocomposites has values are less than (10^4 cm^{-1}) which means they possess indirect energy gap[133].

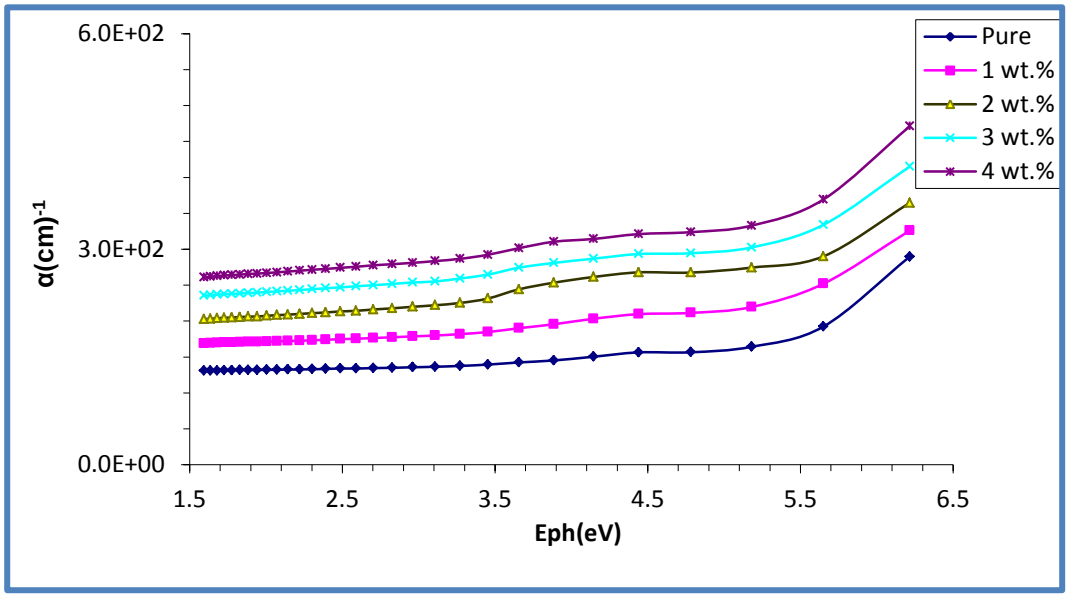

Figure (4-14) Variation of absorption coefficient for PEO-PVA-$SrTiO_3$-NiO nanocomposites with photon energy

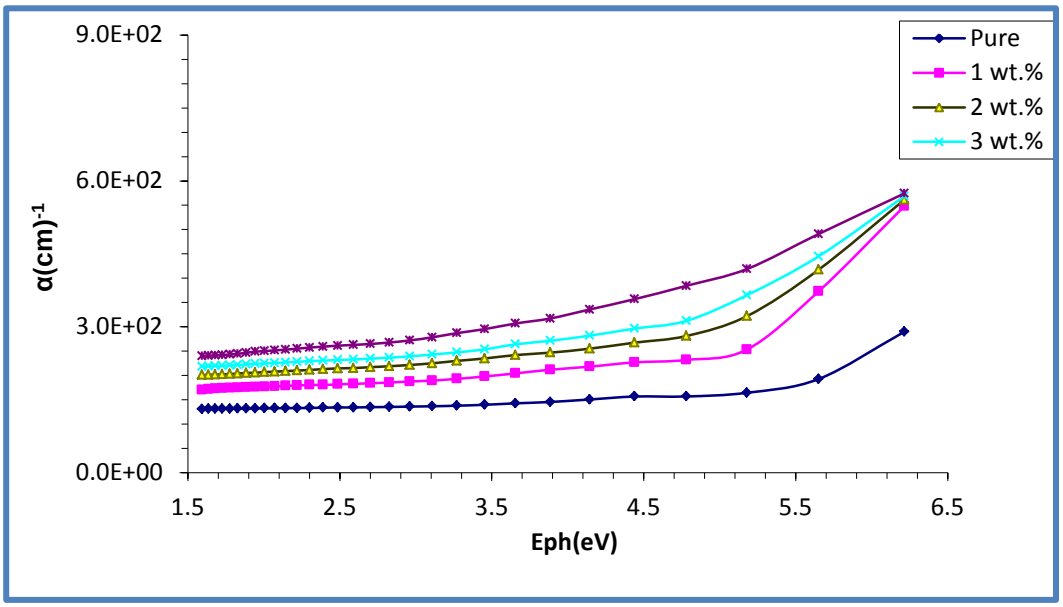

Figure (4-15) Variation of absorption coefficient (α) for PEO-PVA-$SrTiO_3$-CoO nanocomposites with photon energy

4-3-4 Optical Energy Gaps of the Indirect Transition (Allowed and Forbidden) PEO-PVA-$SrTiO_3$-NiO and PEO-PVA-$SrTiO_3$-CoO NCs

Figures (4-16) and (4-17) show the plot of the absorbance edge $(\alpha h\upsilon)^{1/2}$for PEO-PVA-$SrTiO_3$-NiO and PEO-PVA-$SrTiO_3$-CoO nanocomposites versus photon energy and figures (4-18) and (4-19) show the plot of the absorbance edge $(\alpha h\upsilon)^{1/3}$ for PEO-PVA-$SrTiO_3$-NiO and PEO-PVA-$SrTiO_3$-CoO nanocomposites versus photon energy . The values of energy gap decreases with increasing of concentration of nanocomposites as listed in tables (4-2) and (4-3) ,this attributes to great localize levels in the forbidden energy band gap, and the transition of electrons by two stage: the first transition of electron from valence band to localize levels and the second from localize levels to the conduction band in the allowed indirect transition[134].

Thus in indirect forbidden transition, the transition tails of localize of the levels made by the additive .This behavior due to oxygen vacancies of strontium titanate , nickel oxide and cobalt oxide nanoparticles which due to from non-stoichiometry. These nanocomposites are heterogeneous type in other word; the electrons conduction depend on defects and additive impurity, where increasing in the $SrTiO_3$, NiO and CoO nanoparticles additive make several passes of electrons in the PEO-PVA

blend. Therefor passes easy from valence to conduction bands [135].This is explaining the decrease of energy gap by increase the additive .

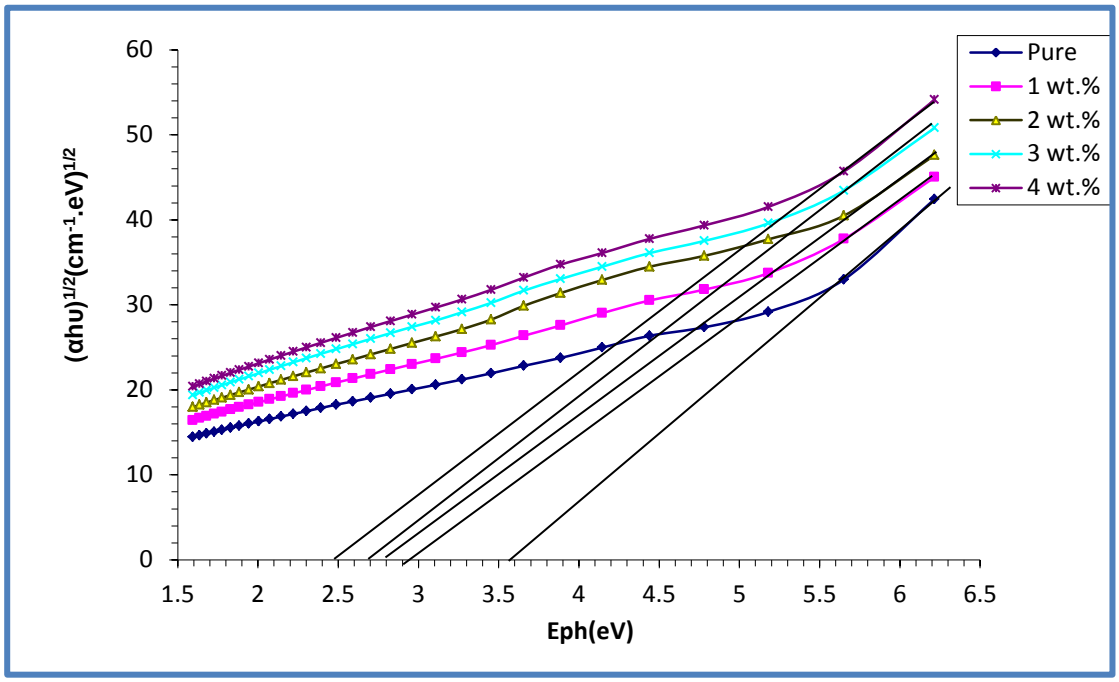

Figure (4-16) Variation of $(\alpha h\upsilon)^{1/2}$ for PEO-PVA-$SrTiO_3$-NiO NCs with photon energy

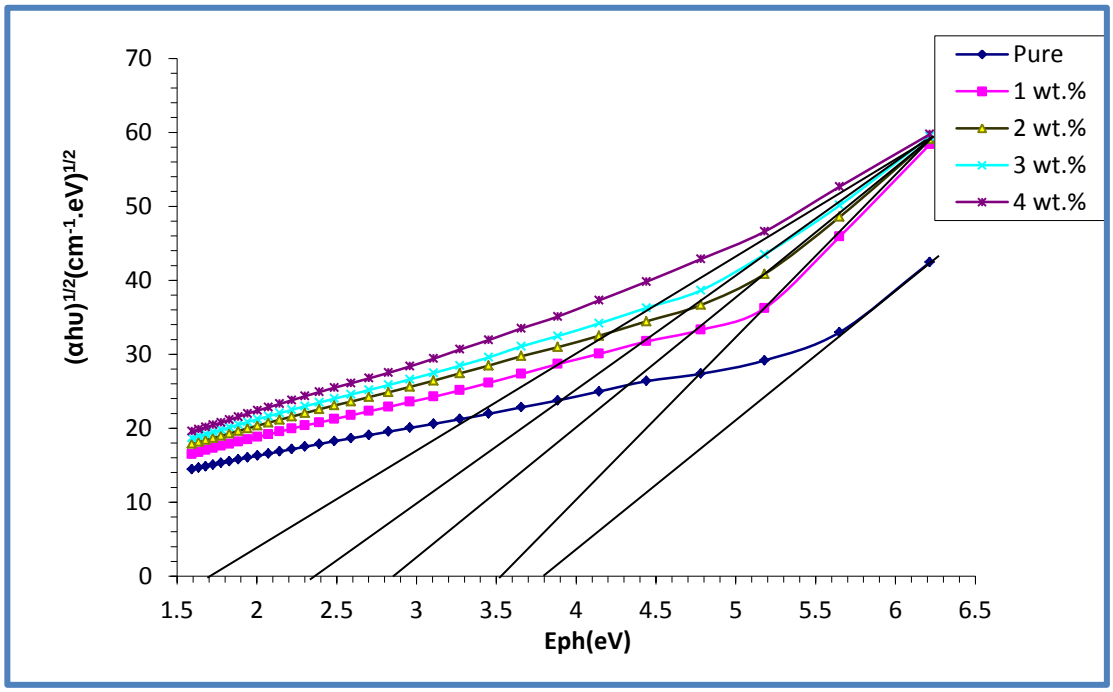

Figure (4-17) Variation of $(\alpha h\upsilon)^{1/2}$ for PEO-PVA-$SrTiO_3$-CoO NCs with photon energy

Tables (4-2) Values of energy gap for the (allowed) indirect transition for PEO/PVA-$SrTiO_3$-NiO nanocomposites

Concentrations of $SrTiO_3$-NiO wt.%	Indirect energy gap (allowed) eV
PEO-PVA blend	3.6
PEO-PVA 1%wt. $SrTiO_3$-NiO NCs	2.9
PEO-PVA 2%wt. $SrTiO_3$-NiO NCs	2.8
PEO-PVA 3%wt. $SrTiO_3$-NiO NCs	2.7
PEO-PVA 4%wt. $SrTiO_3$-NiO NCs	2.5

Tables (4-3) Values of energy gap for the (allowed) indirect transition for PEO-PVA-$SrTiO_3$-CoO nanocomposites

Concentrations of $SrTiO_3$-CoO NPs wt.%	Indirect energy gap (allowed) eV
PEO-PVA blend	3.8
PEO-PVA 1%wt. $SrTiO_3$-CoO NCs	3.5
PEO-PVA 2%wt. $SrTiO_3$- CoO NCs	2.9
PEO-PVA 3%wt. $SrTiO_3$- CoO NCs	2.4
PEO-PVA 4%wt. $SrTiO_3$- CoO NCs	1.7

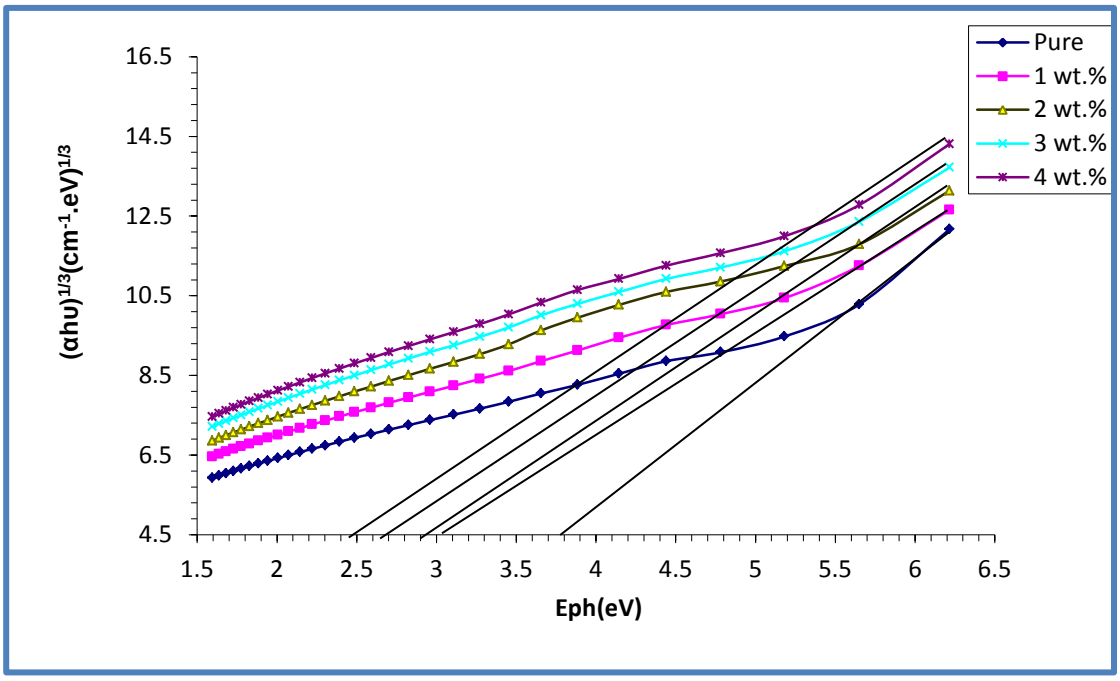

Figure (4-18) Variation of $(\alpha h\upsilon)^{1/3}$ for PEO-PVA-$SrTiO_3$-NiO NCs with photon energy

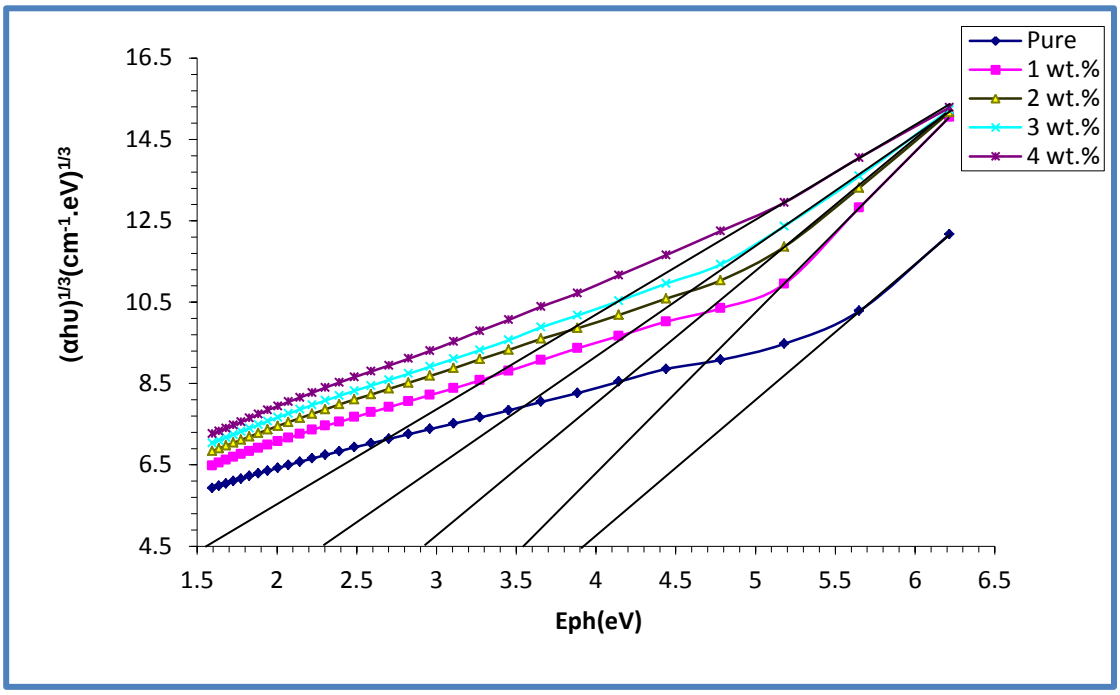

Figure (4-19) Variation of $(\alpha h\upsilon)^{1/3}$ for PEO-PVA-$SrTiO_3$-CoO Nanocomposites with photon energy

Tables (4-4) Values of energy gap for the (forbidden) indirect transition for PEO-PVA-$SrTiO_3$-NiO nanocomposites

Concentrations of $SrTiO_3$-NiO NPs wt.%	Indirect energy gap (forbidden) eV
PEO-PVA blend	3.8
PEO-PVA 1%wt. $SrTiO_3$-NiO NCs	3.1
PEO-PVA 2%wt. $SrTiO_3$-NiO NCs	2.9
PEO-PVA 3%wt. $SrTiO_3$-NiO NCs	2.7
PEO-PVA 4%wt. $SrTiO_3$-NiO NCs	2. 5

Tables (4-5) Values of energy gap for the (forbidden) indirect transition for PEO-PVA-$SrTiO_3$-CoO nanocomposites

Concentrations of $SrTiO_3$-CoO NPs wt.%	Indirect energy gap (forbidden) eV
PEO-PVA blend	3.9
PEO-PVA 1%wt. $SrTiO_3$-CoO NCs	3.5
PEO-PVA 2%wt. $SrTiO_3$-CoO NCs	2.9
PEO-PVA 3%wt $SrTiO_3$-CoO NCs	2.3
PEO-PVA 4%wt. $SrTiO_3$-CoO NCs	1.6

4-3-5 Extinction Coefficient of PEO-PVA-$SrTiO_3$-NiO and PEO-PVA-$SrTiO_3$-CoO NCs

Figures (4-20) and (4-21) show the variation of extinction coefficient versus wavelength for PEO-PVA-$SrTiO_3$-NiO and PEO-PVA-$SrTiO_3$-CoO NCs respectively, by increasing the amount of $SrTiO_3$, NiO and CoO nanoparticles in the PEO-PVA blend, the extinction coefficient increases. The behavior of the extinction coefficient indicates substantial absorption. In addition, the interaction of the carrying charge in the samples with the incident light causes polarization of the medium charges, resulting in a loss of incident photon energy[136].

This implies that the host PEO-PVA blend is modified by the $SrTiO_3$,NiO and CoO nanoparticles. The absorbance in the visible range increases as concentration of nanoparticles increases, which is the interesting observation .

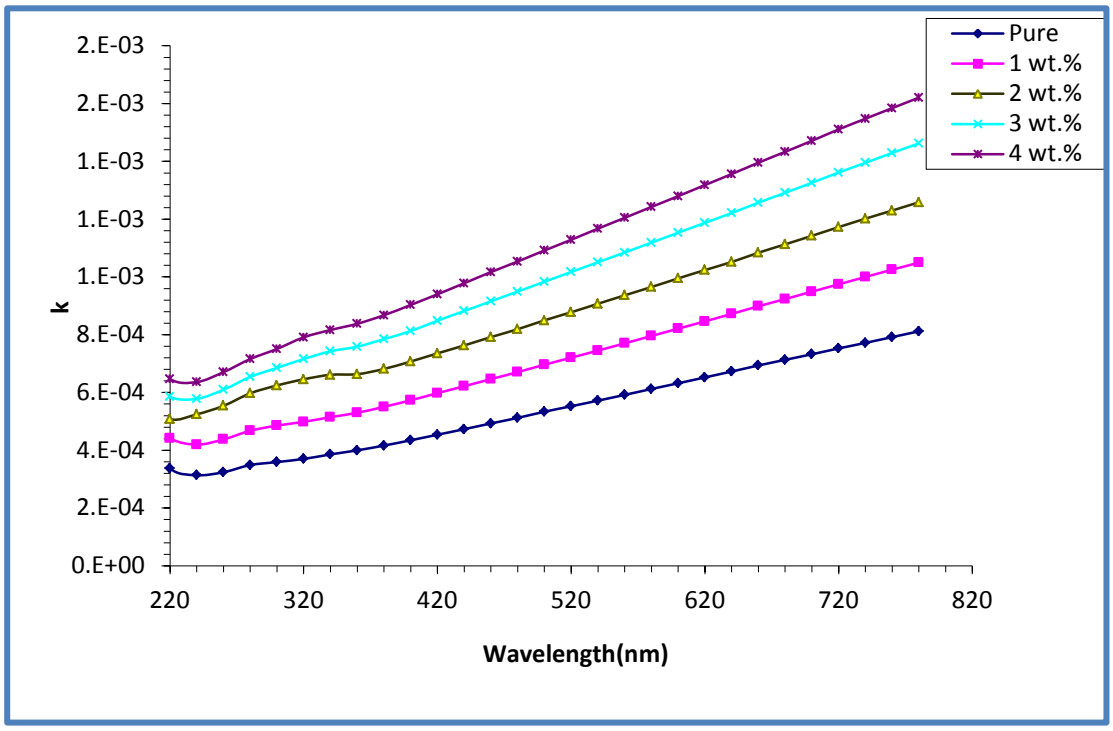

Figure (4-20) Variation of extinction coefficient for PEO-PVA -$SrTiO_3$-NiO nanocomposites with wavelength

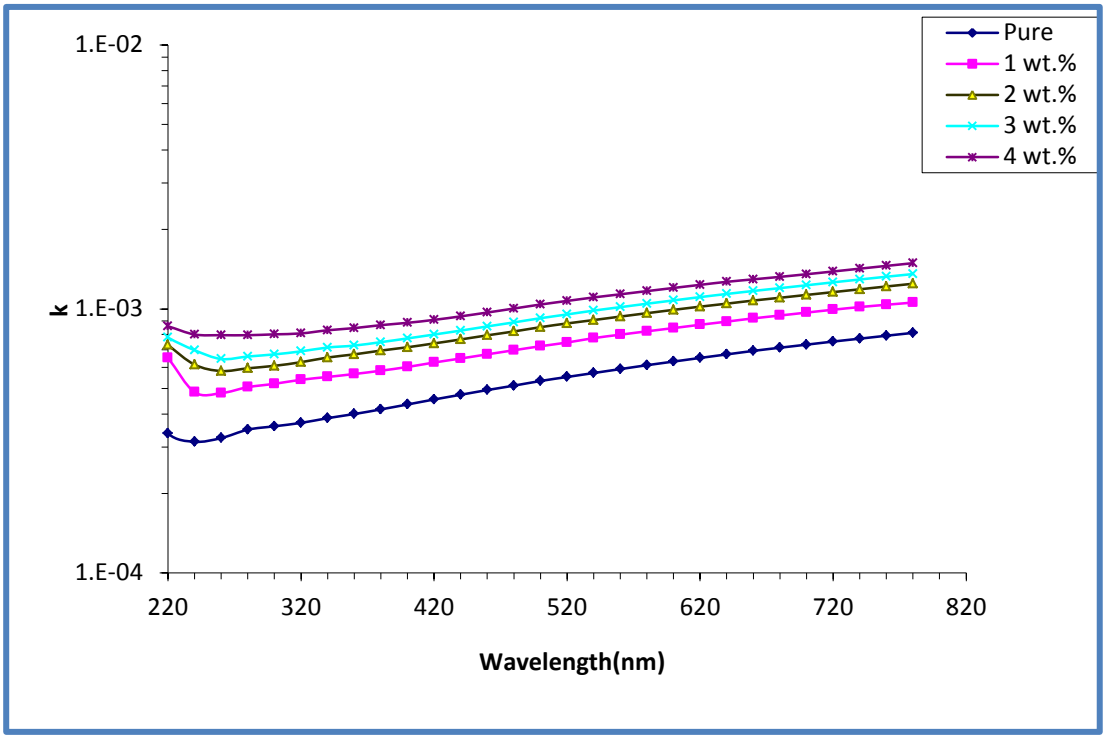

Figure (4-21) Variation of extinction coefficient for PEO-PVA -$SrTiO_3$-CoO nanocomposites with wavelength

4-3-6 Refractive Index PEO-PVA-$SrTiO_3$-NiO and PEO-PVA-$SrTiO_3$-CoO Nanocomposites

Figures (4-22) and (4-23) show viration refractive index as a function of wavelength for PEO-PVA-$SrTiO_3$-NiO and PEO-PVA-$SrTiO_3$-CoO nanocomposites. One of the reasons for the increase in reflectance PEO-PVA-$SrTiO_3$-NiO and PEO-PVA-$SrTiO_3$-CoO NCs is the refractive index increased for the doped samples because the addition of $SrTiO_3$,NiOandCoO NPs enhances the intensity of NCs by raising the PEO-PVA blend's refractive index and thereby, increasing the dispersion of the photon event. It is clear that the refractive index displays an area of dispersion at low wavelengths and practically reaches a plateau at high wavelengths.

One of a material's most fundamental characteristics is its index of refraction،which is directly tied to its electrical polarizability. The electromagnetic field of the light induces polarization in the molecules, which is reflected by the refractive index. Due to the impact of the electric field component of the incident wave, a material exposed to electromagnetic light will experience time-varying forces inside its internal charge structure. The polar character of the samples was attributed to the broad dispersion area. Polar molecules inertia prevents them from following the field alternation at high wavelengths[137].

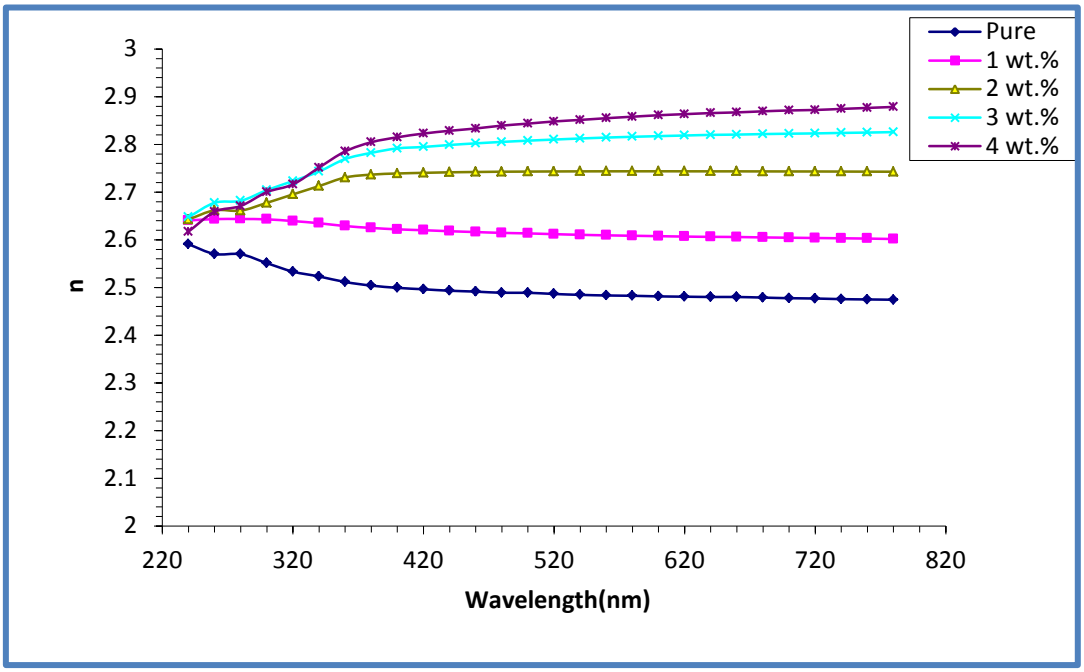

Figure (4-22) Variation of Refractive index for PEO-PVA -$SrTiO_3$-NiO NCs with wavelengt

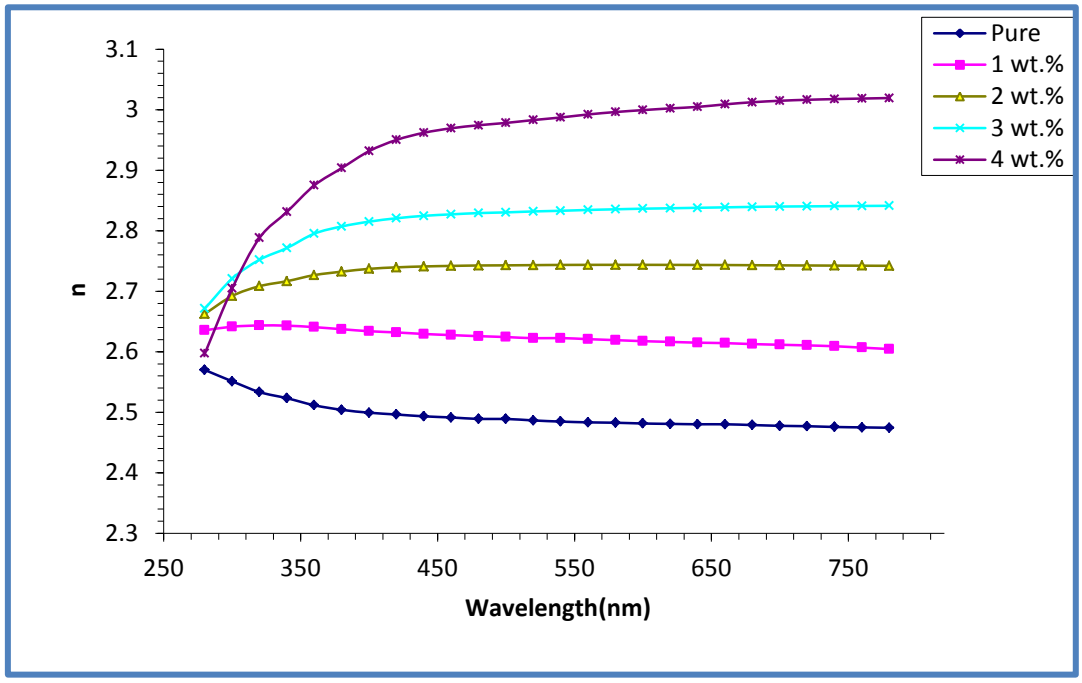

Figure (4-23) Variation of Refractive index for PEO-PVA -$SrTiO_3$-CoO NCs with wavelength

4-3-7 Real and Imaginary part of Dielectric Constant for PEO-PVA-$SrTiO_3$-NiO and PEO-PVA-$SrTiO_3$-CoO NCs

Figures (4-24 and 4-25) , (4-26 and 4-27) show the variations of real and imaginary part (ε_1,ε_2) with wavelength for PEO-PVA-$SrTiO_3$-NiO and PEO-PVA-$SrTiO_3$-CoO NCs respectively. Given that the real component is mostly proportional to the square of the refractive index, it can be seen that the real part is bigger than the imaginary part. The imaginary component is proportional to the extinction coefcient, as shown in figures (4-25) and(4-27) it increas with increasing the $SrTiO_3$,NiO and CoO NPs, but the real part is raised with increasing $SrTiO_3$,NiO and CoO NPs additive [138].

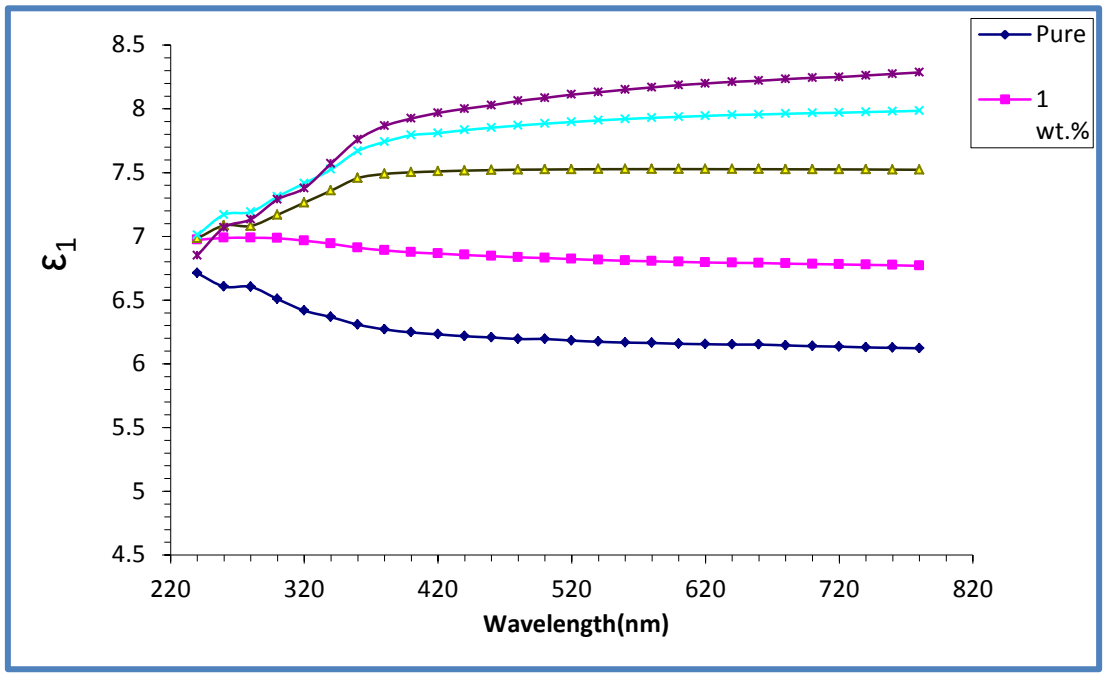

Figure (4-24) Variation real part of dielectric constant for PEO-PVA -$SrTiO_3$-NiO NCs with wavelength

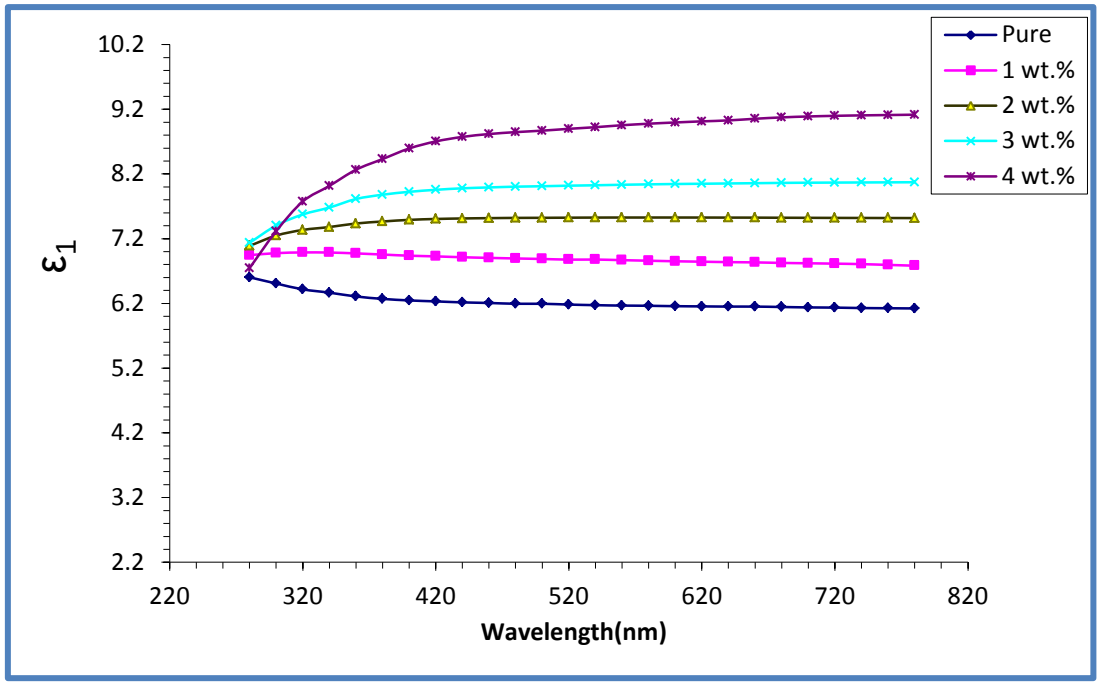

Figure (4-25) Variation real part of dielectric constant for PEO-PVA -$SrTiO_3$-CoO NCs with wavelength

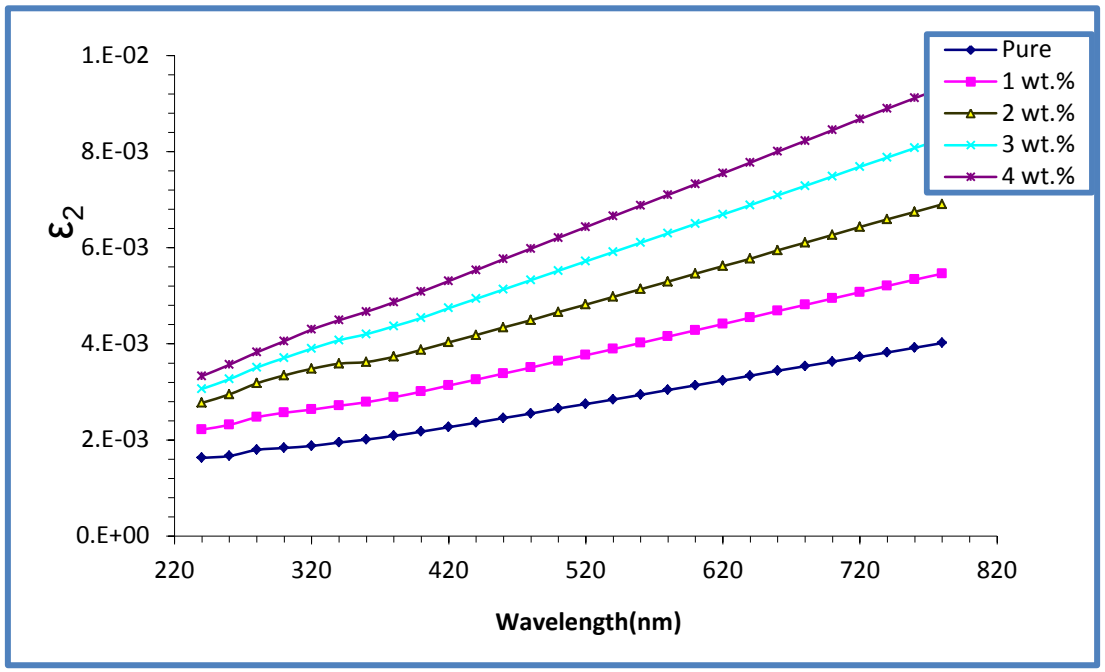

Figure (4-26) Variation imaginary part of dielectric constant for PEO-PVA - $SrTiO_3$-NiO NCs with wavelength

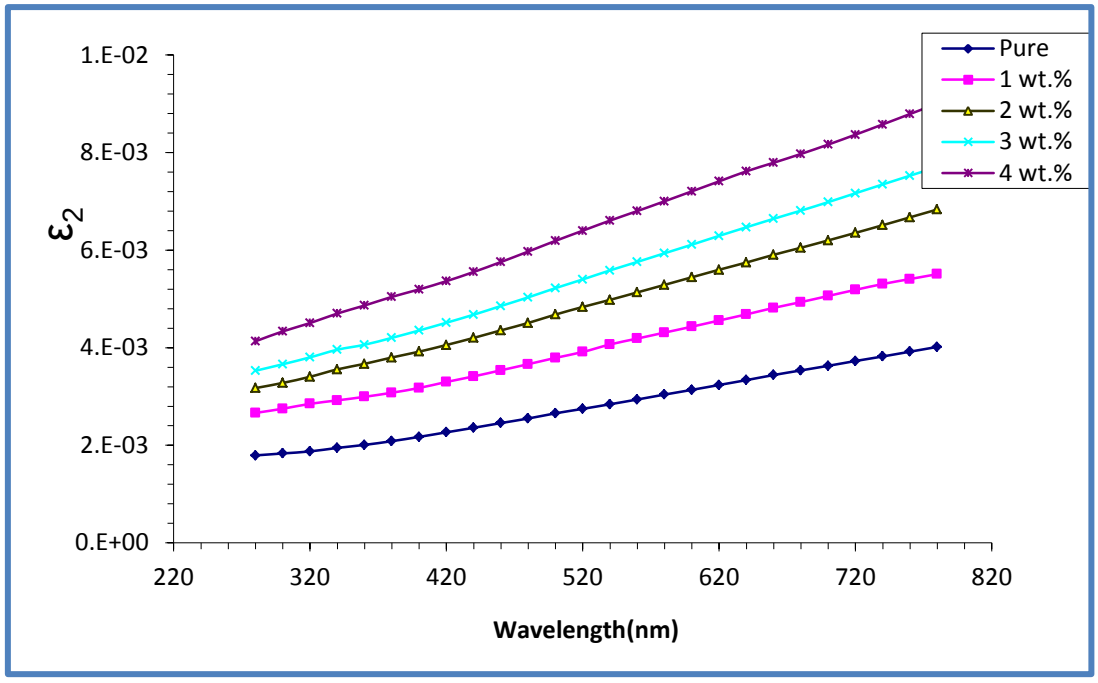

Figure (4-27) Variation imaginary part of dielectric constant for PEO-PVA - $SrTiO_3$-CoO NCs with wavelength

4-3-8 Optical conductivity for PEO-PVA-$SrTiO_3$-NiO and PEO-PVA-$SrTiO_3$-CoO NCs

Figures (4-28) and (4-29) illustrate the variety of the optical conductivity of PEO-PVA-$SrTiO_3$-NiO and PEO-PVA-$SrTiO_3$-CoO NCs with wavelength. The optical conductivity of all NCs samples diminishes as wavelength rises, which is a characteristic linked to how the optical conductivity varies depending on the wavelength of the light impinging on the NCs sample. The optical conductivity spectra shows that all NCs samples in this region have high absorbance, which raises optical conductivity at low photon wavelengths and causes the samples to transmit light in the visible and near-infrared spectrum.

Along with this, it indicates that more $SrTiO_3$,NiO and CoO nanoparticles are produced at greater concentrations, optical conductivity values rise as $SrTiO_3$, NiO and CoO concentrations. The band gap narrows as a result of this increase in conductivity, which is caused by the formation of new local levels in the band gap that make it easier for electrons to move from the valence band to the conduction band. The density of localized stages in the band structure also rises, enhancing optical conductivity and absorption coefficient. Localized levels that have formed in the energy gap are responsible for this behavior in PEO-PVA-$SrTiO_3$-NiO and PEO-PVA-$SrTiO_3$-CoO NCs [139].

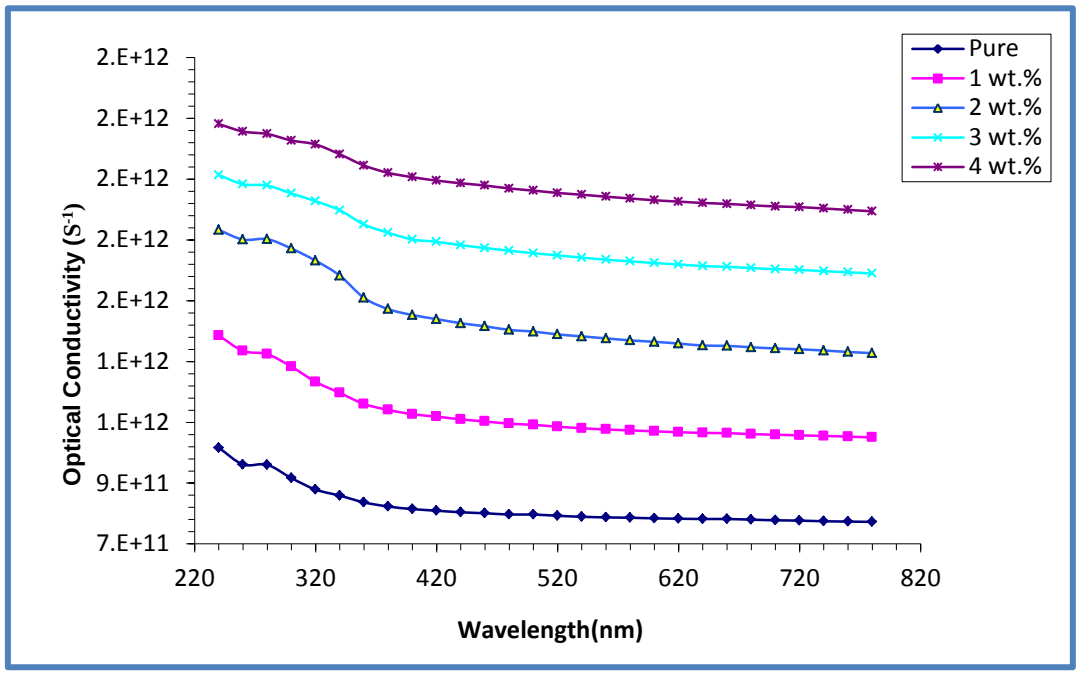

Figure (4-28) Variation of optical conductivity for PEO-PVA -$SrTiO_3$-NiO NCs with wavelength

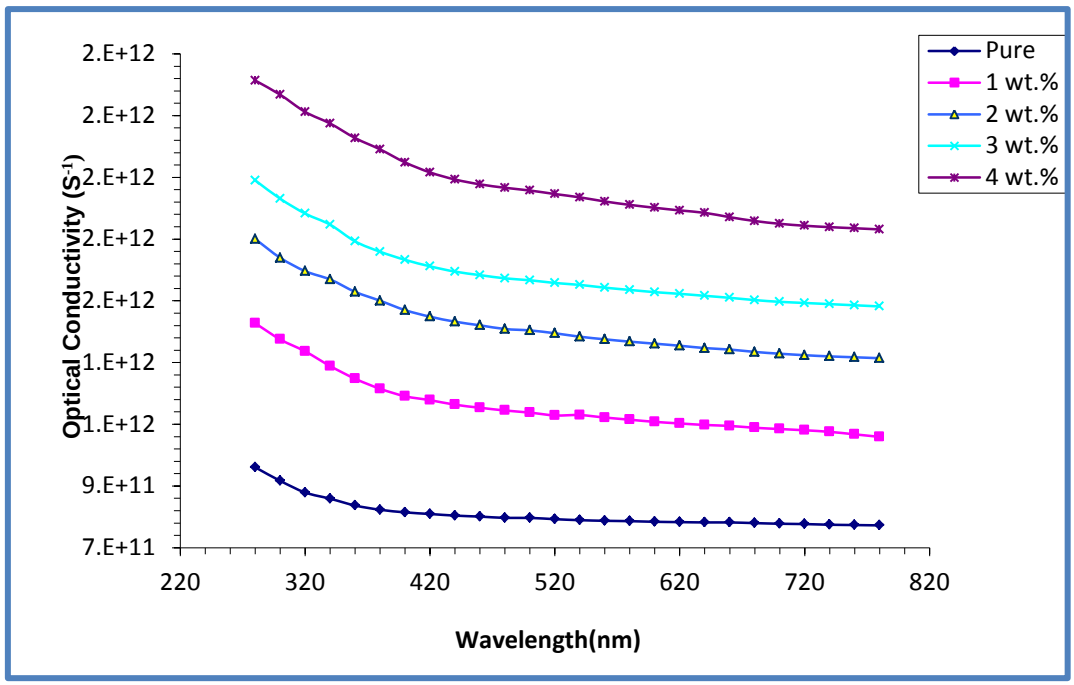

Figure (4-29) Variation of optical conductivity for PEO-PVA -$SrTiO_3$-CoO NCs- with wavelength

4-4 Electrical Measurements of Nanocomposites

4-4-1 A.C Electrical Properties of PEO-PVA-$SrTiO_3$-NiO and PEO-PVA-$SrTiO_3$-CoO Nanocomposites

A.C electrical properties of PEO-PVA-$SrTiO_3$-NiO and PEO-PVA-$SrTiO_3$-CoO nanocomposites are involved dielectric constant, dielectric loss and A.C electrical conductivity were studied in frequency ranging from (100Hz- 5MHz) at room temperature

4-4-1-1 The Dielectric Constant of PEO-PVA-$SrTiO_3$-NiO and PEO-PVA-$SrTiO_3$-CoO Nanocomposites

Figures (4-30) and (4-31) show the variation of dielectric constant versus the weight percentages of strontium titanate , nickel oxide and cobalt oxide nanoparticles in the PEO-PVA-$SrTiO_3$-NiO and PEO-PVA-$SrTiO_3$-CoO NCs , as a result, the ratio of space charge polarization to total polarization decreases. At low frequencies, space charge polarization is the most important sort of polarization, and as frequency increases, it becomes less important .

As the electric field frequency increases, the dielectric constant values for all samples of PEO-PVA-$SrTiO_3$-NiO and PEO-PVA-$SrTiO_3$-CoO NCs decrease, and different types of polarizations occur at higher frequencies. Since an ion's mass is greater than that of an electron, ionic polarized reacts to changes in field frequency in a somewhat different way than electronic polarization. This causes the electrons to react [140].

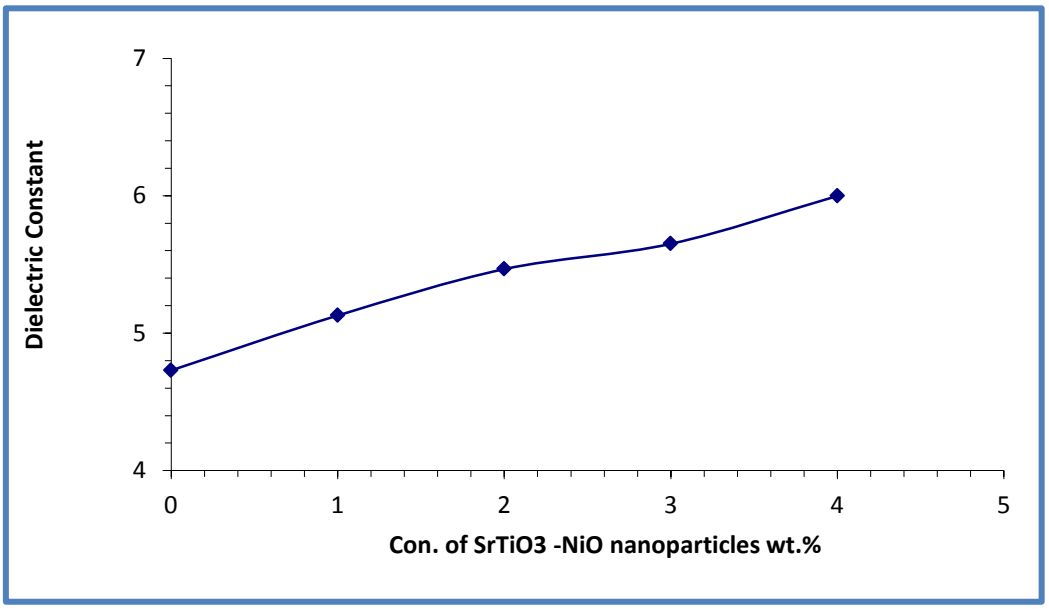

Figure (4-30) Effect of $SrTiO_3$-NiO NPs concentrations on dielectric constant for PEO-PVA blend

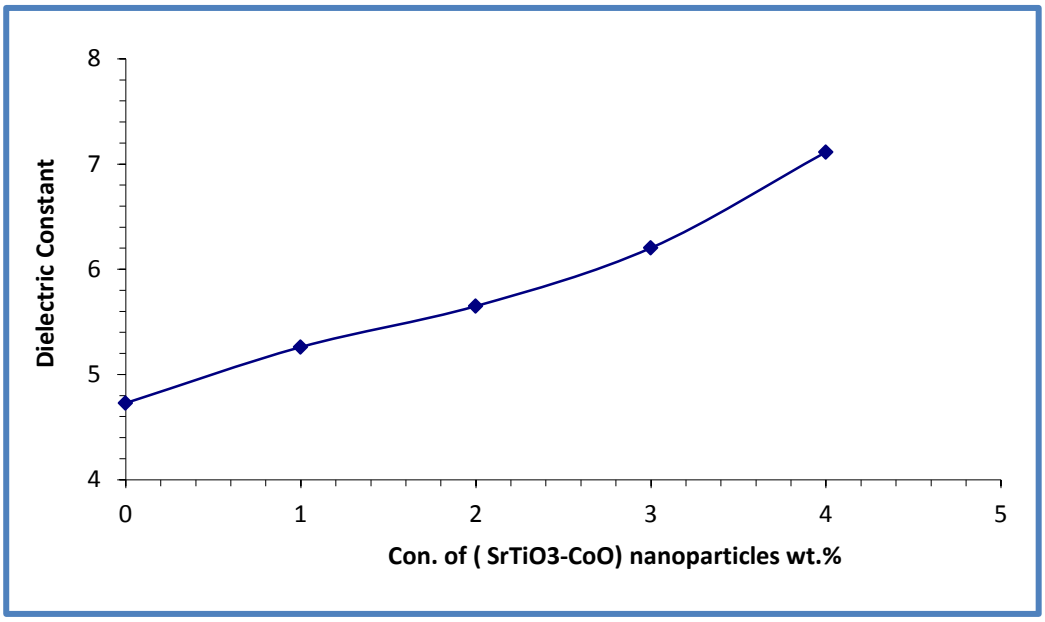

Figure (4-31) Effect of $SrTiO_3$-CoO NPs concentrations on dielectric constant for PEO-PVA blend

The plots of the variation of dielectric constant of PEO-PVA-$SrTiO_3$-NiO and PEO-PVA-$SrTiO_3$-CoO nanocomposites versus frequency are shown in figures (4-32) and (4-33) respectively .With increasing frequency, the dielectric constant for PEO-PVA-$SrTiO_3$-NiO and PEO-PVA-$SrTiO_3$-CoO nanocomposites decreases very fast due to control of the atomic and electronic influence in the PEO-PVA blend and space charge reduces gradually[141] .

At higher frequency, the dielectric constant for PEO-PVA-$SrTiO_3$-NiO and PEO-PVA-$SrTiO_3$-CoO nanocomposites becomes almost frequency independent representing the rotational motion of the polar molecules of the dielectric is not enough rapid for the achievement of equilibrium with the field. In other word, because of the electric dipoles cannot continue the frequency of the electric field and so, it stops [142]. The PEO-PVA-$SrTiO_3$-NiO and PEO-PVA-$SrTiO_3$-CoO nanocomposites have the highest dielectric constant because of the high electrical conductivity for $SrTiO_3$,NiOand CoO nanoparticles.

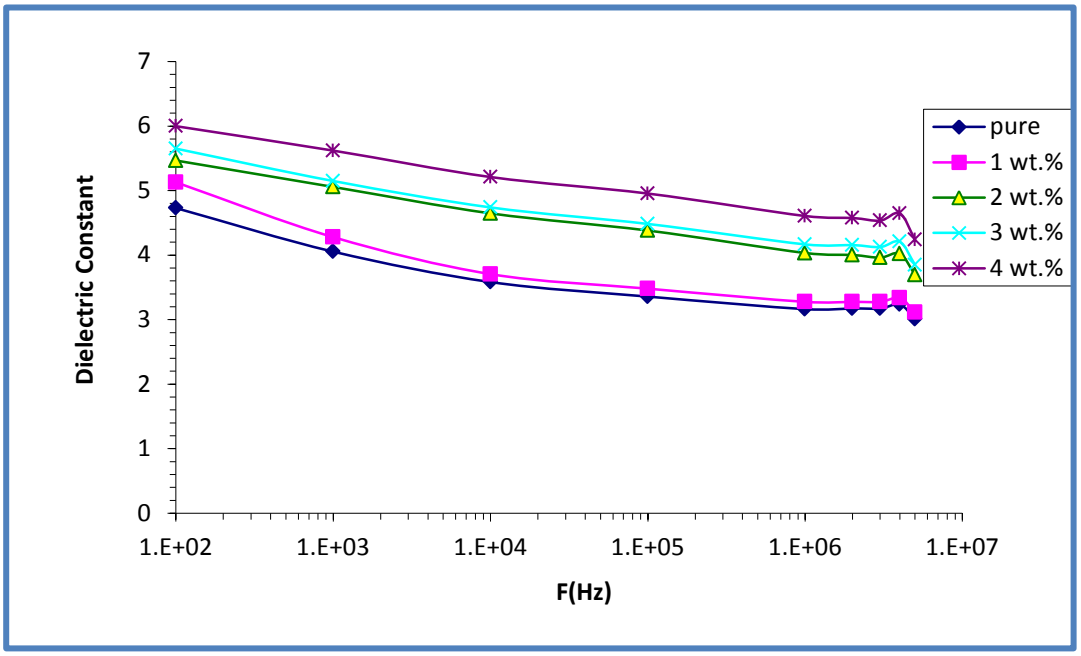

Figure (4-32) Variation of dielectric constant for PEO-PVA -$SrTiO_3$-NiO nanocomposites with frequency.

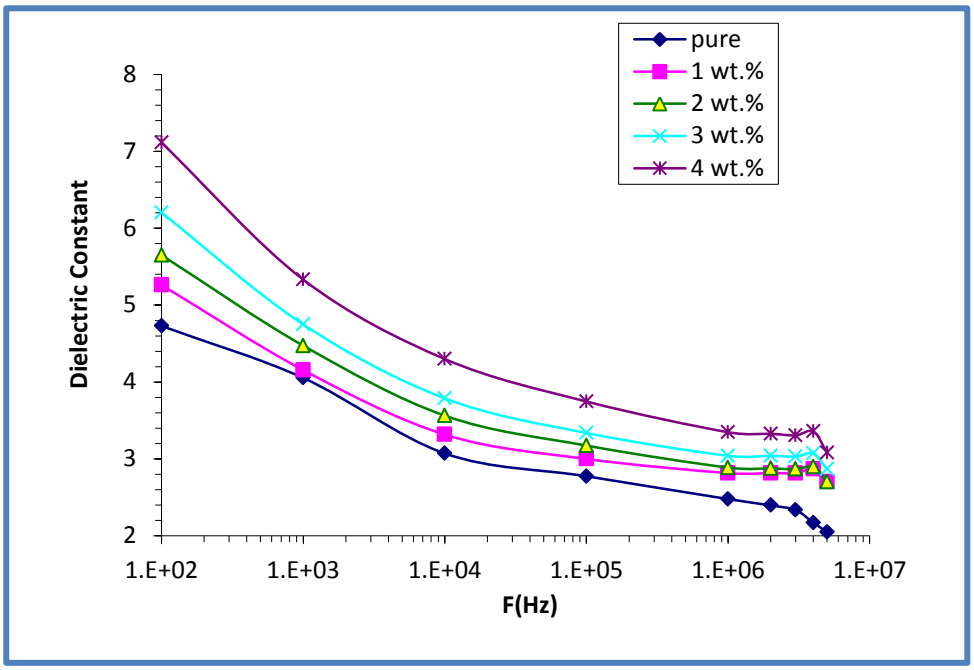

Figure (4-33) Variation of dielectric constant for PEO-PVA -$SrTiO_3$-CoO nanocomposites with frequency.

4-4-1-2 The Electrical Dielectric Loss of PEO-PVA-$SrTiO_3$-NiO and PEO-PVA-$SrTiO_3$-CoO Nanocomposites

The effect of concentrations of $SrTiO_3$, NiO and CoO nanoparticles versus dielectric loss of PEO-PVA blend shows in figures (4-34) and (4-35) at 100 Hz .The dielectric loss of PEO-PVA-$SrTiO_3$-NiO and PEO-PVA-$SrTiO_3$-CoO nanocomposites increases with increasing of the concentrations of nanoparticles . This increases due to the increase of the charge carriers number for PEO-PVA-$SrTiO_3$-NiO and PEO-PVA-$SrTiO_3$-CoO NCs. Filler of strontium titanate ,nickel oxide and cobalt oxide nanoparticles forms as a clusters when the low concentrations, but they are formed a path network in the PEO-PVA-$SrTiO_3$-NiO and PEO-PVA-$SrTiO_3$-CoO NCs when the concentration of nanoparticles reachs 4 wt.%[143].

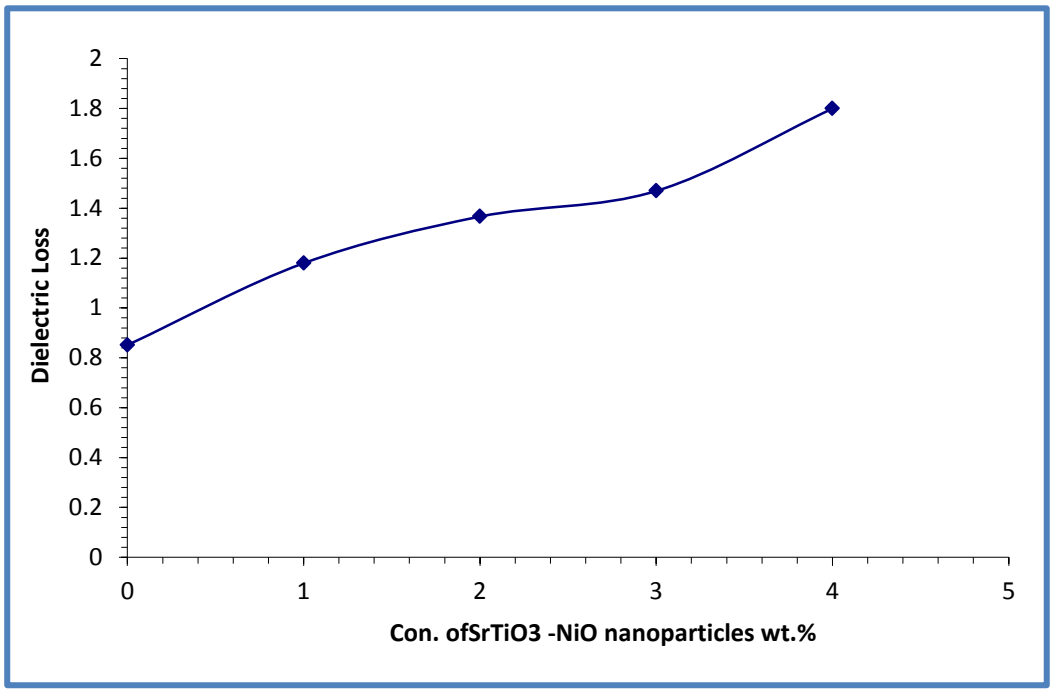

Figure (4-34) Effect of $SrTiO_3$-NiO NPs concentrations on dielectric loss for PEO-PVA blend

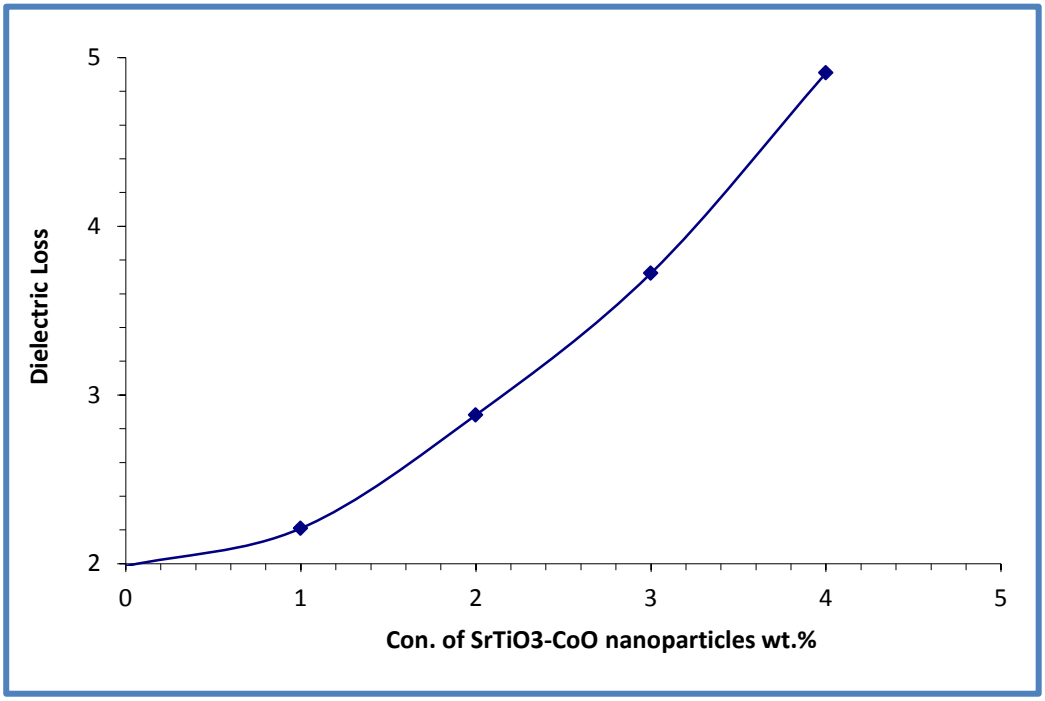

Figure (4-35) Effect of $SrTiO_3$-CoO NPs concentrations on dielectric loss for PEO-PVA blend

Figures (4-36) and (4-37) show the variation of dielectric loss of PEO-PVA-$SrTiO_3$-NiO and PEO-PVA-$SrTiO_3$-CoO NCs versus frequency respectively. For all samples of nanocomposites the dielectric loss decreases with increasing of the frequency of applied electric field, this manner attributed to the decreases of the space charge polarization contribution and associated the inability of dipoles to rotate quickly leading to a gap between frequency of oscillating dipole and that of the applied field . But the dielectric loss becomes very large for PEO-PVA-$SrTiO_3$-NiO and PEO-PVA-$SrTiO_3$-CoO nanocomposites at lower frequencies, due to free charge motion within the material. In addition; the enough time for electric dipoles to align with applied electric field before it variation electric dipoles direction; so the dielectric loss of these nanocomposites is high. These are similar with the results of researchers [144].

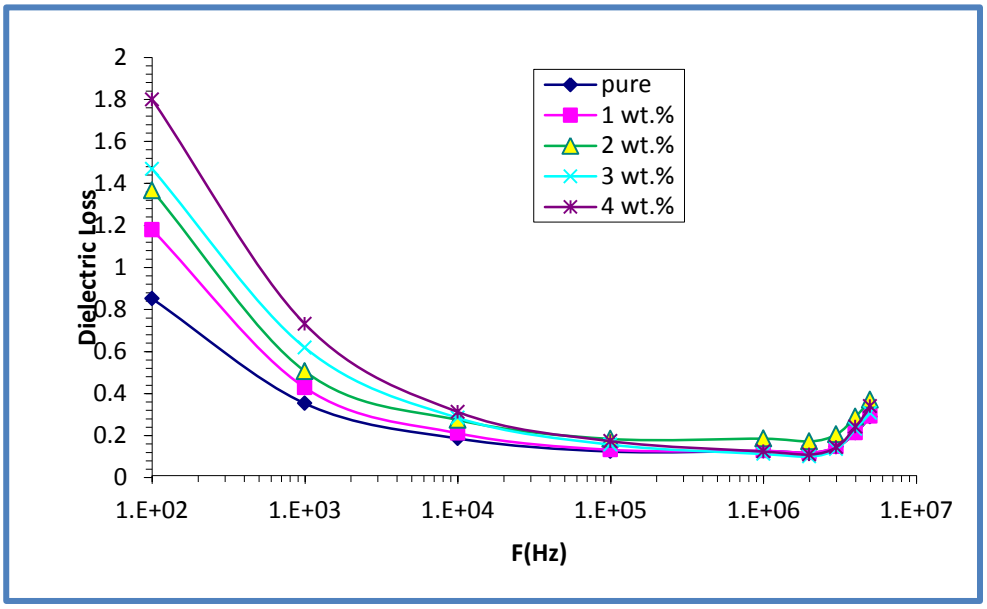

Figure (4-36) Effect of $SrTiO_3$-NiO NPs concentrations on dielectric loss for PEO-PVA blend at 100Hz

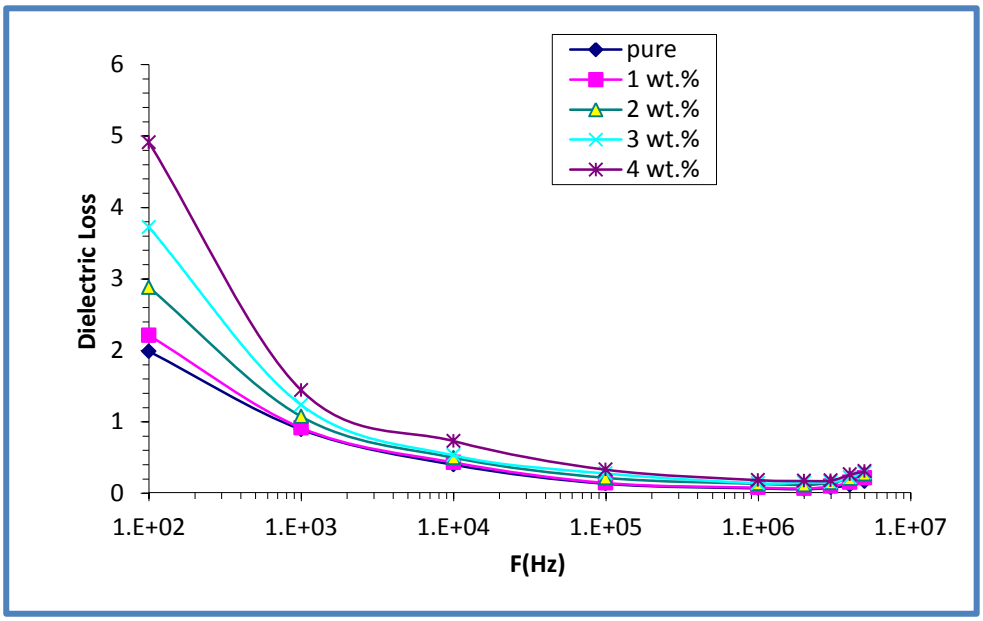

Figure (4-37) Effect of $SrTiO_3$-CoO NPs concentrations on dielectric loss for PEO-PVA blend at 100Hz

4-4-1-3 A.C Electrical Conductivity of PEO-PVA-$SrTiO_3$-NiO and PEO-PVA-$SrTiO_3$-CoO Nanocomposites

Figures (4-38) and (4-39) show the variation of A.C electrical conductivity for PEO-PVA-$SrTiO_3$-NiO and PEO-PVA-$SrTiO_3$-CoO nanocomposites versus concentrations of nanoparticles at100Hz respectively. By increasing strontium titanate , nickel oxide and cobalt oxide nanoparticles concentrations, the A.C electrical conductivity of nanocomposites increases. This is attributed to the increase in the number of charge carriers due to dopant nanoparticles composition which reduces the resistance of nanocomposites gradually and increases the A.C electrical conductivity[145].

Beside that; the strontium titanate , nickel oxide and cobalt oxide nanoparticles form a path network in the nanocomposites especially at concentrations of nanoparticles 4 wt.% for PEO-PVA-$SrTiO_3$-NiO and PEO-PVA-$SrTiO_3$-CoO nanocomposites .

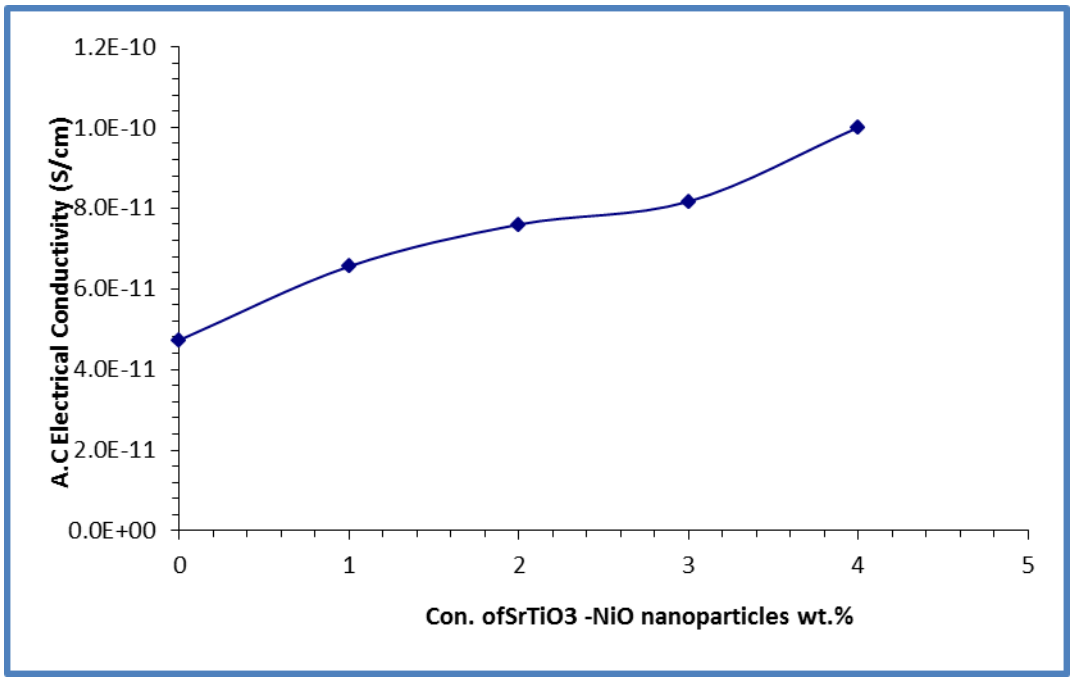

Figure (4-38) effect of $SrTiO_3$-NiO NPs concentrations on A.C electrical conductivity for PEO-PVA blend

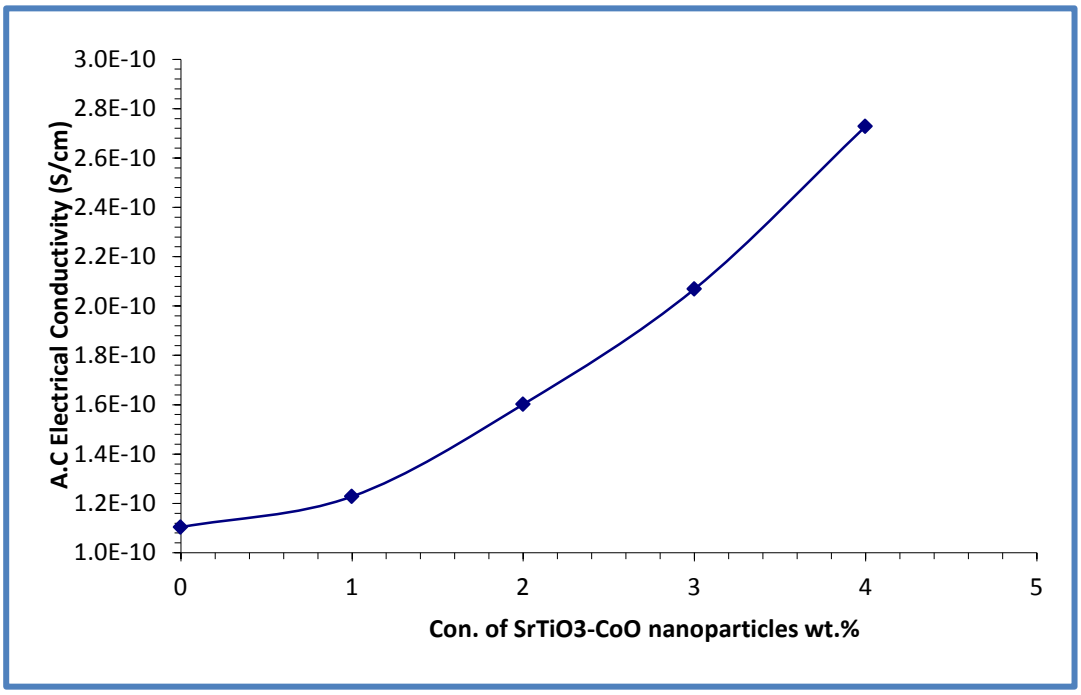

Figure (4-39) effect of $SrTiO_3$-CoO NPs concentrations on A.C electrical conductivity for PEO-PVA blend

Figures (4-40) and (4-41) show the variation of A.C electrical conductivity of PEO-PVA-$SrTiO_3$-NiO and PEO-PVA-$SrTiO_3$-CoO nanocomposites versus frequency at room temperature respectively. By increasing of the frequency of electric field, the A.C electrical conductivity increases for all samples of nanocomposites, where the

frequency acts as a pumping force, pushing the charge carriers between the different conduction states. PEO-PVA blend which form localized levels below the conduction band. This means the mobility of charge carriers and the hopping of ions from the cluster [146] .

In the low frequency, more charge accumulation occurred at the electrode and electrolyte interface, leading to a decrease in the number of the ionization processes for $SrTiO_3$,NiO and CoO nanoparticles for PEO-PVA blend. As high frequency region; the mobility of charge carriers was higher. Hence the electrical conductivity increases with frequency for PEO-PVA-$SrTiO_3$-NiO and PEO-PVA-$SrTiO_3$-CoO nanocomposites . This is similar to the results of the researchers [147].

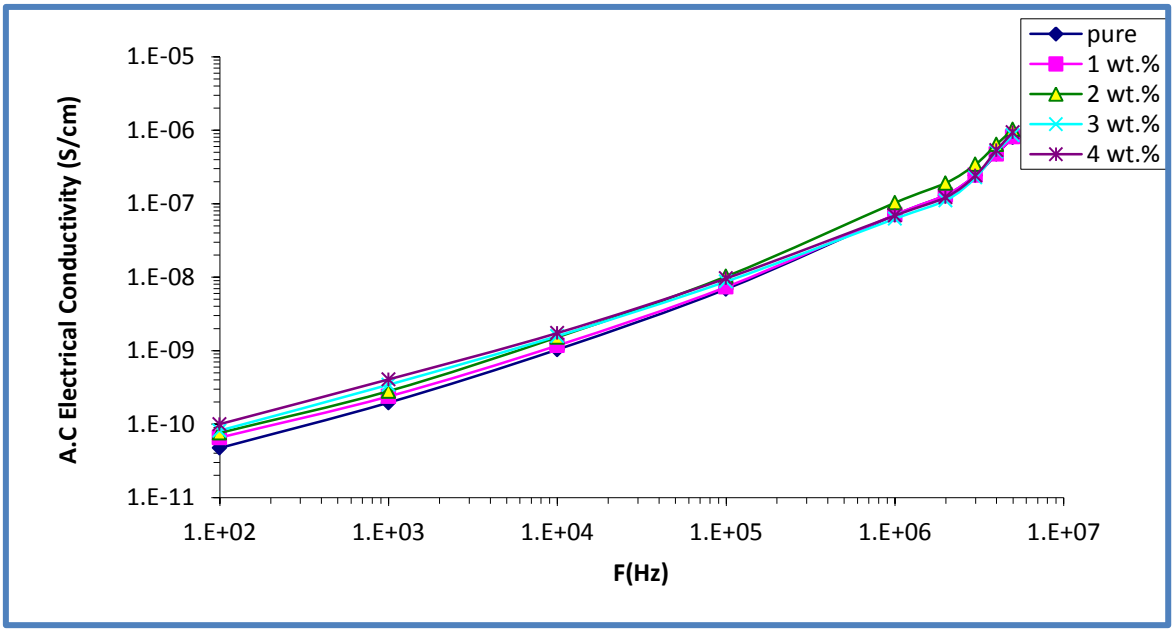

Figure (4-40) Variation of A.C electrical conductivity for PEO-PVA -$SrTiO_3$-NiO nanocomposites with frequency

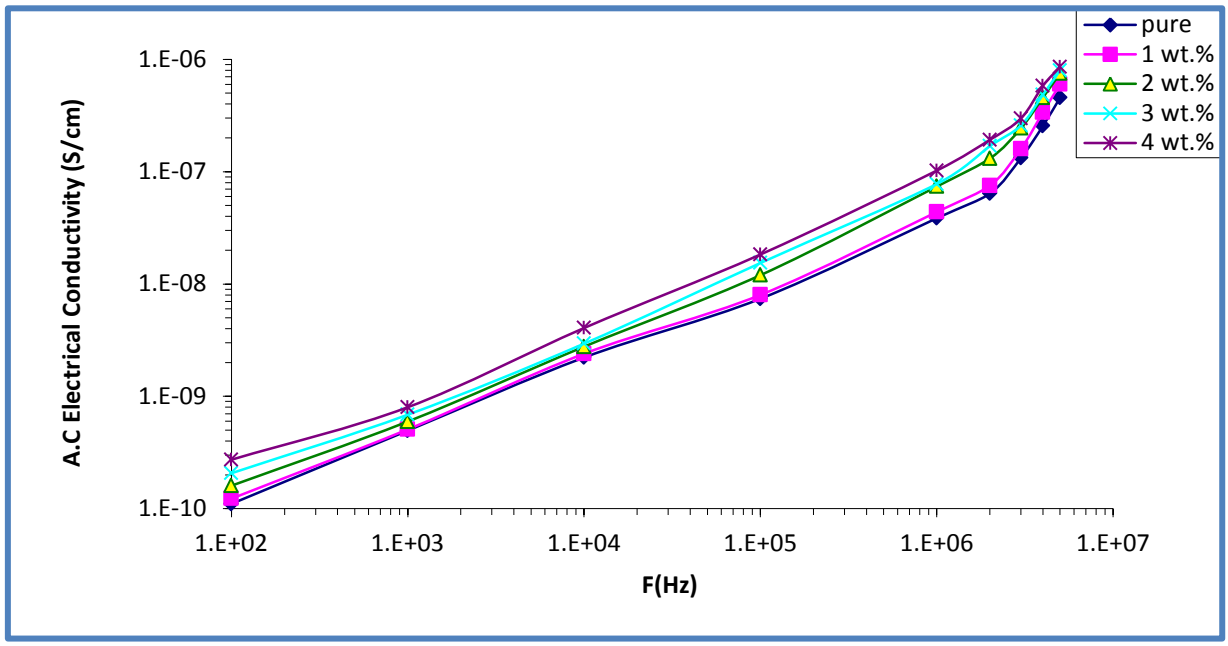

Figure (4-41) Variation of A.C electrical conductivity for PEO-PVA -$SrTiO_3$-CoO nanocomposites with frequency

4-5 Application of PEO-PVA-$SrTiO_3$-NiO and PEO-PVA-$SrTiO_3$-CoO Nanocomposites for Antibacterial Activity

Each of PEO-PVA-$SrTiO_3$-NiO and PEO-PVA-$SrTiO_3$-CoO nanocomposites can be operated as antibacterial.The inhibition zone of the Staphylococcus aureus and Escherichia coli respectively illustrate in images (4-42) and (4-43). The inhibition zone of *S. aureus* and *E. coli* illustration figures (4-44 and 4-45) and figures (4-46 and 4-47) respectively as a function of the concentrations of strontium titanate , nickel oxide and cobalt oxide nanoparticles for nanocomposites. With increasing the percentage of strontium titanate , nickel oxide and cobalt oxide nanoparticles, the inhibition zone of these bacterial is increased.

The possible mechanism of action is that the PEO-PVA-$SrTiO_3$-NiO and PEO-PVA-$SrTiO_3$-CoO nanocomposites are carrying the positive charges and the bacterial are having the negative charges which create the electromagnetic attraction between the nanoparticles of nanocomposites and the bacterial. When the attraction is made, the bacterial get oxidized and die instantly. There is a possibility of another mechanism for the last two concentrations that caused the antibacterial activity of nanocomposites by the nanoparticles that PEO-PVA-$SrTiO_3$-NiO and PEO-PVA-$SrTiO_3$-CoO nanocomposites released (electron-hole)

pairs by exposure to the visible or ultraviolet ray[148,149]. Hence, water can be interacted with electron and hole to form hydroxide (-OH) and ion of hydrogen (^{+}H). Besides that, molecular of oxygen can be interact with each of PEO-PVA-$SrTiO_3$-NiO and PEO-PVA-$SrTiO_3$-CoO nanocomposites to produce peroxide anion (O^{-}_2) which can be react with (^{+}H) to form hydrogen peroxide (H_2O_2) then, hydrogen peroxide (H_2O_2) reacts with (^{+}H) and electron (e) to generates hydrogen peroxide (H_2O_2) molecules which the generation basically depends on the surface of strontium titanate and nickel oxide and cobalt oxide NPs[150] .

Hydrogen peroxide (H_2O_2) is the only can be to penetrates and destroy the membrane of cell bacterial. Due to the negative charges of the membrane of bacterial, Each of the superoxide anion (O^{-}_2) and hydroxyl radicals (OH) cannot be to penetrates its. So, they are stayed on the membrane surface. But the interaction between illumination and (superoxide and hydroxyl) radicals leads to generate oxidative stress finally, inhibit bacterial proliferation.

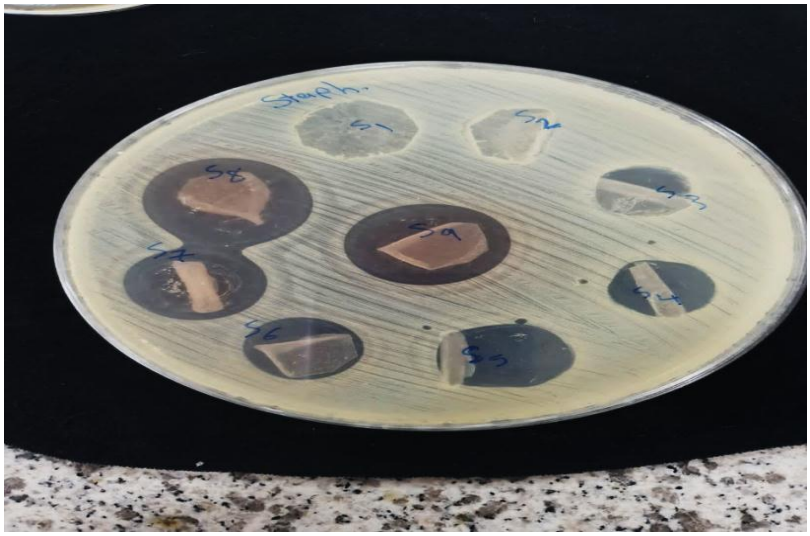

Figure (4-42) images antibacterial effect of PEO-PVA blend as a function of $SrTiO_3$-NiO NPs concentrations on S. aureus

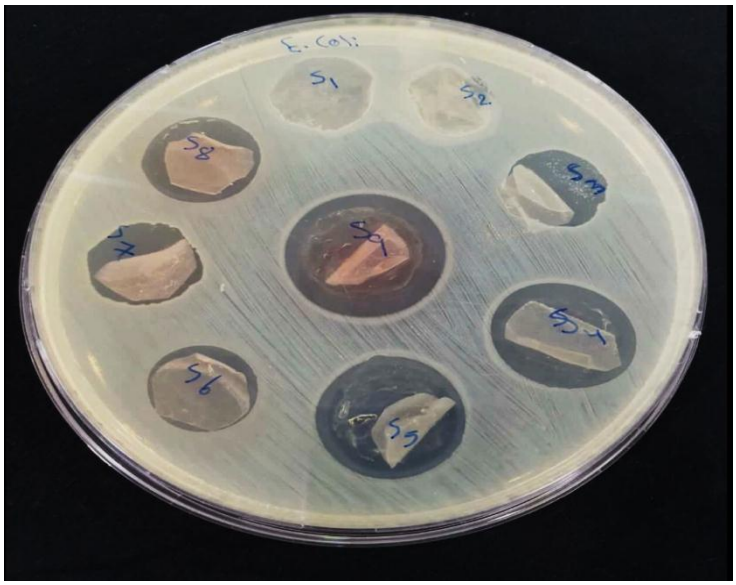

Figure (4-43) images antibacterial effect of PEO-PVA blend as a function of $SrTiO_3$-CoO NPs concentrations on E.coli

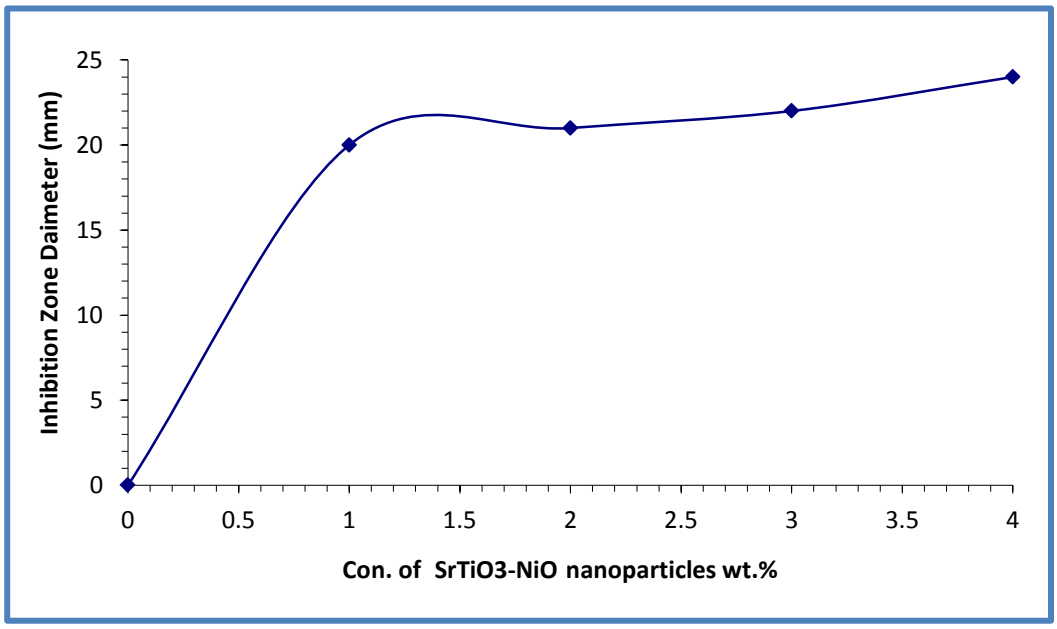

Figure (4-44) Antibacterial effect of PEO-PVA blend as a function of $SrTiO_3$-NiO NPs concentrations on S. aureus

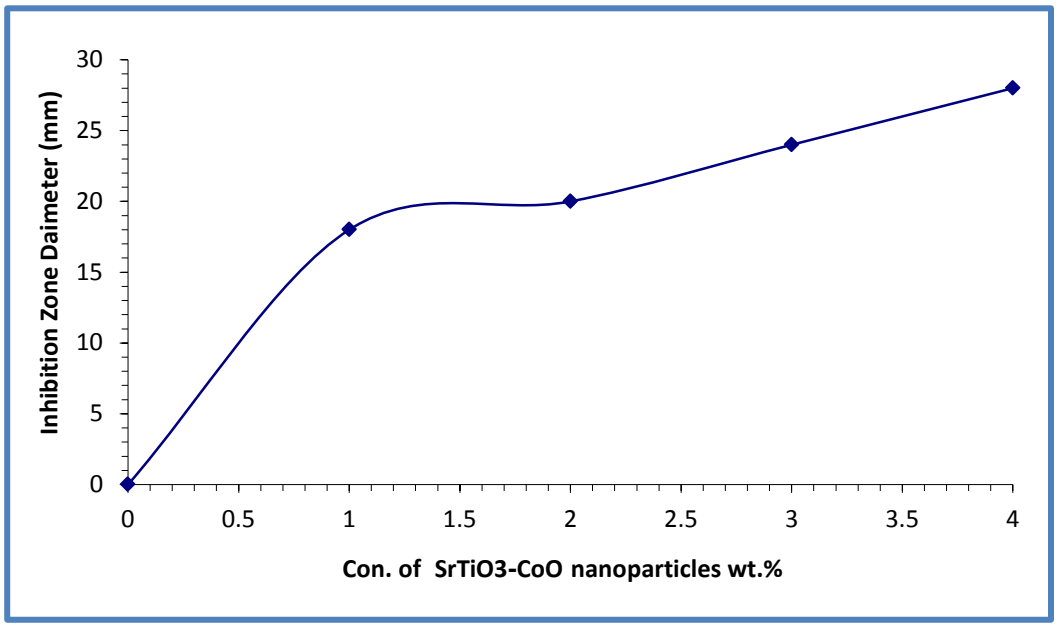

Figure (4-45) Antibacterial effect of PEO-PVA blend as a function of $SrTiO_3$-CoO NPs concentrations on S. aureus

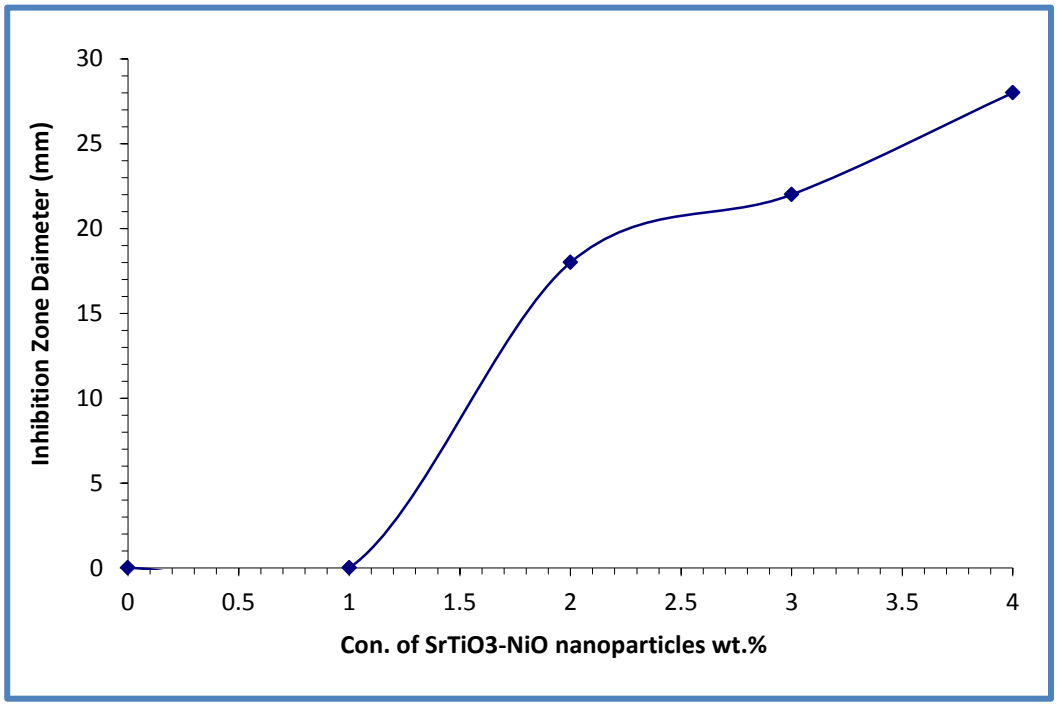

Figure (4-46) Antibacterial effect of PEO-PVA blend as a function of $SrTiO_3$-NiO NPs concentrations on E. coli1

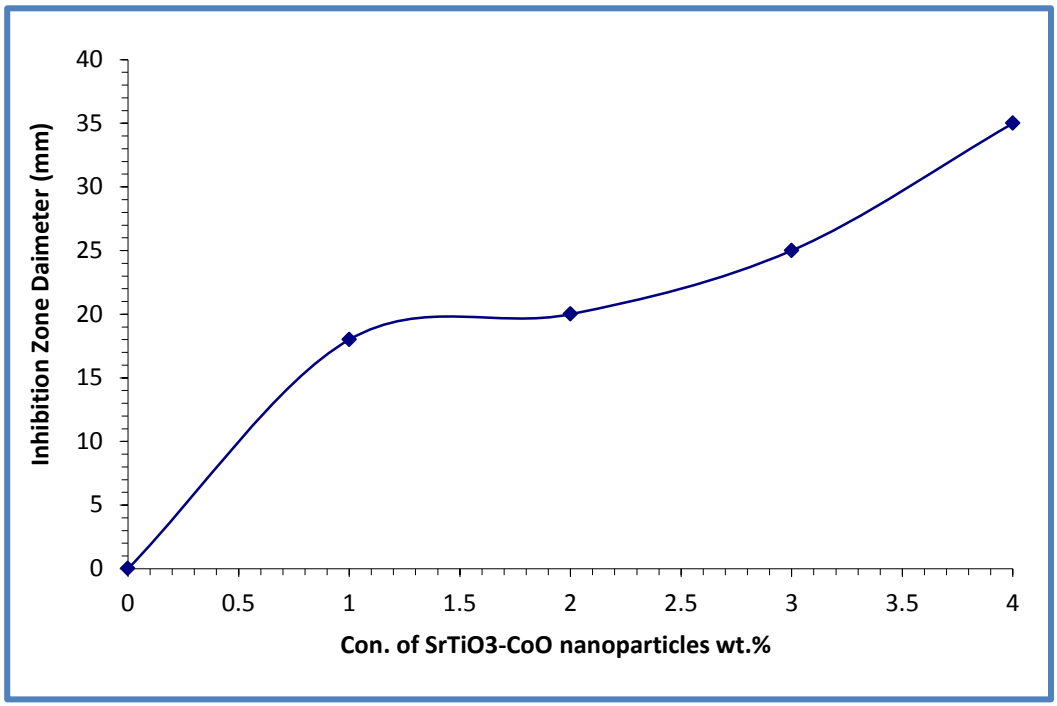

Figure (4-47) Antibacterial effect of PEO-PVA blend as a function of $SrTiO_3$-CoO NPs concentrations on E. coli1

4-6 Application of PEO-PVA-$SrTiO_3$-NiO and PEO-PVA-$SrTiO_3$-CoO Nanocomposites for Pressure Sensors

Figures (4.48) and (4.49) depicts the parallel capacitance of PEO-PVA-$SrTiO_3$-NiO and PEO-PVA-$SrTiO_3$-CoO nanocomposites with the pressure. This figures show that the capacitance of nanocomposites increases as pressure rises . The nanocomposite samples include an internal dipole moment. This is called a dipole moment. If there are no forces (electrical or mechanical), the net dipole is in a straight line, as momentum equals zero. As the strain gets bigger, these dipole moments will cause local distributions to change when they are applied to the samples, creating an electric field. Because of this electric field, there are charges above and below the sample [151].

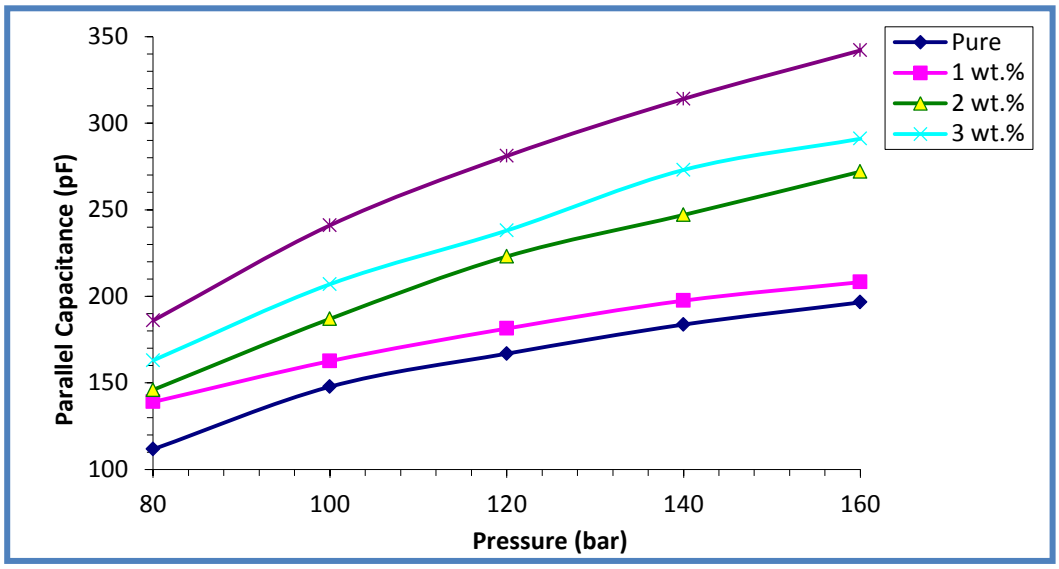

Figure (4-48) Variation of parallel capacitance for PEO/PVA /$SrTiO_3$/NiO nanocomposites with pressure.

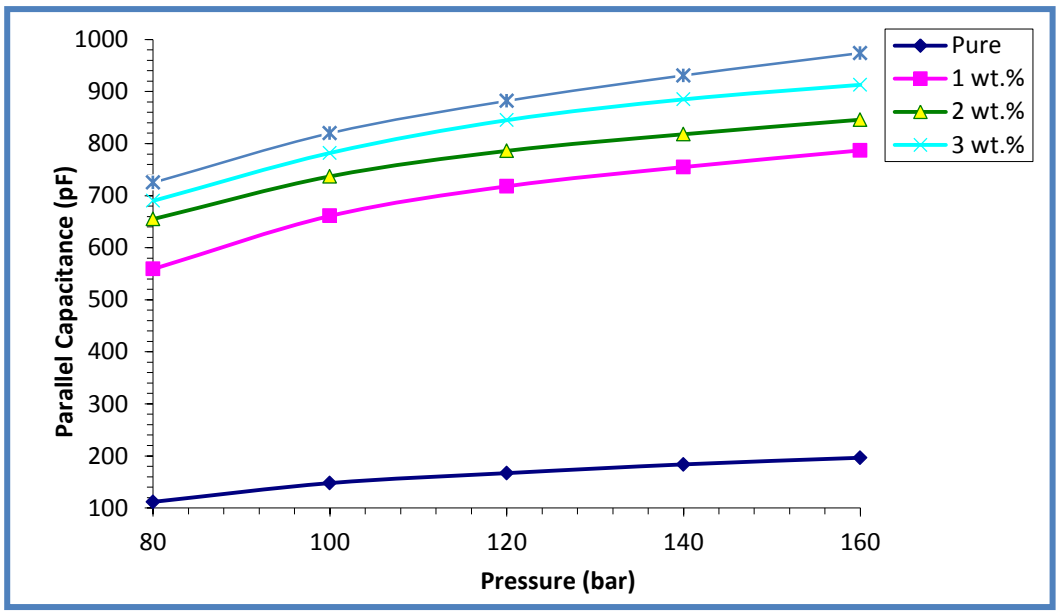

Figure (4-49) Variation of parallel capacitance for PEO-PVA -$SrTiO_3$-CoO nanocomposites with pressure

The influence of $SrTiO_3$,NiO and CoO nanoparticles on the electrical capacitance (Cp) for PEO-PVA-$SrTiO_3$-NiO and PEO-PVA-$SrTiO_3$-CoO NCs is shown in figures (4.50) and (4.51) at 80 bars. It is clear from this graph that the electrical capacitance of nanocomposites increases as the concentration of $SrTiO_3$,NiO and CoO nanoparticles

concentration increases. This might be related to an increase in charge carrier density in nanocomposites [152]

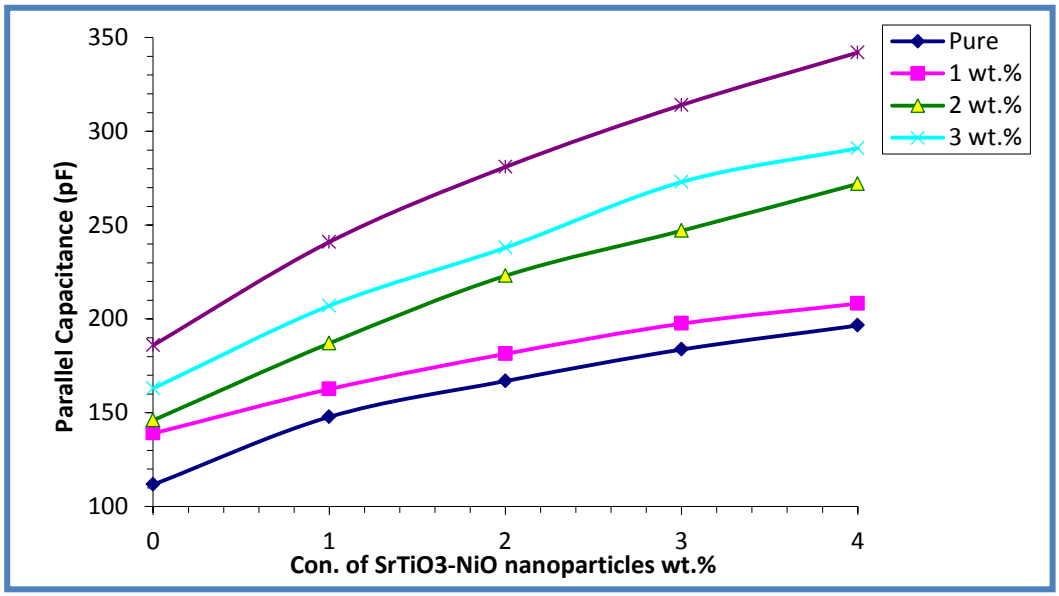

Figure (4-50) Effect of $SrTiO_3$-NiO nanoparticles concentrations on parallel capacitance for PEO-PVA -$SrTiO_3$-NiO nanocomposites.

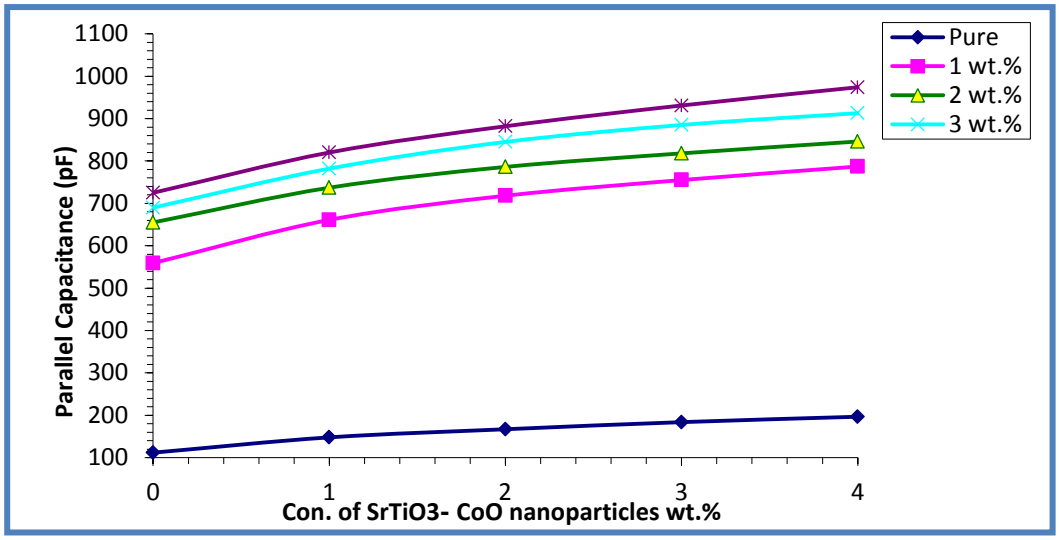

Figure (4-51) Effect of $SrTiO_3$-CoO nanoparticles concentrations on parallel capacitance for PEO-PVA -$SrTiO_3$-CoO nanocomposites

The influence of $SrTiO_3$,NiO and CoO nanoparticles on sensitivity for PEO-PVA-$SrTiO_3$-NiO and PEO-PVA-$SrTiO_3$-CoO NCs is shown in figures (4-52) and (4-53). It is clear from this graph that the sensitivity of nanocomposites increases as the concentration of $SrTiO_3$,NiO and CoO nanoparticles concentration increases. This is due to internal dipole moment [153].

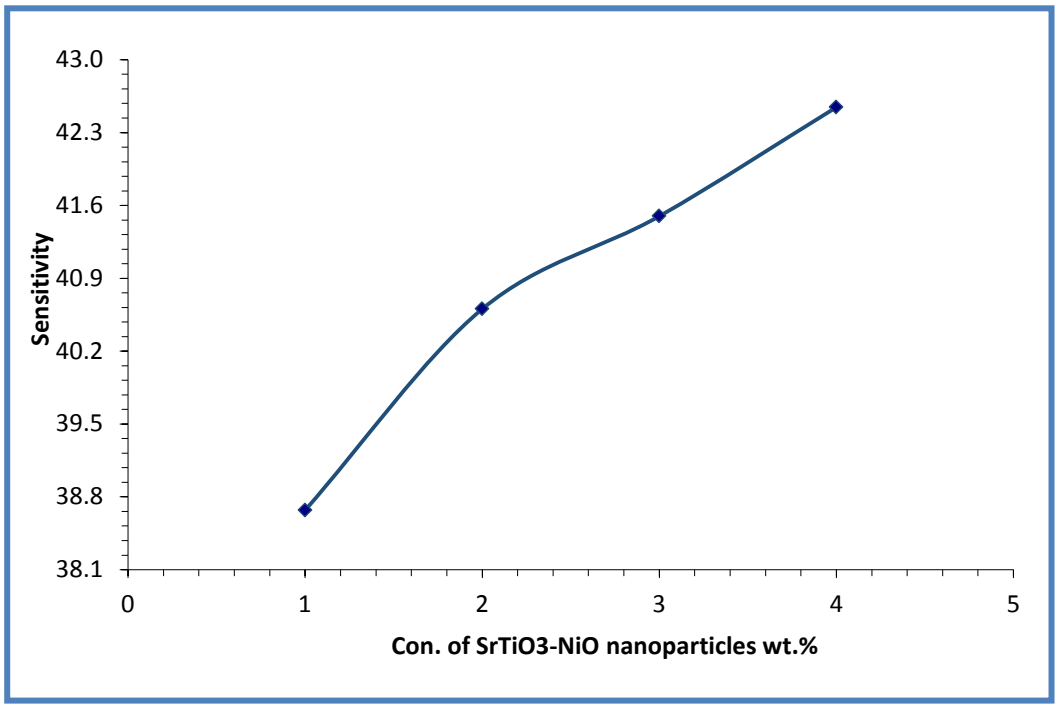

Figure (4-52) The influence of $SrTiO_3$-NiO NPs concentration on sensitivity for PEO-PVA-$SrTiO_3$-NiO NCs.

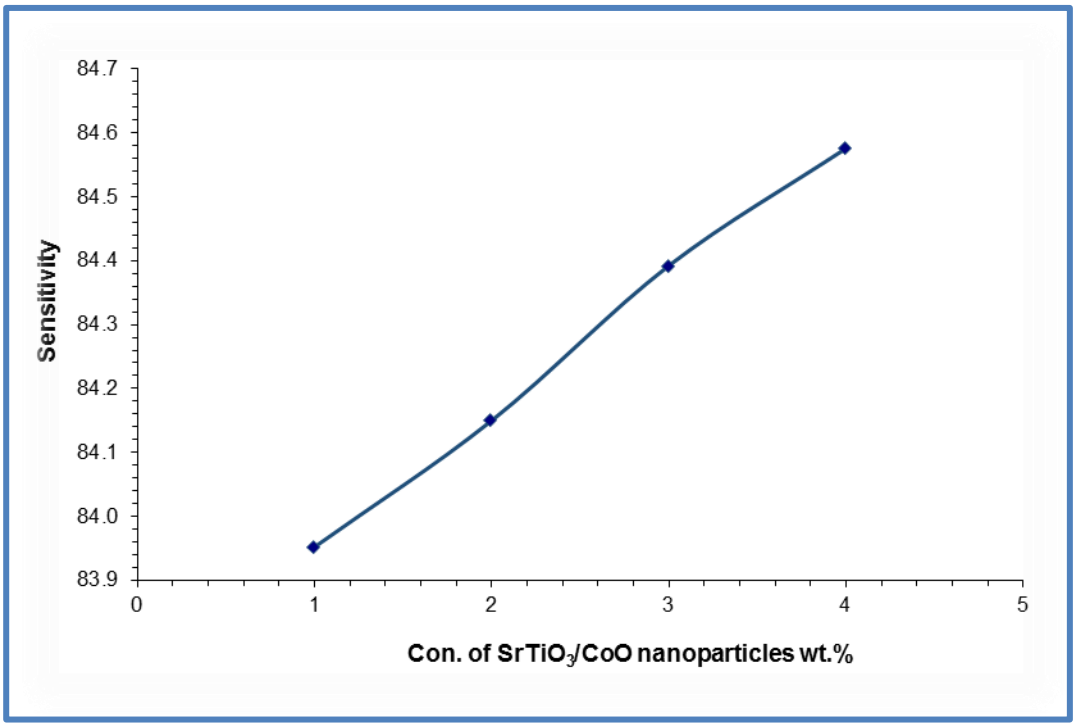

Figure (4-53) The influence of $SrTiO_3$-CoO NPs concentration on sensitivity for PEO-PVA-$SrTiO_3$-CoO NCs

4-7Application of PEO-PVA-$SrTiO_3$-NiO and PEO-PVA-$SrTiO_3$-CoO NCs For Gamma Ray Shielding.

Fluctuation of (N/No) for a mixture of PEO-PVA with various quantities of $SrTiO_3$, NiO and CoO nanoparticles is shown in figures(4-54)and (4-55) . When increasing concentration of SrTiO3,NiO and CoO nanoparticles, the transmission radiation decreases. This happens due to an increase in the attenuation radiation [154]. Figures (4-56)and (4-57) shows increasing Ln(N/No) of PEO-PVA mixture with increasing $SrTiO_3$,NiO and CoO NPs concentrations[155].

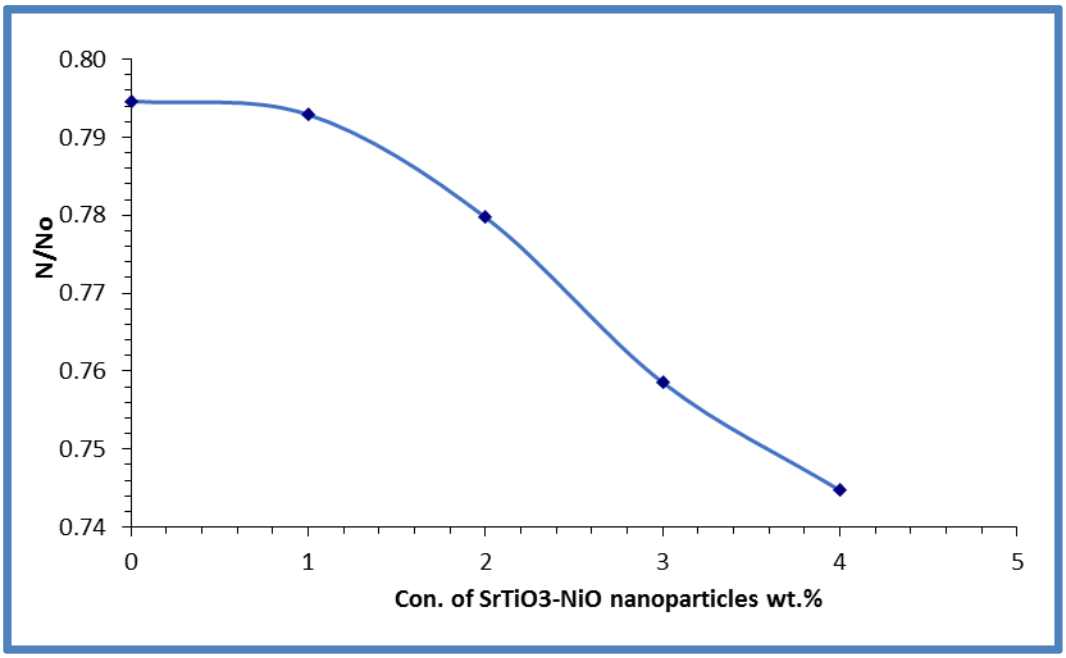

Figure (4-54) of (N/No) for PEO-PVA blend with various $SrTiO_3$-NiO Variation nanoparticle concentrations

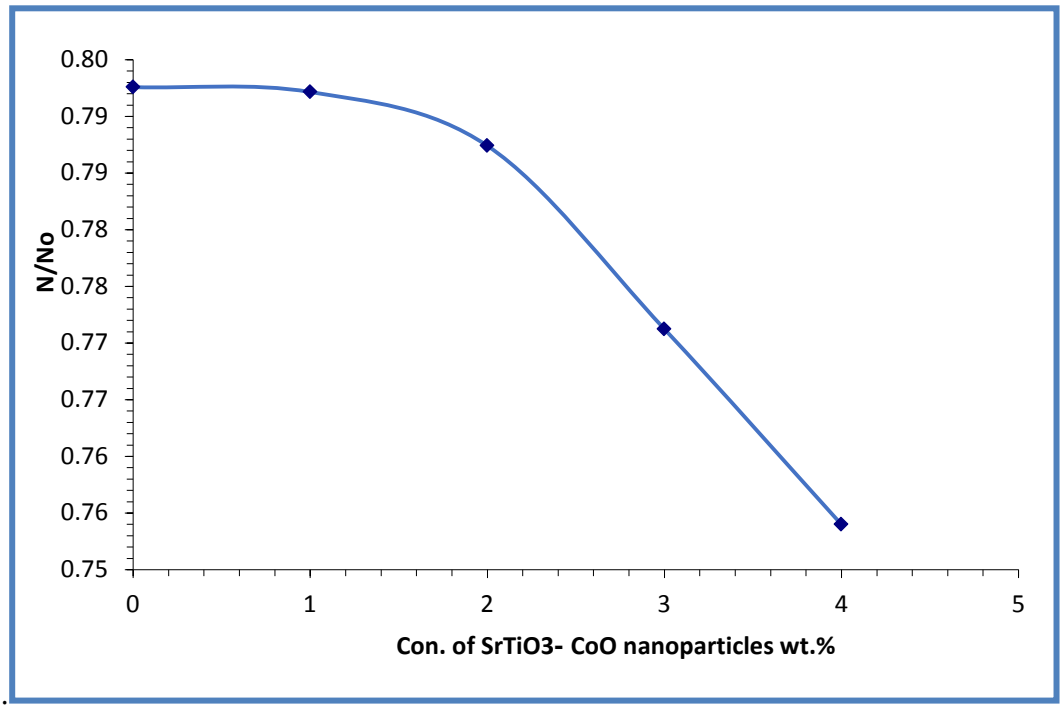

Figure (4-55) of (N/No) for PEO/PVA blend with various $SrTiO_3$-CoO Variation nanoparticle concentrations

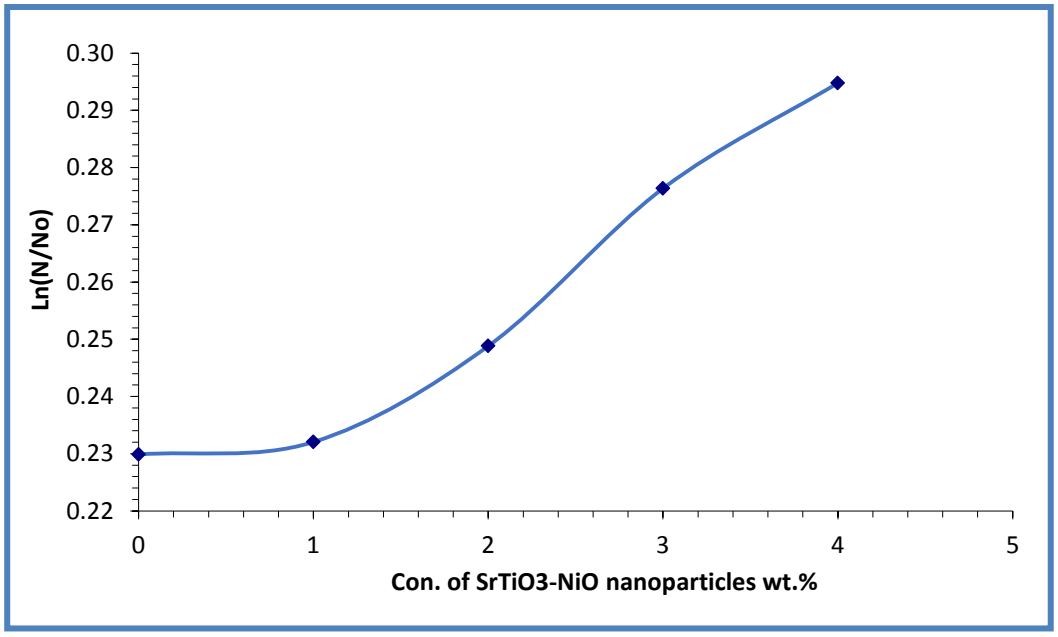

Figure (4-56) Change of Ln(N/No) for PEO-PVA mixture with different concentrations of $SrTiO_3$-NiO nanoparticles.

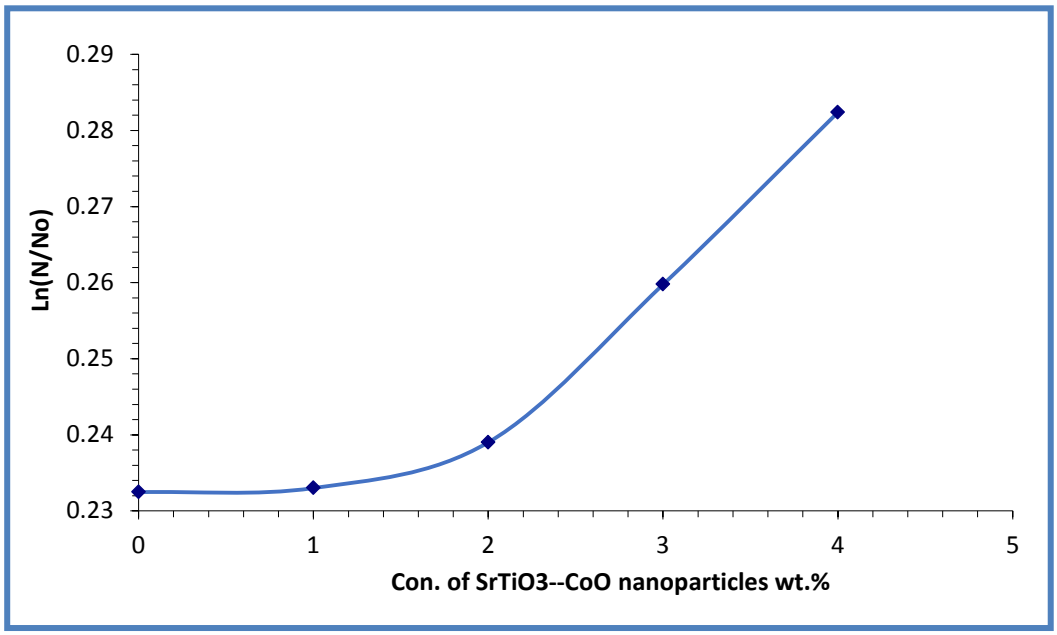

Figure (4-57) Change of Ln(N/No) for PEO-PVA mixture with different concentrations of $SrTiO_3$-CoO nanoparticles.

Figures(4-58)and (4-59) shows attenuation coefficient for the PEO-PVA mixture, with varying of $SrTiO_3$,NiO and CoO nanoparticles. When the results of polymer nanocomposites and concrete in the figure below were compared, they looked very similar. However, the composite polymer was better than concrete because it was more mobile, had no electrical properties and could prevent neutrons from escaping. The attenuation coefficients rise with increasing $SrTiO_3$,NiO and CoO nanoparticles. This is because shielding materials are made of nanocomposites, which either absorb or reflect gamma rays [156]

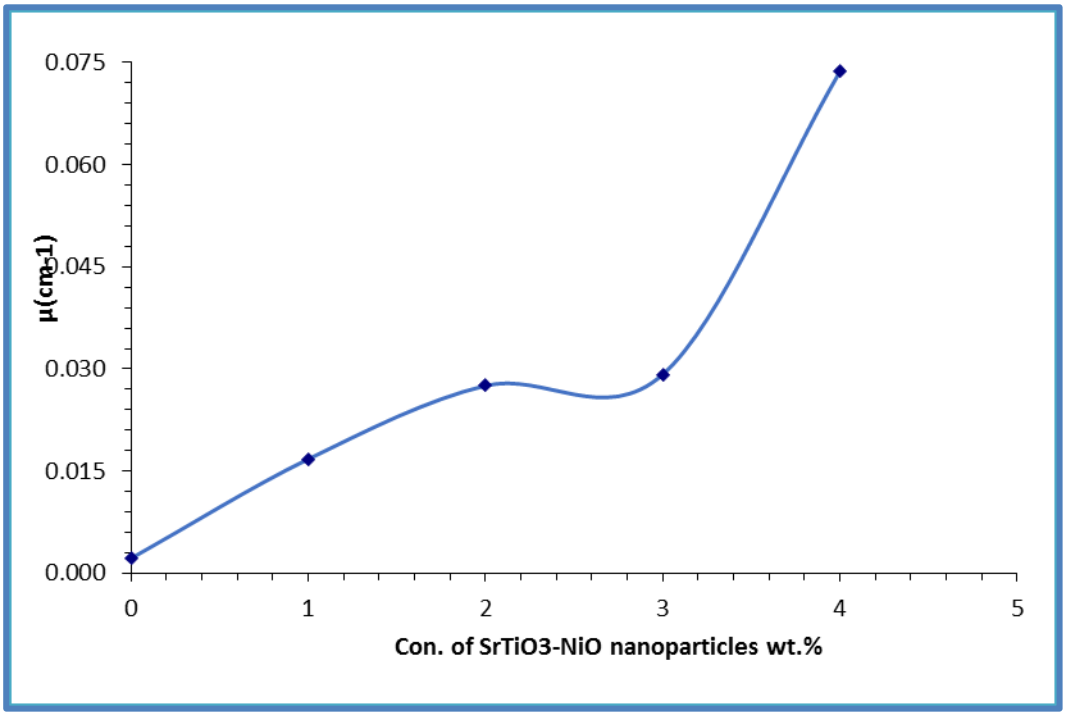

Figure(4-58) Variation of gamma radiation attenuation coefficients for PEO-PVA blends with different $SrTiO_3$-NiO NPs concentrations

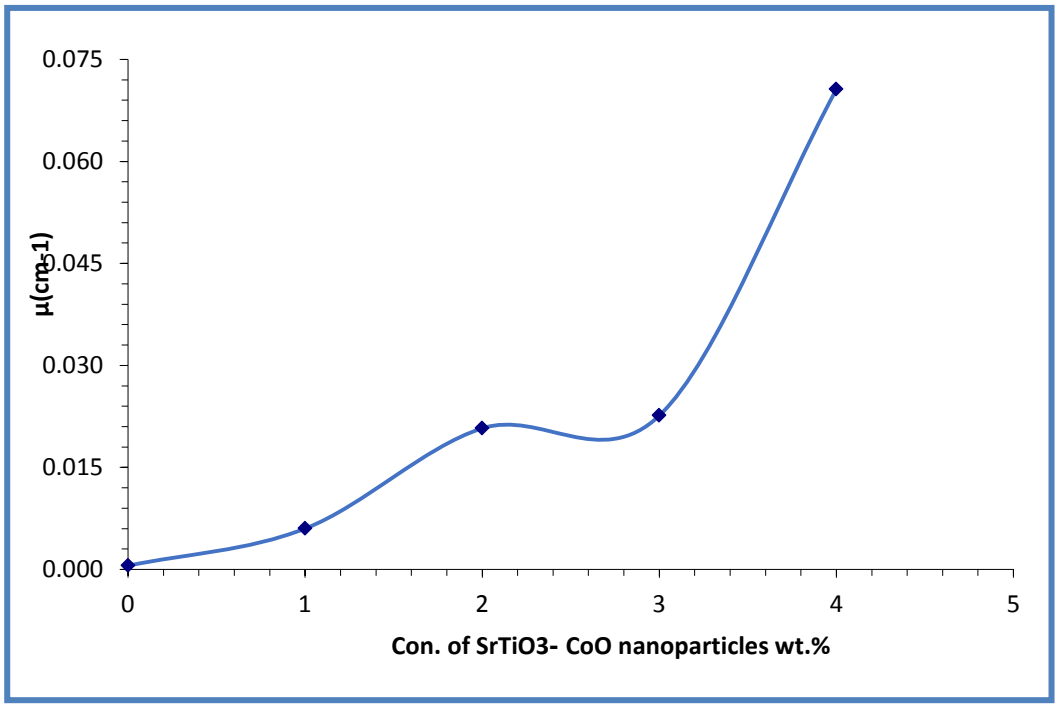

Figure(4-59) Variation of gamma radiation attenuation coefficients for PEO-PVA blends with different $SrTiO_3$-CoO NPs concentrations.

Figures (4-60)and (4-61) show the mass attenuation coefficient (μ/ρ) as a function of concentration of NPs. From this figure, mass attenuation coefficient increases by increasing the concentration of NPs. This is

because shielding materials are made of nanocomposites, which either absorb or reflect gamma rays [157]

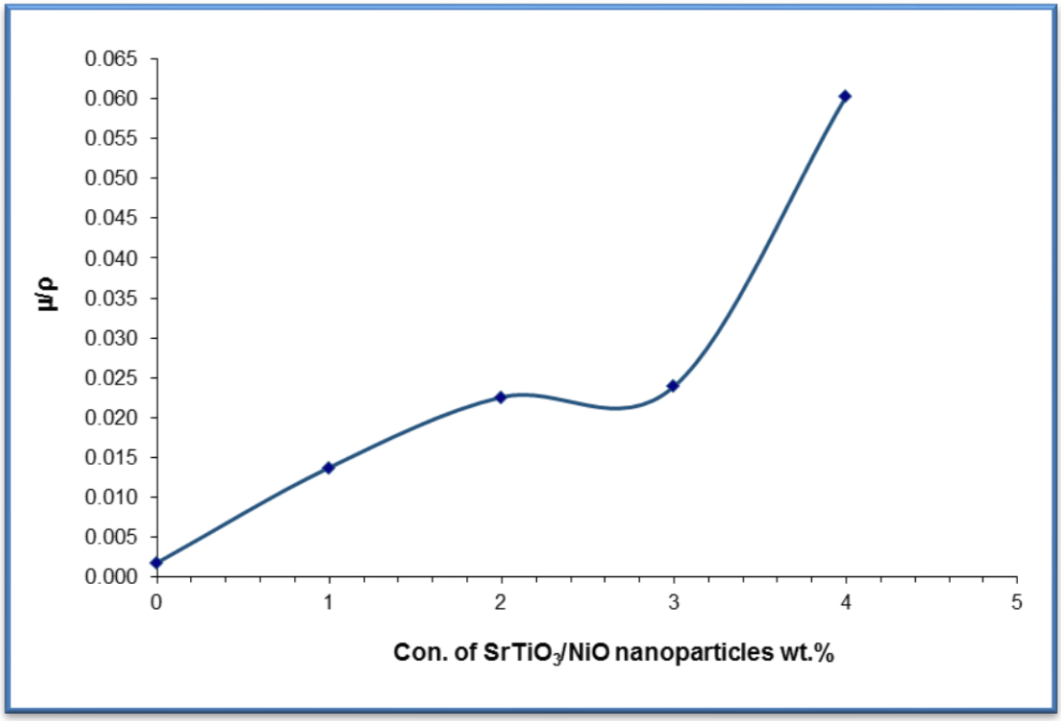

Figure(4-60) Attenuation mass of gamma-irradiation of a PEO-PVA mixture with different concentration of $SrTiO_3$-NiO nanoparticles

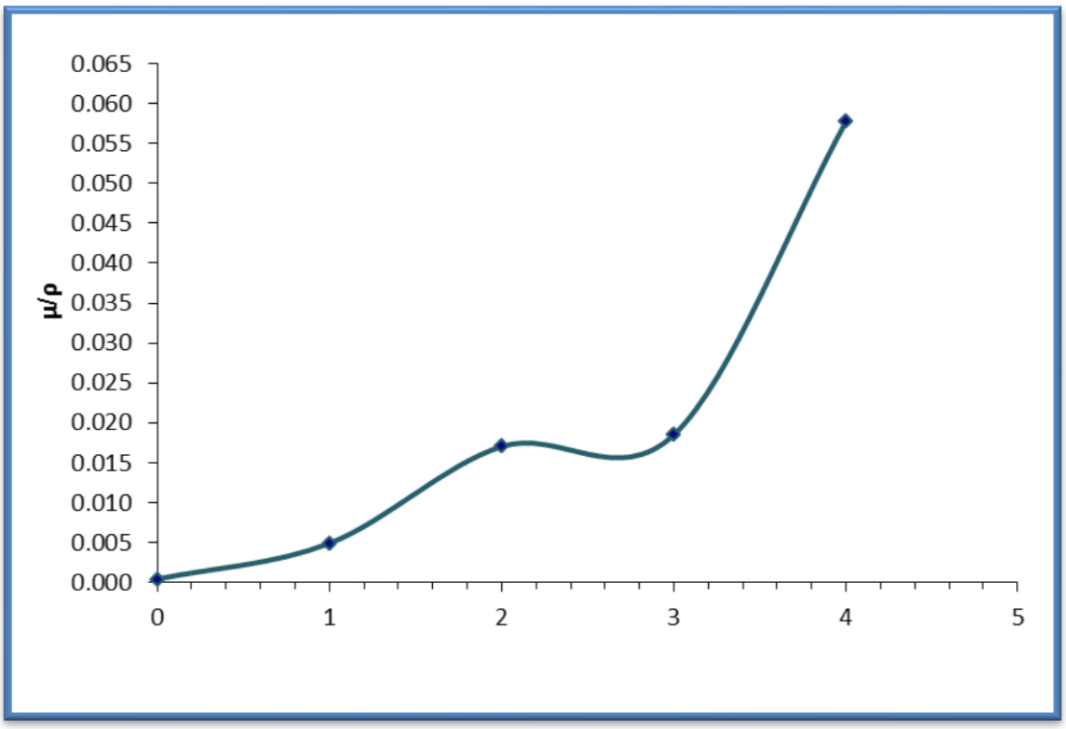

Figure(4-61) Attenuation mass of gamma-irradiation of a PEO-PVA mixture with different concentration of $SrTiO_3$-CoO nanoparticles

4-8 Conclusions

From the obtained results and discussions, the following points are concluded:

1- The optical microscope images show that $SrTiO_3$,NiO and CoO nanoparticles form a continuous network inside the polymers when the ratio of 4wt.%

2-FTIR spectra show a shift in some bands and change in the intensities of other bands comparing with pure PEO-PVA-$SrTiO_3$-NiO and PEO-PVA-$SrTiO_3$-CoO NCs films, this indicates there is no interaction between the polymers and the added nanoparticles.

3- SEM shows the surface morphology of the PEO-PVA-$SrTiO_3$-NiO and PEO-PVA-$SrTiO_3$-CoO NCs films with many aggregates or chunks randomly distributed on the top surface, homogeneous and coherent.

4- The absorbance and absorption coefficient of PEO-PVA-$SrTiO_3$-NiO and PEO-PVA-$SrTiO_3$-CoO NCs increase with the increasing of the concentrations of the $SrTiO_3$,NiO and CoO nanoparticles. The absorption coefficient for all films is less than $10^4 cm^{-1}$ ·Refractive index, extinction coefficient, and dielectric constant) real, imaginary) are increasing with the increasing of concentrations of $SrTiO_3$,NiO and CoO nanoparticles, while the energy gap for indirect transition (allowed‹forbidden) decreases with the increasing of the concentrations of $SrTiO_3$,NiO and CoO nanoparticles, the optical conductivity increases as the concentrations of $SrTiO_3$, NiO and CoO in the PEO-PVA increase to 4 wt.%

5- The dielectric constant, dielectric loss and A.C electrical conductivity for PEO-PVA-$SrTiO_3$-NiO and PEO-PVA-$SrTiO_3$-CoO NCs are increasing with the increasing $SrTiO_3$, NiO and CoO nanoparticles concentration and decreasing with the increase of frequency of the applied electric field, on the other hand, the A.C electrical conductivity increases with the increase of frequency, these properties can be used for films in capacitors, transistor, and electronic circuits.

6- The inhibition zone diameter increases with the increase in $SrTiO_3$, NiO and CoO nanoparticles concentratios

7-The results indicate that when pressure increases, the electrical capacitance of PEO-PVA-$SrTiO_3$-NiO and PEO-PVA-$SrTiO_3$-CoO NCs increases

8- The attenuation coefficient increase with increased of concentration of nanoparticles

4-9 Future Work

1-Study the thermal and mechanical properties of PEO-PVA-$SrTiO_3$-NiO and PEO-PVA-$SrTiO_3$-CoO NCs .

2- Study the effect of temperature, frequency and relative humidity on the capacitance of PEO-PVA-$SrTiO_3$-NiO and PEO-PVA-$SrTiO_3$-CoO NCs as humidity sensors application.

3- Study the effect of radiation on some physical properties of PEO-PVA-$SrTiO_3$-NiO and PEO-PVA-$SrTiO_3$-CoO NCs

4- Study the rheological properties of PEO-PVA-$SrTiO_3$-NiO and PEO-PVA-$SrTiO_3$-CoO nanocomposites

5- Effect of dye optical and electrical properties of PEO-PVA blend and used as smart windows applications

References

[1] Qian L. ,"Application of Nanotechnology for high performance textiles",J. of textile and apparel ,Technology and management ,Vol. 4,No. 1, pp.12-23,(2004).

[2] Krešimir M. and Zeljko M.," Nanotechnology and Diabetes", Vuk Vrhovac Institute, University Clinic for Diabetes, Endocrinology and Metabolic Diseases, Vol.34, No.4,pp.105-110(2006).

[3] Anita R., J.S Rana, Poonam R., Ashok K., Manoj R.," Antimicrobial Nanocomposite of Silver and Gelatin Nanofibers for Medical Applications", International Journal for Technological Research in Engineering Vol.1, No.4,pp.177-182(2013).

[4] Yuan-C.,Wenjun W.,Jiyan L.,QingliangY.,Feiyan L.,Qian L., Chang Z.,Chang L.,and Jinxing Z.," The Preparation of Graphene Reinforced Poly(vinyl alcohol) Antibacterial Nanocomposite Thin Film", International Journal of Polymer Science,Vol.2015,p.1(2015)

[5] Doulabi A. H, Mequanint K., and H. Mohammadi," Blends and Nanocomposite Biomaterials for Articular Cartilage Tissue Engineering", Materials, Vol. 7, No. 7, pp.5327-5355, (2014).

[6] Mohamad H.,Sana S. and Shaima A.,"Electrical properties for (ppab) thin films", Journal of Babylon,Vol.23,No.3,pp.1006-1114(2015).

[7] Abdul-Kareem J., Burak Y. K., Layth T. H.," Preparation and study the mechanical properties of CMC/PVA composites by sound waves", Journal of Advances In Physics Theories And Applications ,Vol.15,pp.11-20(2013).

[8] Muthuraj .R., M. Misra and A. K. Mohanty, "Biodegradable compatibilized polymer blends for packaging applications: A literature review ", Journal of Applied Polymer Sciences, Vol. 135, No. 24, pp. 1-35،(2017)

[9] Alkhayatt A. H, Al-Azzawi O., A. H. and Z. Alakayashi, "Rheologicaland optical characterization of polyvinyl pyrrolidone (PVP) - polyethyleneglycol (PEG) polymer blends", IOSR Journal of Applied Physics, Vol. 8,No.1, pp. 11-18, (2016)

[10] Utracki. J. L. A ," Polymer Blends Handbook" , printed in poston , London, Vol .1 , pp. 951–976 (2002).

[11] Shan J., Sha L. and Wenhao F.," PVA Hydrogel Properties for Biomedical Application", Journal of the mech. Behavior of biomedical materials, Vol.4 No 481, ,pp.1228-1233(2011).

[12] Lau K. Y., Piah M. A.," Polymer Nanocomposites in High Voltage Electrical Insulation Perspective: A Review", Malaysian Polymer Journal, Vol. 6, No. 1,pp.58-69(2011)

[13] Manocha L M,Jignesh V.,Nikesh P.,Ashidh W. and Manocha S. ,"Nanocomposites for structural applications",Indian Journal of pure &applied physics, Vol.44,pp.135-142(2006).

[14] Mansor B. A.,Kamyar S., Wan M. Z., Nor A. I.and 2Majid D.," Synthesis and Characterization of Silver/Clay/Starch Bionanocomposites by Green Method", Australian Journal of Basic and Applied Sciences.,Vol. 4,No.7,pp.2158-2165(2010).

[15] Rohan A. H and Darrin J.P," Polymer Nanocomposites for biomedical Applications",Mrs Bulletin . Vol. 32,pp,354-358(2007).

[16] Chia-Jung W., Akhilesh K. G., Patrick J. S. and Gudrun S.," Development of Biomedical Polymer-Silicate Nanocomposites: A Materials Science Perspective", Journal of Materials Vol.3,pp.2986-3005 (2010).

[17] William G. E., Aldo B. A. and Jinwen .Z,"Polymer Nanocomposites: Synthetic and Natural Fillers", Maderas. Ciencia y tecnología,Vol. 7,No.3,pp.159-178(2005).

[18] Kumar .K. Kiran, M. Ravi, Y. Pavani, S. Bhavani, A. K. Sharma, and V. V. R. Narasimha Rao, “Investigations on the effect of complexation of NaF salt with polymer blend (PEO/PVP) electrolytes on ionic conductivity and optical energy band gaps,” Phys. B Condens. Matter, Vol. 406, No. 9, pp. 1706–1712, 2011, doi: 10.1016/j.physb.(2011).

[19] Silva T. L. da, F. P. de Araujo, E. C. da Silva Filho, M. B. Furtini, and J. A. Osajima, “Degradation of poly (ethylene oxide) films using crystal violet,” Mater. Res., Vol. 20, pp. 869–872, (2017) .

[20] Zhu, Junmin. "Bioactive modification of poly(ethylene glycol) hydrogels for tissue engineering"s Vol 31. pp. 4639–4656 (2014).

[21] Jolanta S., Mārtiņš K., Anda D. and Velta T.," Poly(vinyl alcohol) hydrogels", Proceedings of the Estonian Academy of Sciences ,Vol 58,No. 1,pp.63-66 (2009) .

[22] Mudigoudra B.S., Masti S.P., Chougale R.B.," Thermal Behavior of Poly (vinyl alcohol)/ Poly (vinyl pyrrolidone)/ Chitosan Ternary Polymer Blend Films", Research Journal of Recent Sciences, Vol.1,No.9, pp.83-86 (2012).

[23] Maria S. P.,Youssef H., Arja H. V., Orlando J. R., Joel J. P. and Jukka V. S.," Effect of Moisture on Electrospun Nanofiber Composites of Poly(vinyl alcohol) and Cellulose Nanocrystals", Journal of Biomacromolecules, Vol. 11, No. 9,pp.2471-2477 (2010).

[24] Veeran G. K. and Guru V. B.," Water Soluble Polymers for Pharmaceutical Applications",Journal of Polymers Vol.3,pp.1972-2009 (2011).

[25] Abdul kareem G.,Safa A.,"Study optical properties of CMC by additive PVA",Journal of Babylon uni., Vol.22,No.1,pp.171-183 (2012).

[26] Muller K. A. & H. Burkard. "$SrTiO_3$: An intrinsic quantum paraelectric below 4 K". Phys. Rev. Vol.19 No .7, pp 3593–3602. Bibcode:1979PhRvB..19.3593M. doi:10.1103/PhysRevB.19.3593(1979).

[27] Read, P. G. "Gemmology, second edition. Great Britain: Butterworth-Heinemann". pp. 173, 176, 177, 293. ISBN 0-756-4411-7(1999).

[28] Benthem K. van, C. Elsässer and R. H. French. "Bulk electronic structure of $SrTiO_3$: Experiment and theory". Journal of Applied Physics. Vol 90 No 12 pp.6156. doi:10.1063/1.1415766. S2CID 54065614(2001).

[29] Rodenbücher C.; P. Meuffels; W. Speier; M. Ermrich; D. Wrana; F. Krok; K. Szot. "Stability and Decomposition of Perovskite-Type

Titanates upon High-Temperature Reduction". Phys. Status Solidi RRL. Vol 11 No 9: 1700222. Bibcode:2017PSSRR..1100222R. doi:10.1002/pssr.201700222. (2017)

[30] Hassan.A. J, "Study of Optical and Electrical Properties of Nickel Oxide(NiO) Thin Films Deposited by Using a Spray Pyrolysis Technique", Journalof Modern Physics, Vol. 5,pp. 2184-2191, (2014).

[31] Dooley. K.M, Chen. S.Y, J.R. Ross "Stable Nickel- Containing Catalysts for the Oxidative Chupling of Methane" Journal of Catalysis, 145, pp. 402-408 (1994).

[32] McKee ,R. A., Walker .F. J, & Chisholm .M. F.: Crystalline Oxides onSilicon:TheFirstFiveMonolayers.PhysRev.Lett.81(14):.Bibcode:PhRvL .81.3014M.(1998),Doi:10.1103/PhysRevLett.81.3014 (1998).

[33] Gulati .K, S. Lal, P. K. Diwan, and S. Arora, Int. J. of Appl. Eng. Res., Vol.14, No. 1: pp 170, (2019).

[34] B. Svegl, Orel, M.G. Hutchins, K. Kalcher, J. Electrochem. Soc. Vol 143 No (5) pp 1532–1539(1996)

[35] Zhu .X, Wang .J, D. Nguyen, J. Thomas, R. A. Norwood, and N.Peyghambarian, "Linear and nonlinear optical properties of Co_3O4 nanoparticle-doped polyvinyl-alcohol thin films," Opt. Mater. Express, Vol.2, No. 1, pp. 103, (2012)

[36]Du N, Zhang H, Chen BD, Wu JB, Ma XY, Liu ZH, et al. (17 December 2007). "Porous Co3O4 Nanotubes Derived From Co4(CO)12 Clusters on Carbon Nanotube Templates: A Highly Efficient Material For Li-Battery Applications". Advanced Materials. Vol 19 No (24): pp 4505–4509. doi:10.1002/adma.200602513. S2CID 55881828

[37] Patel and Sureshkuma," Spectroscopic Investigation and Characterizations of PAM/PEO Blends Films" Vol.4 No.2 (2014) DOI: 10.4236/soft.2015.42002

[38] Dawood .K. A, Ali. M, F. Lafta, B. Nasih, S. Nayyef, and A. Hashim, "Preparation of Polyvinyl alcohol-Poly-acrylic acid-Cobalt Oxide Nanoparticles Nanocomposites and Study their Optical Properties," Int. J. Sci. Res., Vol. 3, No. 12, (2014).

[39] Sugumaran S, C. Bellan .S., and M. Nadimuthu, “Characterization of composite PVA–Al 2 O 3 thin films prepared by dip coating method,” Iran. Polym. J., Vol. 24, No. 1, pp. 63–74,(2015).

[40] Chatterjee .B, Kulshrestha .N and P. N. Gupta, "Electrical properties of starch-PVA biodegradable polymer blend", Physica Scripta Journal, Vol. 90, No.2, (2015)

[41] Mathen J. J., G. P. Joseph, and J. Madhavan, “Improving the optical and dielectric properties of PVA matrix with nano-ZnSe: Synthesis and Characterization,” Int. J. Eng. Res, Vol. 4, pp. 1054–1062,(2016).

[42] Karpuraranjith .M., and S. Thambidurai, "Chitosan/zinc oxide-polyvinyl pyrrolidone (CS/ZnO-PVP) nanocomposite for better thermal and antibacterial activity", International Journal of Biological Macromolecules, Vol .104. pp 1753-1761, (2017).

[43] Goswami A, Bajpai .A. K, J. Bajpai, and B. K. Sinha, “Designing vanadium pentoxide-carboxymethyl cellulose/polyvinyl alcoholbased bionanocomposite films and study of their structure, topography, mechanical, electrical and optical behavior,” Polym. Bull., Vol. 75, No. 2, pp. 781–807,(2017).

[44] Guruswamy .B, Ravindrachary V, C. Shruthi, S. Hegde, R. N.Sagar, and S. D. Praveen, “Optical, electrical and thermal properties of SnO2 nanoparticles doped poly vinyl alcohol-poly vinyl pyrrolidone blend polymer electrolyte,” Indian J. Adv. Chem. Sci.,Vol. 6, No. 1, pp. 17–20,(2018).

[45] Ningaraju .S, Gnana .A.P, Prakash,and H.B. Ravikumar," Studies on free volume controlled electrical properties of PVA/NiO and PVA/TiO2 polymer nanocomposites" Solid State Ionics, VoL. 320, pp. 132–147,(2018).

[46] Ueda.K, Tanaka .K, and Y. Chujo ," Optical, Electrical and Thermal Properties of Organic–Inorganic Hybrids with Conjugated Polymers Based on POSS Having Heterogeneous Substituents", Polymers, VoL 11, No 44,(2019).

[47] Jebur. Q, Hashim.A , & M. Habeeb, " Fabrication, Structural and Optical properties for (Polyvinyl Alcohol–Polyethylene Oxide–Iron

Oxide) Nanocomposites", Egyptian Journal of Chemistry,Vol. 63,No. 2, pp. 611-623, (2020).

[48] Abid .A. A, Sameer H. Al-nesrawy and A. R. Abdulridha, "New Fabrication (PVA-PVP-C.B) Nanocomposites: Structural and Electrical Properties "Journal of Physics: Conference Series ,Vol. 1804 ,pp. 1203,(2021)

[49] Cao.Y, Shen C, Z.Yang, Z. Cai, Z. Deng, & D. Wu,"Polycaprolactone/polyvinyl pyrrolidone nanofibers developed by solution blow spinning for encapsulation of chlorogenic acid". Food Quality and Safety Vol 6, fyac014, https://doi.org/10.1093/fqsafe/fyac014 (2022)

[50] Zainab.S.J, Majeed .A.H,Waleed.H, Synthesis and Characterization of(PVA-CoO-ZrO2)Nanostructures for Nano optoelectronic Fields East European Journal of Physics Vol 2. pp 228-233 (2023) DOI:10.26565/2312-4334-2023-2-25 (2023)

[51] A. A. Al-Shamari, A. M. Abdelghany،H. Alnattar, and A. H. Oraby"،Structural and optical properties ofPEO/CMC polymer blend modified with gold nanoparticles synthesized by laser ablation in water," J. Mater. Res. Technol., Vol. 12, pp. 1597–1605,doi: 10.1016/j.jmrt.2021.03.050. (2021)

[52] Lee, J.-K.; Lee, Y.-J.; Chae, W.-S.; Sung, Y.-M. Enhanced ionic conductivity in PEO-LiClO4 hybrid electrolytes by structural modification. J. Electroceramics, No 17, pp 941(2006)

[53] Mansour, A.F., S.F. mansour and M.A. Abdo,. "Enhancement of structural and electrical properties of ZnO/ PVA nanocomposites", IOSR Journal of Applied Physics, No 7(2): Vol 97- pp 106 (2015)

[54] Suryanarayana. C and M. G. Norton, "X-ray Diffraction, A Practical Approach". Plenum Press, New York, (1998).

[55] E. Bacaksiz , S.Aksu , B.M.Basol , M.Altunbas , M.parlak and E. Yanmaz , " Structural , Optical and Magnetic Properties Of Zn1-xCoxO Thin Films Prepared by Spray Pyrolysis " Thin Films ,Vol.516 , PP.7899-79029 ,(2008)

[56] Ilican .S, Caglar ,M., and Y. Caglar, “The effect of deposition parameters on the physical properties of CdxZn1-xS films deposited by spray pyrolysis method,” J. Optoelectron. Adv. Mater., Vol. 9, No. 5, pp. 1414–1417(2007).

[57] Abdullah .O. G and Saeed. S. R, “Effect of NaI doping on same physical characteristic of (PVA) 0.9-(KHSO4) 0.1 composite films,” Chem. Mater. Res., Vol. 3, No. 11, pp. 19–24, (2013).

[58] Kumar. S, "Infrared spectroscopy: method development and ligand binding studies", Licentiate thesis, Stockholm University, Stockholm, Sweden pp 83.(2010).

[59] Nandiyanto .A. B, Oktiani D. R, and R. Ragadhita, "How to read and interpret FTIR spectroscope of organic material", Indonesian Journal of Science & Technology, Vol. 4, No. 1, PP. 97-118,(2019)

[60] Stehr .F. J. M, "Fourier transform infrared spectroscopy (FTIR) for detection and quantification of milk components for cattle health monitoring", M.Sc. Thesis, Norwegian University of Life Sciences(2017).

[61] S. M. Hassan," Optical Properties of Prepared Polyaniline and Polymethyl methacrylate blends", International Journal of Application or Innovation in Engineering & Management (IJAIEM) ,Vol. 2,No. 9,pp. 232-235, (2013)

[62] Diez-Pascual .A. M, "Nanoparticle reinforced polymers", Polymers, Basel, Vol. 11, No. 4 (2019).

[63] Roppolo. I, Sangermano .M, and A. Chiolerio, "Optical properties of polymer nanocomposites", Functional and Physical Properties of Polymer Nanocomposites, Vol. 31, PP. 139-157(2016).

[64] Gupta .A., S. Das, C. J. Neal, and S. Seal, "Controlling the surface chemistry of cerium oxide nanoparticles for biological applications", Journal of Materials Chemistry B, Vol. 4, PP. 3195-3202(2016).

[65] David W.Greve," Semiconductor devices and technology", 2nd,USA. (2012).

[66]Edition, Addison-Wesley Publishing Company, London (Molecular Biology of Gene) (1975).

[67] Van Z., Bart. "Principles of semiconductor devices" Colarado University (2004).

[68] Chiad .S. S, Habubi .N. F., S. F. Oboudi and M. H. Abdul-Allah, "Effect of Thickness on The Optical Parameters of PVA: Ag", Diyala Journal for pure Sciences, Vol. 7, No. 3, (2011).
[69] Hashim. A, "Experimental Study of Electrical Properties of (PVA $CoNO_3$, $AgCO_3$) Composites", American J. of Sci., Vol 68, pp. 56-61,(2012).

[70] Dhakal .T. R, Mishra, R. Sanjay, Glenn, Zachery, Rai, K. Binod " Synergistic Effect of PVP and PEG on the Behavior of Silver Nanoparticle Polymer Composites", J. of Nanoscience and Nanotechnology, Vol.12, pp. 6389-6396**,** (2012).

[71] Hassan. S. M," Optical Properties of Prepared Polyaniline and Polymethyl methacrylate blends", International Journal of Application or Innovation in Engineering & Management (IJAIEM) ,Vol. 2,No. 9,pp. 232- 235, (2013).

[72] Shekhar .S, Prasad. V, Subramanyam .S. V, "Structural and electrical properties of composites of polymer-iron carbide nanoparticle embedded incarbon"J.Els.,Sci.,Vol.18,(2006).
[73] Stenz .O," The physics of thin film optical spectra", An Introduction, Winzerlaer Str. Vol 10, 07745 Jena Germany, pp.71-72, (2005).
[74] Mwolfe .C, N. Holouyak and G. B. Stillman, "Physical properties of semiconductor",prenticeHall,NewYork,(1989).
[75] AL-Dawodi.H. R. A," A study of the structural and optical properties of obliquely deposited (CdS) thin films", M.Sc. Thesis, University AlMustansiriyah,CollegeofScience,(2010).
[76] Nilens. A. G, "deep imparity in semiconductors" , Wiley – Interscience pub., (1973).

[77] Sauer .M., J. Hofkens and J. Enderlein, Handbook of Fluorescence Spectroscopy and Imaging, from Single molecules to Ensembles , WileyVCH Verlag GmbH & Co. KGaA, Weinheim, Germany, (2011).
[78] Al-Alousi .M. A., "The Effect of Substrate Temperature and The

Annealing Time on the Optical Properties of The AgInS2 Thin Films Prepared by chemical spray Pyrolysis Technique", J. of University ofAnbar for pure science Vol 4, (2010).
[79] Abdelazizand .M , Abdelrazek .E. M, Effect of Dopant Mixture on Structural, Optical and Electron Spin Resonance Properties of Polyvinyl Alcohol, Physica B, Vol. 390,pp. 1-9, (2007).
[80] Najeeb .H. N, Wahab .G. A, Ali, A. K. Kodeary, J. Ali, "Doping Effect on Optical Constants of Poly-Vinyl Chloric (PVC)", Academic Research International, Vol.4, pp. 53-62, (2013).
[81] Baker .M. I., Walsh .S, Z. Schwartz and B. D. Boyan, A Review of Polyvinyl Alcohol and it is Uses in Cartilage and Orthopedic Applications, Journal of Biomedical Materials Research: Applied Biomaterials,(2012).
[82] Meyyappa. M, Nanotechnology Measurement Handbook, A Guide to Electrical Measurements for Nanoscience Applications, 1st Edition, KeithleyInstruments,Inc.,USA,(2007).
[83] Tyagi. M and D. Tyagi, "Polymer Nanocomposites and their Applications in Electronics Industry", International Journal of Electronics and Electrical Engineering,Vol. 7, pp. 603-608, (2014).
[84] Abbas .N. K, M. A. Habeeb, and A. J. K. Algidsawi," Influence of Prepared Chloropenta Amine Cobalt (III) Chloride Nanoparticles on The Dielectric Properties of PVA Film", Australian Journal of Basic and Applied Sciences, Vol. 9,pp. 26-34, (2015).
[85] Azahari ,N. A, N. Othman and H. Ismail," Biodegradation Studies of Polyvinyl Alcohol/Corn Starch Blend Films in Solid and Solution Media", Journal of Physical Science, Vol. 22, pp.15-31, (2011).

[86] Kumar .N. B. R, Crasta .V, R. F. Bhajantri and B. M. Praveen, "Microstructural and Mechanical Studies of PVA Doped with ZnO and WO3 Composites Films", Journal of Polymers,Vol. 2014, (2014).
[87] Jeevan .N. C, B. Babu .R. N., and K. Chandrashekara, "Characteristic Analysis of Mechanical Properties on Carbon Fiber Reinforced Plastic",International Journal of Research in Engineering & Advanced Technology (IJREAT),Vol. 3,pp. 305-308, (2015).

[88] Gaponenko, Sergey V.,"Optical properties of semiconductor nanocrystals", 1st,Cambridge university press, (1998)

[89] Alias .A. N., Zabidi .Z. M,A.M.M. Ali,M. K. Harun," Optical Characterization and Properties of Polymeric Materials for Optoelectronic and Photonic Applications",International Journal of Applied Science and Technology,Vol. 3, No. 5,pp.11-38 (2013).

[90] Aziz .S. B, Brza .M. A, M. M. Nofal, R. T. Abdulwahid, S. A. Hussen, A. M. Hussein, and W. O. Karim, "A comprehensive review on optical properties of polymer electrolytes and composites", Materials, Basel, Switzerland, Vol. 13, No. 17, (2020).

[91] Jafar .H. I, Ali. N. A. and A. Shawky, "Study of A.C Electrical Propertiesof Aluminum-Epoxy Composites", Journal of Al-Nahrain University,Vol.14,pp.77-82,(2011).

[92] Seghier .T and Benabed .F, Dielectric Properties Determination of HighDensity Polyethylene (HDPE) by Dielectric Spectroscopy, International Journal of Materials, Mechanics and Manufacturing 3, (2015).

[93] Blythe .T and Bloor .D, Electrical Properties of Polymers, 2nd Edition, Cambridge University Press, UK, (2005) .

[94] F. Yakuphanoglu, "Electrical conductivity and electrical modulus properties of α, ω-dihexylsexithiophene organic semiconductor," *Physica B: Condensed Matter*, vol. 393, no. 1-2, pp. 139–142, (2007).

[95] M. M. El-Nahass, A. A. Atta, M. A. Kamel, and S. Y. Huthaily, "AC conductivity and dielectric characterization of synthesized p-N,N dimethyl laminobenzy Iidenemalononitrile (DBM) organic dye," *Vacuum*, vol. 91, pp. 14-19, (2013)

[96] J. C. Giuntini, J. V. Zanchetta, D. Jullien, R. Eholie, and P. Houenou, "Temperature dependence of dielectric losses in chalcogenide glasses," *Journal of* Non-crystalline Solids, vol. 45, no. 1, pp. 57–62, (1981).

[97] Parravicini .G. B., E. R. Mognaschi, D. Comoretto, G. Dellepiane, and A. Brillante, "Dielectric studies on conjugated polymers," Synthetic Metals, Vol. 101, No. 1-3, pp.467-468,(1999).

[98]R. C. Dorf, The Electrical Engineering Hand Book, CRC Press LLC, 2nd Edition, Piscataway, New Jersey, USA, (2000).

[99] Radivojevic .V. M, Rupcic .S., M. Srnovic, and G. Bensic, "Measuring the dielectric constant of paper using a parallel plate capacitor", International Journal of Electrical and Computer Engineering Systems, Vol. 9, No. 1. PP. 1-10,(2018).

[100] Wen .S,and D. D. L. Chung, "Electric Polarization in Carbon FiberReinforced Cement", Cement and Concrete Research,Vol. 31, pp.141-147,(2001).

[101] Solymar .L. and D. Walsh, "Electrical Properties of Materials, 7th Edition", Oxford University Press, Oxford, New York, (2004).

[102] Griffith .D. J, Introduction to Electrodynamics 3rd Edition , PrenticeHall, Inc., New Jersey, USA, (1999).

[103] Gladkov .S. O, Dielectric Properties of Porous Media, Springer-Verlag Berlin Heidelberg, New York , USA, (2003).

[104] Zohdi .T. I, Electromagnetic Properties of Multiphase Dielectrics, Primer on Modeling, Theory and Computation , Springer-Verlag Berlin, Heidelberg, Berkeley, USA, (2012) .

[105] Gao .W. and N. M. Sammes, An Introduction to Electronic and IonicMaterials, World Scientific Publishing Co. Pte. Ltd., Singapore, (1999).

[106] A.Chelkowski, "Dielectric physics", 1st edition, pwin-polish sci. Pub.(1980).

[107] Abdullah .O. G, Hussen .S. A, and A. Alani, "Electrical Characterization of Polyvinyl Alcohol Films Doped with Sodium Iodide", Asian Transactions on Science & Technology ,Vol. 1,No. 4, (2011).

[108] Prystaj .L. A, Effect of Carbon filler Characteristics on the Electrical Properties of Conductive Polymer Composites Possessing Segregated Network Microstructures, MSc. Thesis, The Academic Faculty, Georgia Institute of Technology, (2008).

[109] Srivastava, N. K. and Mehra, R. M.. “Study of electrical properties of polystyrene/foliated graphite composite”, J. Materials Science-Poland,27(1):pp.110-122.(2009).

[110] Saini, I.; Rozra, J.; Chandak, N.; Aggarwal, S.; Sharma, P. K. and Sharma,A.. “Tailoring of electrical, optical and structural properties of PVAby addition of Ag nanoparticles”, Materials Chemistry and Physics, 139(2-3):pp.802-810.(2013).

[111] Demir, H. O.; Sacak, M. and Digrak, M. "Investigation of Poly-2-[(4-Pyridilmethylene)-Imino] Phenol's Some Properties: Electrical Conductivity,Antimicrobial Activity and Synthesis of Its Metal Complexes", Journal of Materials Science and Engineering B 3, 3(1):pp.19-24. (2013).

[112] Hashim. A , and Hadi A. , Novel Pressure Sensors Made From Nanocomposites (Biodegradable Polymers–Metal Oxide Nanoparticles): Fabricat and Characterization. Ukrainian Journal of Physics, 63(8), DOI: https://doi.org/10.15407/ujpe63.8.754 , (2018).

[113] Hashim .A, and Jassim, . A, "Novel of biodegradable polymersinorganic nanoparticles: Structural, optical and electrical properties as humidity sensors and gamma radiation shielding for biological applications," J. Bionanoscience, Vol. 12, No. 2, pp. 1–7, 2018.

[114] Ahmed .K, A., H. Sroor, Obaid F., and A. Hashim, "Fabricationof novel (carboxy methyl cellulose – polyvinylpyrrolidone – polyvinyl alcohol)/ lead oxide nanoparticles : structural and optical properties for gamma rays shielding applications," Int. J. Plast. Technol., Vol. 23, No. 1,pp. 39–45, 2019.

[115] Obaid. M, Roy .K, Mahloniya .R. G, J. Bajpai, and A. K. Bajpai, "Spectroscopic and morphological evaluation of gamma radiation irradiated polypyrole based nanocomposites," J Adv Mater Lett, Vol. 3, No. 5, pp. 426–432,2012.

[116] Jana, S.; Thapa, R.; Maity, R. and Charropadhyay, K. K.. "Optical and dielectrical properties of PVA capped nanocrystalline PbS thin films synthesized by chemical bath deposition", Physica E, 40(10): pp. 3121-3126(2008).

[117] Su .C, Huang .K, H.-H. Li, Y.-G. Lu, and D.-L. Zheng,"Antibacterial properties of functionalized gold nanoparticles and their application in oral biology," J. Nanomater., vol. (2020).

[118] Vimbela. G. V, S. M. Ngo, C. Fraze, L. Yang, and D. A. Stout,"Antibacterial properties and toxicity from metallic nanomaterials," Int. J. Nanomedicine, vol. 12, p. 3941, 2017.

[119] Ashraf . Pelaz .S, B, P Pino, M Carril, A Escudero, "Gold-based

nanomaterials for applications in nanomedicine," Light. Nanostructured Syst. Appl. Nanomedicine, pp. 169–202, (2016).
[120] Bapat .R. A, TV Chaubal, S Dharmadhikari, "Recent advances of gold nanoparticles as biomaterial in dentistry," Int. J. Pharm., p. 119596,(2020).
[121] Rithin Kumar .N. B, V. Crasta, R. F. Bhajantri, and B. M. Praveen,"Microstructural and mechanical studies of PVA doped with ZnO and WO3 composites films," J. Polym., vol. 2014, (2014)

[122] Salman .S. A, Z. A. Al-Ramadhanand Z. F. Nazal," Optical PropertiesOf Polyvinyl Alcohol (PVA) Films Doped With CoCH3COOH salt", Diyala journal for pure sciences,Vol. 10,No.3, pp. 30-38, (2014).
[123] Bhavani .S, M. Ravi, and V. V. R. N. Rao, "Studies on Electrical Properties of PVA: NiBr2Complexed Polymer Electrolyte Films for BatteryApplications", International Journal of Engineering Science and Innovative Technology (IJESIT),Vol. 3, pp. 426-434, (2014).
[124] Habeeb .M. A and L. A. Hamza, "Structural, Optical and DC Electrical Properties of (PVA-PVP-Y2O3) Films and Their Application for Humidity Sensor," J. Adv. Phys., Nol. 6, No. 1, pp. 1–9, (2017).
[125] Sangawar, V. S.; Dhokne, R. J.; Ubale, A. U.; Chikhalikar, P. S. and Meshram, S. D. "Structural characterization and thermally stimulated discharge conductivity (TSDC) study in polymer thin films", Bull. Mater.Sci., 30 (2): pp. 163-166. (2007).

[126] S. Mustafa, "Engineering Chemistry", Library of Arab society for publication and distribution, Jordan, (2008).
[127]G. A. AL-Dahash, H. N. Najeeb, A. Baqer and R. Tiama," The Effectof Bismuth Oxide Bi2O3 on Some Optical Properties of Poly vinyl Alcohol",British Journal of Science, Vol. 4, pp.117-124, (2012).
[128] Abed. R. A. and M. A. Habeeb," Preparation and Study Optical Properties of (PVA-PVP-CrCl2) Composites", Industrial Engineering Letters,Vol.3,pp.60-66,(2013).
[129] Neama .H, N. AL-Khegani, "The Effect of Ferrous Chloride (FeCl2) onSome Optical Properties of Polystyrene", Academic Research International,Vol,5,pp.161-166,(2014).
[130] Md J. Uddin, B. Chaudhuri, K. Pramanik, T. R. Middya and B. Chaudhuri ," Black tea leaf extract derived Ag nanoparticle-PVA composite film: Structural and dielectric properties", J. Materials science

andEngineering B, Vol. 177 ,No.20, pp.1741- 1747, (2012).
[131] Bachari .T. S, "Electric Properties of Polyvinyl Acetate (PVA)-Polyoland Prepared Sulfonated Phenol-formaldehyde Resin (SPF) Bulk SamplesComposite", Asian Journal of Applied Science and Engineering,Vol.3,pp.33-44,(2014).
[132] Salsa .T. H. C, C. B. Lombellob and M. Akira, "Electro spinning ofGelatin/Poly (Vinyl Pyrrolidone) Blend from Water/Acetic Acid Solutions",Materials Research,Vol. 18,pp. 509-518, (2015).
[133] Gaza .T. S, A, Sulong M. N. Akhtar, A. H. Kadhum, A. Mohamad, and A. A. Al-Amery, "Properties and Applications of Polyvinyl Alcohol, Halloysite Nanotubes and Their Nanocomposites", Molecules, Vol. 20,No.12,pp.22833-22847,(2015).
[134] Kadajji .V. G, and G. V. Betageri, "Water Soluble Polymers for Pharmaceutical Applications", Polymers, Vol. 3,No.4,pp. 1972-2009, (2011).

[135] Stenz .O," The physics of thin film optical spectra", An Introduction,Winzerlaer Str. 10, 07745 Jena Germany, PP.71-72, (2005).

[[136] Mohd H.H., Elias S., Anuar K., Muhd Y., Iskandar S. M. and Muhd Ahmad A. O.," Temperature Dependence of AC Electrical Conductivity of PVA-PPy-$FeCl_3$ Composite Polymer Films",Malaysian Polymer Journal ,Vol 3, No. 2,pp.24-31 (2008).

[137] İbrahim U., Selda K., Ali G., Tutku C. K., Mehmet L. A.," Preparation and Properties of Electrospun Poly(vinyl alcohol) Blended Hybrid Polymer with Aloe vera and HPMC as Wound Dressing", Hacettepe Journal of Biology and Chemistry.,Vol. 38 ,No.1,pp. 19-25 (2010).

[138] Prajakta J. ,Dinesh K.K.,Poonam S. & Nirali G.,"Effect of nano-filler on electrical properties of PVA-PEO blend polymer electrolyte",Indian Journal of Pure and Applied Physics, Vol.51, pp.350-353 (2013).

[139] B Chatterjee, N Kulshrestha and P N Gupta," Electrical properties of starch-PVA biodegradable polymer blend", Physica Scripta,Vol.90 (2015).

[140] Sunil G R., Rajashekhar B., P. K. Pujari, and V. Ravindrachary," Pressure sensitive dielectric properties of TiO_2 doped PVA/CN-Li nanocomposite", Journal of Polymer Research ,Springer (2015).

[141] Mustafa B. M., Konul A. Y., Goncha M. E., Rasim K. M., and Aytan Z. S.," Study of Dielectric Properties of CdS/PVA Nanocomposites Obtained by Using Successive Ionic Layer Adsorption and Reaction", World Journal of Condensed Matter Physics, Vol.3,pp.82-86 (2013).

[142] Nixon. G. S. V., M. Rathnakumarib , and P.Sureshkumarb," Synthesis, dielectric, AC. conductivity and non-linear optical studies of electrospun copper oxide nanofibers", Archives of Applied Science Research, Vol. 3 ,No.5,pp.514-525 (2011).

[143] Sheha .E, Mona N. and M K El-Mansy," Characterization of poly (vinyl alcohol)/poly(3,4-ethylenedioxythiophene) poly(styrenesulfonate) polymer blend: structure, optical absorption, electrical and dielectric properties", Physica Scripta Vol.88,No.3 (2013).

[144] Ahmad. F , E. Sheha.," Preparation and physical properties of $(PVA)_{0.7}(NaBr)_{0.3}(H_3PO_4)_{xM}$ solid acid membrane for phosphoric acid – Fuel cells",Journal of Advanced Research, Vol. 4,pp.155–161 (2013).

[145] Thomasukutty J., Soney C. G., Maya M. and Sabu T.," Functionalized MWCNT and PVA Nanocomposite Membranes for Dielectric and Pervaporation Applications",J. Chemical Engineering and Process echnology,Vol.6,No.3,pp.1-8 (2015).

[146] Divya .R, Meena .M, C. K. Mahadevan and C. M. Padma," Investigation on CuO Dispersed PVA Polymer Films", Journal of Engineering Research and Applications, Vol. 4, No.5, pp.1-7 (2014).

[147] Hussein H., Naheda H. and Ahmed H.," The Effect of Aluminum Oxide Nanoparticles on Optical Properties of (Polyvinyl alcohol-Polyethylene glycol) Blend", Journal of Industrial Engineering Research, Vol.1,No.4,pp. 94-98 (2015).

[148] RithinKumar N.B ,VincentCrasta, and B.M.Praveen," Advancement in Microstructural, Optical, and Mechanical Properties of

PVA (Mowiol 10-98) Doped by ZnO Nanoparticles",Physics Research International Vol. 9 (2014).

[149] Abdelrazek .E.M, Abdelghany AM, and Tarabih AE," Characterization and Physical Properties of Silver/PVA Nano-composite",Journal of Pharmaceutical, Biological and Chemical Sciences,Vol.3,No.4 (2012).

[150] Melinte .V, Buruiana .T, I. D. Moraru, and E. C. Buruiana, "Silver-Polymer Composite Materials with Antibacterial Properties",Digest Journal of Nanomaterials and Biostructures Vol. 6, No 1,pp.213 -223 (2011).

[151].George F. F., Leon M. C., Ayo A. and Russell B.,"Metal Oxide Semi-Conductor Gas Sensors in Environmental Monitoring",Journal of Sensors,Vol.10, pp.5469-5502 (2010).

[152] Habeeb.M.A., W.K. Kadhim, "Study the optical properties of (PVA-PVAC-Ti) nanocomposites", Journal of Engineering and Applied Sciences, Vol. 9, No.4, pp. 109-113,(2014), doi: 10.36478/jeasci.2014.109.113

[153] Narsimha. P, .Shilpa .J, K Syed., M. Revansiddappa, S.V. Bhoraskar ,and M.V.N. Ambika P.," Electrical and humidity sensing properties ofpolyaniline/WO3 composites", Journal of Sensors and Actuators B 114,pp. 599–603(2006).

[154] Wangchang. G, Nan.L, Xiaotian L., Rui W.,Jinchun T., and Tong Z.,"Effect of polymerization time on the humidity sensing properties of polypyrrole",Journal of Sensors and Actuators B ,Vol.125 ,pp. 114–119 (2007).

[155] Roy .M. K, R. Mahloniya G, J. Bajpai, and A. K. Bajpai, “Spectroscopic and morphological evaluation of gamma radiation irradiated polypyrole based nanocomposites,” J Adv Mate r Lett, Vol. 3, No. 5, pp. 426–432,(2012).

[156] Raja, V.; Sharma, A. K. and Rao, V. V. R. N. “Impedance spectroscopic and dielectric analysis of PMMA-CO-P4VPNO polymer films”, Mater. Lett. , 58(26): pp. 3242–3247. (2004).

[157] Choudhary S Structural, optical, dielectric and electrical properties of (PEO–PVP)–ZnO nanocomposites. J Phys Chem Solids No121, pp 196–209(2018)